HIGH FLASH-POINT FLUID FLOW SYSTEM AEROSOL FLAMMABILITY STUDY AND COMBUSTION MECHANISM ANALYSIS

A Dissertation

by

SZU-YING HUANG

Submitted to the Office of Graduate and Professional Studies of
Texas A&M University
in partial fulfillment of the requirements for the degree of

DOCTOR OF PHILOSOPHY

Chair of Committee,	M. Sam Mannan
Committee Members,	James Holste
	Zhengdong Cheng
	Eric Petersen
Head of Department,	M. Nazmul Karim

December 2013

Major Subject: Chemical Engineering

ABSTRACT

The existence of flammable aerosols creates fire and explosion hazards in the process industry. Due to the operation condition of high pressure circumstances, heat transfer fluids tend to form aerosols when accidental leaking occurs on pipelines or storage vessels. An aerosol system is a complicated reactive system; there are neither systematic flammability data similar to the case with pure gases, nor clearly described ignition-to-combustion process of a droplet-air mixture system.

The flammable regions of three main, widely-used commercial heat transfer fluids: Paratherm NF (P-NF); Dowtherm-600 (D-600); and Plate Heat Exchange Fluid (PHE), were analyzed by electro-spray generation with laser diffraction particle analysis method. The aerosol ignition behavior depends on the droplet size and concentration of the aerosol. From the adjustment of differently applied electro-spray voltages (7-10 kV) and various liquid feeding rates, a flammable condition distribution was obtained by comparison of droplet size and concentration. All of the fundamental study results are to be applied to practical cases with fire hazards analysis, pressurized liquid handling, and mitigation system design once there is a better understanding of aerosols formed by high-flash point materials.

On the other hand, the process of combustion from initial stage to global flame formation was simulated with COMSOL-multi-physics in terms of heat transfer, droplet evaporation, and fluid dynamics of liquid-air interaction. The local temperature change

through time, as an indicator of luminous flame appearance, was analyzed to describe the flame development and ignition delay time of aerosols. We have conducted a series of simulation regarding physical formula in description of this combustion process, and will conclude with how temperature distribution influenced the appearance of luminous flames, which was the symbol of successful ignition of aerosol. The mitigation implementing timing and location can be characterized with further understanding of this combustion process. The potential application of the ignition delay will be beneficial to the mitigation timing and detector sensor setting of facilities to prevent aerosol cloud fires.

Finally, the scientific method of aerosol flammability study was discussed for its potential impacts on experimental results. A modeling point of view was introduced, with the analysis of electric field application on fuel droplets, and the related fundamental study of the ignition phenomenon on aerosol system. Existing charges from electrospray is beneficial for the monodispersity and control of aerosols for fundamental study. However, the additional charges accumulated on the droplet surfaces are likely to have impacts on flammability due to the excess energy they applied to the aerosols system and droplet-droplet distraction or turbulences. This is a re-visit of aerosol flammability study method, with a conclusion that charges did have positive impact on droplets' ignition concentration range with a balancing effect on turbulence increase to reduce the ignition chance.

DEDICATION

My true thanks to those who supported me throughout the years

To my beloved family in Taiwan

ACKNOWLEDGEMENTS

I cannot believe this chapter of my life is coming to a stepping stone end right now. Everything is just like yesterday; the frenzied sunshine in Texas, the shiny glass windows of the Jack E. Brown building, and the enormous new things for me to discover in the world of chemical engineering. Four wonderful years have passed, which were not all smooth or easy. I sincerely appreciate everyone I have met so far in this great place. You have enlightened this long path of my graduate study.

First, I owe a lot of appreciation to my advisor, Dr. Sam Mannan, who provided his students with endless help, care, and precious guidance. Making the decision to join Mary Kay O'Connor Process Safety Center (MKOPSC) in the chemical engineering department was one of the best things I have ever done in life. Dr. Mannan's kindness and selfless devotion were the strong resources I needed to continue.

I appreciate my committee members, Dr. Eric Petersen, Dr. James Holste, and Dr. Zhengdong Cheng, for their guidance and suggestions. To my great project leaders and research scientists in MKOPSC, Dr. Xinrui Li, Dr. Yi Liu, Dr. Victor Carreto, Dr. Xiaodan Gao, thanks to all of their contributions to my studies and career consulting and assistance. Same appreciation is given to my former and present colleagues who have offered me a lot of help: Dr. Peng Lian, the pioneer in aerosol research here; Yan-ru Lin, the next leader in the aerosol lab. Thanks to both of you for making this interesting

research sustain; and to all the MKOPSC members who accompanied me through these years as well.

Finally, my most appreciated family: there are neither accurate words I can use nor enough paragraphs I can put here to explain my gratitude. Their love and selfless support helps me fly to my dreams all the time. Aunt, Dad, and especially to Grandma: she passed away in my first day studying here, but her blessing has always been with me. This is all for them.

NOMENCLATURE

P-NF	Paratherm-NF
D-600	Dowtherm-600
PHE	Plate Heat Exchanger (Fluid)
LFL	Lower Flammability Limit
UFL	Lower Flammability Limits
P	Pressure
T	Time
MIE	Minimum Ignition Energy
D	Diameter (of droplet)
SMD	Sauter Mean Diamater
Sh	Sherwood number
Nu	Nusselt number
Cpa	Heat capacity of ambient air
vf	Stoichiometric coefficient of fuel chemical
ka	Thermal conductivity of air
M	Mass
N	Number(s)
d	Droplet diameter
ρ	Liquid density of fuel
D	Mass diffusivity

Sh^*	Modified Sherwood number
B_M	Mass transfer number
F_M	Correction factors of mass diffusivity
Y	Mass Fraction
k	Boltzmann constant (of reaction)
h	Planck's number
R	Ideal gas constant
q	Droplet charge at the Rayleigh instability limit
r	Droplet radius
ε_0	Electric permittivity of the surrounding medium
γ	Surface tension
σ	Surface charge density
C_l	Liquid specific heat
$L(T_d)$	Latent heat of vaporization
B_d	Droplet breakup transition probability function
K_{air}	Heat conductivity of air,
$(\rho D)_{air}$	Fuel-vapor diffusivity in ambient conditions
C	Coulomb, the charge quantity number
NMR	Nuclear Magnetic Resonance

TABLE OF CONTENTS

Page

LIST OF FIGURES

Page

LIST OF TABLES

Page

CHAPTER I

INTRODUCTION

The creation of aerosols from accidental leaking of pressurized operations in process industries is considered one of the most hazardous scenarios of explosion and fire. Heat transfer fluids, the group of commercially used hydrocarbon materials with high flash points, are operated under relatively high pressure, which can form a flammable aerosol cloud near the release point (Bowen and Shirvill, 1994; Durkee, 2003). There are already more than 60 reported incidents resulting from the formation of mists under specifically lower temperatures than the expected flash points, including hydrocarbon extracts from the oil industry and chemical processing facilities. These incidents have caused more than $500 million in losses (Febo and Valiulis, 1995).

In general, an aerosol is a mixture of fuel droplets in the surrounding air and often exhibits a two-phase physical state. The potential droplet size distribution of either mono- or poly-dispersity depends on the chemical properties of the fuel, such as viscosity. Compared to gaseous matter, aerosols contain more combustible material and more enthalpy per unit volume and can disperse to larger areas over bulk liquids (Krishna, Rogers, and Mannan, 2003). There is a general misconception that fluids are safe below their flash points, when in fact, aerosols can be ignited below the fluid's flash point due to the drastically increased evaporation rates for liquids dispersed in the form of fine aerosol droplets with large droplet surface area (Lian, Mejia, Cheng, and Mannan, 2010).

The fire hazards can be separated into two parts for discussion: ignitability and combustion. For ignitability, fuel aerosols require different diagnostics, such as minimum ignition energies (MIE) and lower/upper flammability limits (LFL/UFL) (Maragkos and Bowen, 2002), which are frequently studied in gaseous materials. For combustion, simple scenarios of a flame front traveling through the flammable mixture are not applicable to aerosols, for fuels are continuously evaporating from aerosol droplets to sustain the flame. Therefore, the heat release rates of flash fires from aerosols are expected to be significantly higher than that of fires from vapor mixtures, which may result in more severe damaging effects to the surrounding areas (Lian, Ng, Mejia, Cheng, and Mannan, 2011). Due to the complexity of the mixture, analyzing these indicating parameters has become difficult. There is no strictly defined terminology to describe aerosol flammability. The droplets interact with each other as well as the surrounding air. Energy transfer rates differ among liquid droplets, evaporated vapors, and the surrounding air; droplet evaporation rates differ in various locations, with respect to the relative distance of the spraying source. The combustion is also a multi-stage process including droplet heating, droplet evaporation, vapor ignition, flame formation, flame sustenance, and flame propagation. Each stage of the combustion process may be affected by spatial distribution of fuel droplets, local concentration at the flame path, and stability of fuel feeding rates (Abramzon and Sirignano, 1989). Based on these factors, it is concluded that a clearer and more complete definition and a more referable tool for aerosol fire hazard characterization are needed for loss prevention in the process industries.

There are several published works on aerosol flame front propagation or expansion regarding flame diffusion, droplet suspension, and fuel vapor pressure (Lian, Mejia, Cheng, and Mannan, 2010; Lawes and Saat, 2011; Nomura, Kawasumi, Ujiie, and Sato, 2007). The macroscopic behavior of an aerosol system shows a special flame development mechanism; flame propagation speed and flame diameter are highly influenced by droplet size and volumetric concentration (Lian, Mejia, Cheng, and Mannan, 2010). There is a lack of study focusing on predicting the "flammability limits" in terms of concentration to find the region of combustible conditions. In an early physical phase study, Eichhorn (1955) made a distinction between mist (aerosol) flammability and other physical states as shown in Figure 1. The diagram shows the dew point curve cuts through the vapor-liquid phases. The upper and lower limits are relatively clear of vapor. However, in the aerosol region, the limits are unclear and not well documented or evaluated thoroughly. Flash point is not a clear limiting value for mists. This diagram has been analyzed, modified, and reused throughout the field, but the mist segment remains unclear.

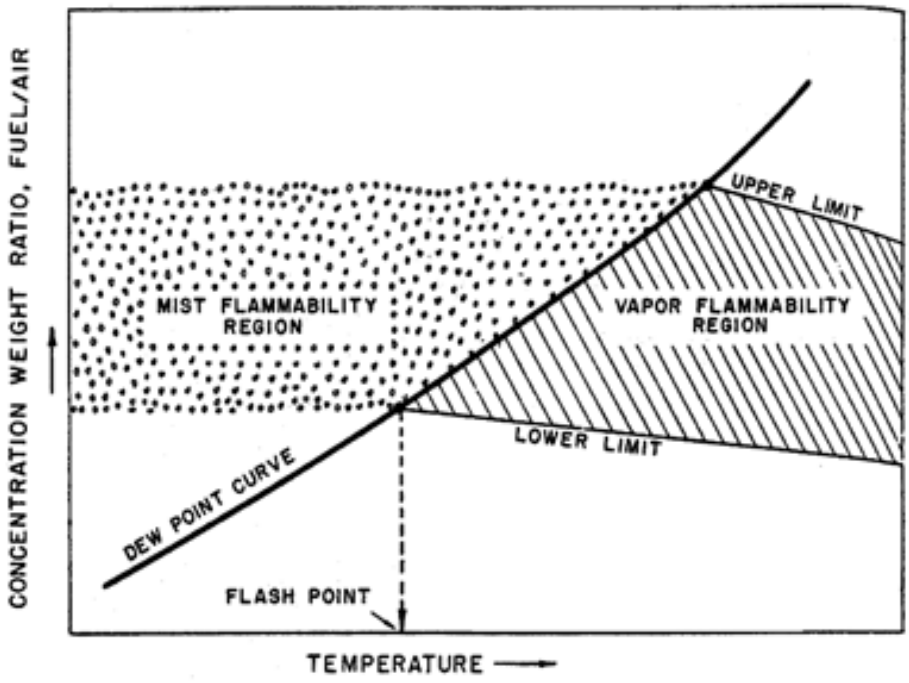

Figure 1. Flammability Diagram of Different Physical States at Fixed Pressure, Eichhorn (1955).

The concept of ignitability was introduced by Aggarwal and Cha (1987) and Aggarwal and Sirignano (1984), explaining that aerosol ignition and combustion behavior occur due to statistical performance rather than deterministic phenomenon. Generally, the flame formation frequency, defined as the successful global flame appearances divided by specific times of ignition attempt, is a point factor used to show the tendency of an aerosol flammability region in a transitional way between "being ignited and form exact flames" and "not ignitable." The reciprocal of the flame appearance frequency, ignition delay time, is another significant indicator of ignition analysis for a better understanding of the time lag after ignition until a global flame forms. Following the logic to introduce

the concept and describe the group behavior of aerosol droplets, a statistical diameter description should be defined. Sauter Mean Diameter (SMD) is the droplet size characterization unit applied to this study. The equation is:

$$D_{[3][2]} = \frac{\sum_{i-1}^{m} D_i^3 \Delta n_i}{\sum_{i-1}^{m} D_i^2 \Delta n_i}$$ (Lian, Mejia, Cheng, and Mannan, 2010)

where D_i and n_i are droplet diameter and the number of the droplets, respectively.

The mean diameter is a value of surface area moment. Similarly, there are other statistical mean diameters such as $D_{[N]}$ with under/within N% of the total droplets in the group of measurement having the average droplet size. To apply the statistical analysis to research, Fritsching (2005) has explained thoroughly the atomization of the droplets through spray, and there are clustering, evaporation, liquid bindings, and other forces which may affect the individual droplet state. The comparison of change among these statistical droplet sizes will be discussed in the results of the study and will show why SMD can be one of the most stable, referable, and well-implemented sizing units in aerosol system studies.

In summary, previous researchers have indicated various aspects of aerosol hazards. The formation from different scenarios, the influence of fuel property and droplet profile on flame propagation, and tools for aerosol characterization are well developed. However, the connection between aerosol formation and combustion, or the ignition condition requires more discussion and tests to complete and define. Thus, this paper intends to propose a systematic approach and obtain experimental data in order to draw the range

of the aerosol flammable region. The flammability data were obtained after adopting the methodology from the research by Lian, Mejia, Cheng, and Mannan (2010) to generate aerosol by electro-spray with specific control of droplet diameters, apply non-intrusive laser particle analysis to characterize the droplet sizes and concentration distribution, ignite the aerosol system to test the ignitability, and observe the combustion flame development. After achieving the experimental information, a useful, organized flammability reference on heat transfer fluid aerosol system was developed. The methodology and experimental setup may also be available to offer a framework on other studies of aerosol types, providing a potential way to analyze the flammability of this complicated physical system, and prevent hazards from industrial or lab scale liquid handlings during an accidental release (Huang, Li, and Mannan, 2013).

In addition to the flammability criteria of high flash point fluid aerosol, the combustion process of flow system aerosol was also of our concern. Previous studies paid attention to the flame propagation and expansion (Lian *et al.*, 2010; Lawes and Saat, 2011), which are the external effect of the burning behavior; this research took a closer look into the inherent process of combustion, *i.e.* the sustainable flame appearance and propagation. The special three-stage combustion of fuel aerosol flame was observed, but has not yet been analyzed in a matter of temperature distribution, energy transfer, and the relation of aerosol properties with ignition source energy. Considering all the factors influencing the luminous flame appearing in aerosol, a better modeling tool is truly needed. To better understand the combustion process, a deeper look into aerosol formation procedure and its effects is also necessary. Electrospray methods can help experimentalists control the

droplet sizes, but the charges accumulating in aerosols may also cause turbulence in the results of combustion and ignition initiation. Thus, the side parameters are to be analyzed to make the research a complete logic. Combining with the studies on aerosol formation and flame propagation, a clear framework of aerosol fire and explosion prevention can be launched properly.

This research has four objectives, which are as well the following chapters of the dissertation:

1) Formation control of heat transfer fluid aerosols (from three commercial fuels) by electro-spray. This objective is to make the sample system well-defined: fuel selection (compounds with high flash points which are stable in regular conditions), and droplet dispersion and sizing (by Laser Diffraction Particle Analysis). This is also a verification of previous study on the best method to control droplet sizes in flow system aerosols.
2) Systematic ignitability tests of aerosol system. This is the approach to obtain a useful reference which can explain the flammability of aerosols in terms of droplet size, concentration, *etc*. The result shall be able for the initial screening during hazards evaluation on high flash point fuel aerosols.
3) Combustion process analysis of aerosol. This objective is focusing on the burning behavior after the droplets are ignited, including flame development mechanism, ignition delay time (global flame formation time), and flame propagation. This is the

consequence analysis portion of aerosol fire, while mitigation can be considered using the results.

4) The fundamental study of aerosol combustion research. Electrospray is an innovative method for smaller scale analysis for aerosol combustion, while understanding of the charge impact on aerosol shall be discussed as the accessibility to scale up for practical applications. This objective is to offer deeper thoughts on the electric field, energy material properties, and the related industrial-scale ignition occurrence. This is the objective to improve the fundamental research on aerosol, and to offer a better frame work on future research.

The overall study flow chart can be simply shown as Figure 2.

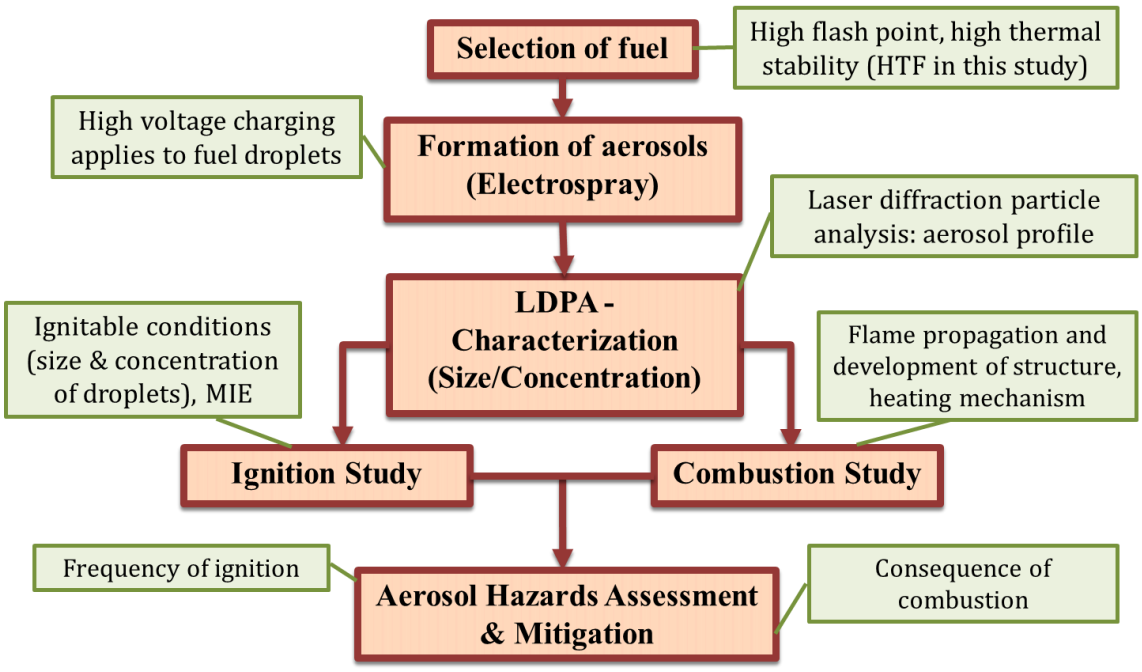

Figure 2. The schematic flow chart for the study overall

CHAPTER II

FLOW SYSTEM AEROSOL IGNITABILITY

Background and Problem Statement

Aerosol studies have been carried out for years, and the comparison of other non-homogeneous system fire hazards is frequently discussed. However, due to the uniqueness of flow systems, liquid-air mixture aerosols have not been brought into general, systematic studies yet. The complexity of the ignition condition, or the "flammability," remains unsolved. The major problems are the definition of combustible concentration range, droplet sizes, and other possible factors. The ultimate goal is to generate a useful tool which can be used to provide adequate prediction to handle fuels, especially high flash point liquids which are considered to be safe under the critical temperature. In this chapter, we are able to offer a better definition of a flow system aerosol, which reflected the practical case on pilot plant level liquid handling and operating; then a series of testing will be applied using relatively recent methods developed to analyze droplets in controlled electric field.

Methodology

Selection of Fuel

The materials we chose for the study are three kinds of heat transfer fluids. The properties are listed in Table 1. As we can see from the table, the heat transfer fluids are widely used in process industries due to its thermal stability of high flash point and high viscosity. These heavy-oil extracted products can be considered as a thermally stable element while dealing with process fluids of more unstable, flammable materials. However, due to the complication of aerosol, the physical property may change after the fluids changed from liquid to mist. The criterion we used to select the experimental materials is a flash point to be higher than 150˚C and with smaller reactivity in regular operating conditions. This is the topic we are interested in. The experiment would be set in room temperature, atmospheric pressure, and regular humidity. We attempted to imitate the NTP operation circumstances in facility and idealized the environment, trying to get more out of the material property change and the detailed reactions.

Table 1. The physical properties of Heat Transfer Fluids (Lian, Mejia, Cheng & Mannan, 2010)

Heat Transfer Fluid	D-600	P-NF	PHE
Appearance	Crystal clear	Transparent	Transparent pale yellow
Composition	Paraffinic hydrocarbon	Hydrotreated mineral oil	Hydrotreated heavy paraffinic hydrocarbon
Recommended	121-315˚C	49-343˚C	66-316˚C
Average Molecular	372	350	445
Flash Point	224˚C (435˚F)	174˚C (345˚F)	227˚C (440˚F)
Fire Point	240˚C (464˚F)	196˚C (385˚F)	260˚C (500˚F)
Density	0.850g/ml	7.25 lb/gal	7.22 lb/gal
Viscosity	32.1 cSt as	11.0 cSt at 40˚C	40.25 cSt at 40˚C

Formation of Aerosols System: Electrospray

The fuel is contained in syringes for spraying use. The method we used to produce aerosols from liquid is electrospray, which is mainly the application of high voltage (up to 10 kV) onto the droplet streams, making the droplets charged and form minute droplet streams, which is the aerosol state we defined. This method was taken from a study of Mejia, He and Cheng (2009), introducing the electric control of the fine distribution of aerosol droplets. The size and space distributions can be varied by different applied voltages and liquid flow rate. The liquid meniscus at the outlet of each capillary took a

conical shape, *i.e.* cone-jet mode under the influence of the electric field between the nozzles and the grounding electrode (Lian, Mejia, Cheng, and Mannan, 2010). The distance between the grounding electrode (attached to a metal mesh) and the nozzle fronts is 2.5 inch and remains the same condition for every test.

The electrospray setup consisted of a function generator (Stanford Research System, Ds-345) to generate the voltage signal; there was a high voltage amplifier (Trek Inc. 610E) attached to achieve the applied voltage to attempted level. An electric wire was connected the high voltage amplifier output to the top of the nozzles, clipped onto the metal side of nozzles. PNF fluid was pumped from 10 infusion syringe propellers (KDS 220). The size of the syringe was 2.5 mL. The nozzles used in the experiment are stainless steel capillary tubing of 0.01 i.d. and 0.02 o.d., with 10 nozzles lined up on the metal rack to pour flows down to the mesh for the electric field formation. Figure 3 shows the schematic electrospray system used.

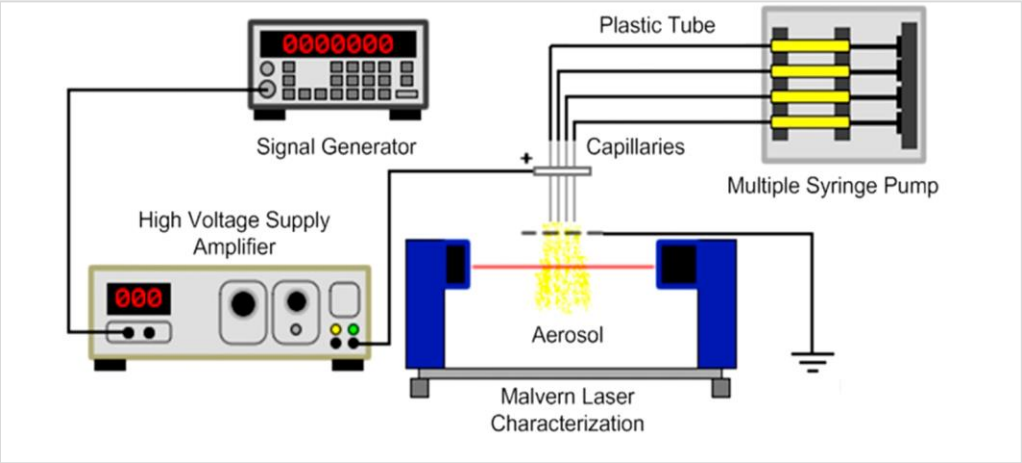

Figure 3. Schematic electrospray system (Lian, Mejia, Cheng, and Mannan, 2010)

Particle Characterization

Properties of the spray generated must be constantly monitored throughout the ignition process. Non-intrusive laser technique is an important and effective tool in this regard (Barth 1984; Hamidi 1986a). Malvern Spraytec for spray/aerosol droplet size and concentration measurements applies laser diffraction techniques, which is called Laser Particle Diffraction Analysis (LDPA). It relies on the fact that particles passing through a laser beam will scatter light at an angle that is directly related to their size. As particle size decreases, the observed scattering angle increases logarithmically. Scattering intensity is also dependent on particle size, diminishing with particle volume. Mie scattering is the background theory of this analysis. The measurement is shown schematically in Figure 4.

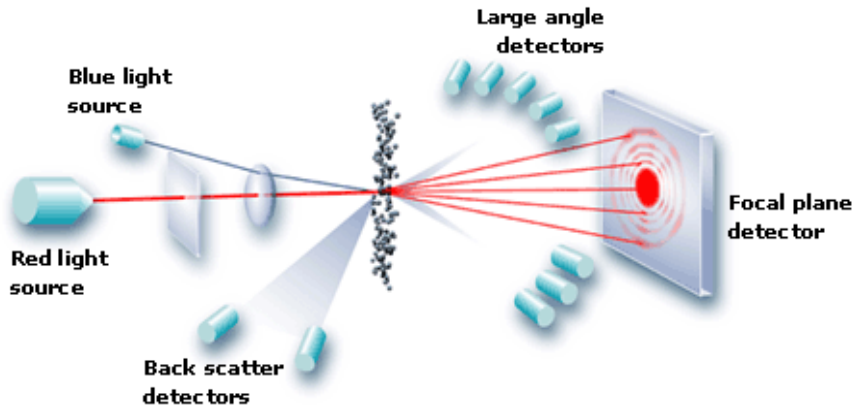

Figure 4. Schematic figure of Mie scattering in tests (Lian, Mejia, Cheng, and Mannan, 2010)

The Malvern SprayTec Laser consists of a 2mW Helium-Neon laser tube and a ring diode detector. The laser beam is a collimated monochromatic beam of wavelength 780-662 nm and 1.8 mm in diameter. Intensities of the diffracted light on the diodes in the detector are converted into drop-size data by a computer. The laser technology realizes instantaneous and non-intrusive measurements on characteristics of aerosol droplets suspended in the air, without specific sampling operations, which will change the existing conditions of the droplets and interrupt the test process, resulting in measurement data not reflecting the real in-situ conditions. The Malvern Spraytec instrument has been registered and approved for use in the lab research by the Environmental, Health and Safety Department of Texas A&M University. The software was licensed and upgraded with the subscription of Malvern to ensure the quality of measurement. There are many other ways of droplet size analysis; however, from previous research data we observed that Spraytec provides most widely-used reference information on droplet diameter distribution.

Testing Chamber of Aerosols

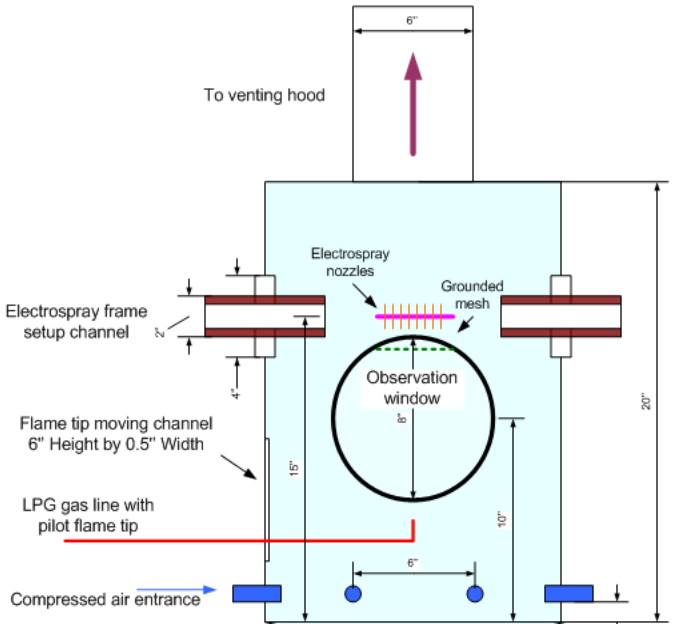

Figure 5. Aerosol formation/igniton chamber

The aerosol ignition chamber is shown as Figure 5. Basically, the system is setting up a plastic glass hood box around the electrospray device, making sure that the combustion procedure is controlled in a region from which we can easily calculate the volumetric concentration, reaction system parameters, and prevent the aerosol accumulation on lab desks or ground. A rack is designed in kind for the box to stand on the corner of the lab, providing a good position for the laser device, air supply, and other equipments to be put in the space we have.

The ventilation tubing attachment is at the top of the chamber, being connected to an aluminum tube and linked to the ventilation system in lab. There are three access points

to the interior of the chamber, created by two sliding doors and one handled door. We use these entrances to set up or remove the equipment needed. The two sliding doors are specifically for laser observation and camera capturing. There are eight air input nozzles attached to the bottom side of the box, providing enough air for later combustion.

Ignition of Aerosol

Aerosols introduced into the chamber will be ignited by an open flame. The third series of openings on the chamber wall will be used to accommodate the relevant components as shown in the above section.

For the open flame as ignition source, liquid propane gas, or LPG, is used as the fuel gas. It flows through a 1/8-inch ID stainless steel tubing. The tubing protrudes into the ignition chamber through the same opening for the spark electrodes. The inside end of the tubing is bent 90° up as the flame tip. LPG gas will flow upwards before ignition upon exiting of the tubing. The flame length is adjusted by controlling the LPG flow rate through a flow regulating valve on the LPG flow line.

The flame will be captured by a high speed camera with a resolution of 512*512, 1000 pictures per minute. This accuracy helps us take better control of when and where the luminous flames appear in the combustion process, and how they propagate along the stream lines. We will be able to calculate flame appearance numbers from the captures and compare them with laser signals while the flame is formed.

Connecting all the setups, Figure 6 shows the whole experiment area for aerosol testing.

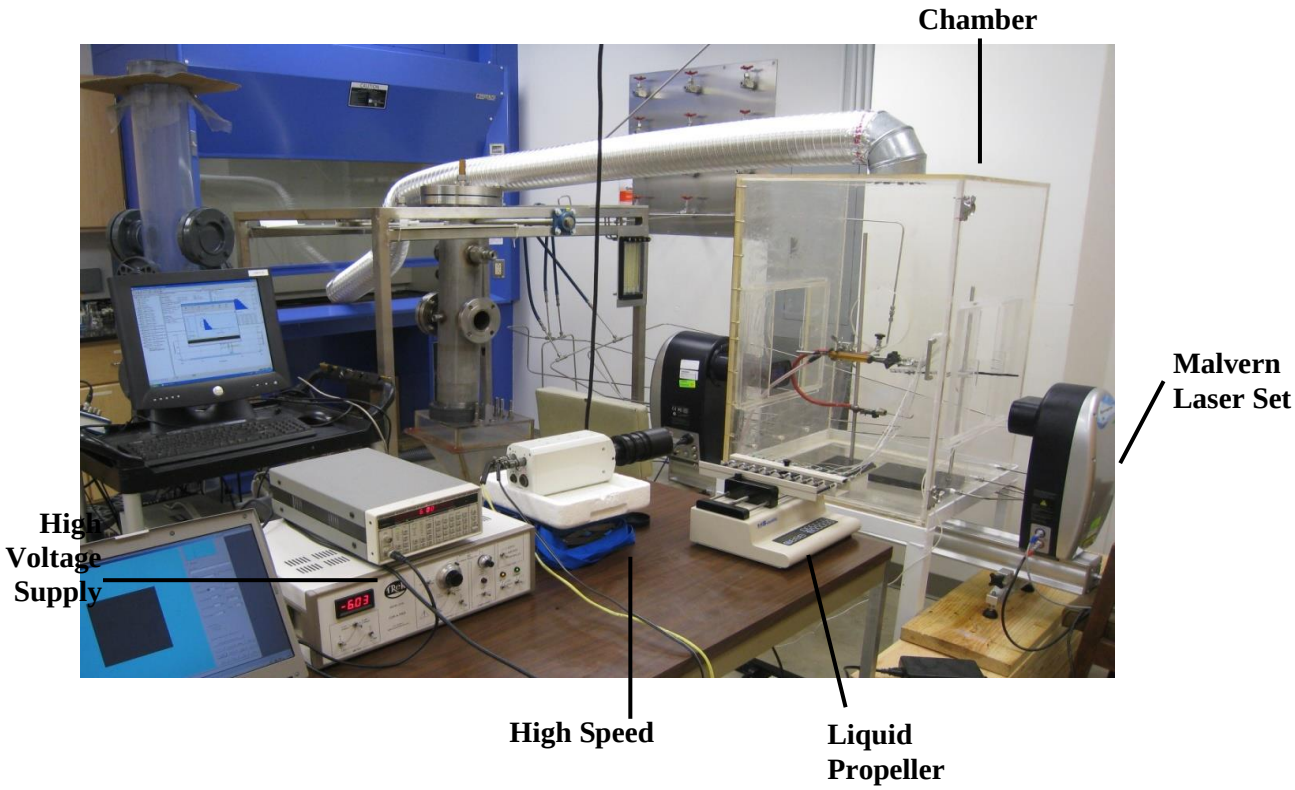

Figure 6. Experiment Setup overview. (Huang, Li, and Mannan, 2013)

Experiment Steps

We planned to use the experiment setup to produce heat transfer fluid aerosol for ignition tests. The startup steps and measurements are listed as the following.

Start-up process:

(i) Start the compressed air flow line and open the compressed air supply; the air flow rate is controlled by rotameter. Start the electrospray system: aerosol droplets are generated and flow downward through the ignition chamber.

(ii) Start the Malvern SprayTec laser diffraction particle analyzer and the computer for measurement and recording of the aerosol droplet size data within the ignition chamber.

(iii) Step (i) and (iii) go on for 30min until properties of aerosols droplets in the ignition chamber become stable (judgment based on data from SprayTec). Care should be taken to ensure that the aerosol purge line and the lab's venting hood are working properly. The temperature and pressure within the ignition chamber should also be kept constant.

Ignition test process:

(iv) For the open flame ignition, stop the compressed air flow, and connect the LPG gas flow tubing with the flame tip to the chamber; open the LPG flow control valve, and ignite the LPG gas upon outlet of the flame tip. Use the regulating valve on the LPG gas flow line to control the gas flow rate and the open flame length. Restart the compressed air flow.

(v) When the open flame becomes stable, restart the electrospray fluid flow, and start the stopwatch. Upon aerosol ignition and appearance of combustion flame, stop the stopwatch and the aerosol flow. Record the time value from the watch.

(vi) Test of ignition behavior of aerosols with different droplet size and concentration values: change the aerosol droplet size by adjusting the electrospray syringe pump flow rate and electric voltage on the spray

nozzle. When the aerosols droplet properties become stable, steps in (iv), (v), and (vi) are followed to get the ignition frequency values for aerosols of new properties with different spark generation settings.

(vii) Analyze the droplet size and concentration with the changing of experiment parameters, understand what extent of the control we have over the setup, and we can proceed to reproduce and adjust the experiment for other sets of times for accurate results, so that we will be able to determine the flammable region.

Results and Discussion

Aerosol Formation and Droplet Characterization

The characterization of droplets was applied with LDPA testing of the fuel streams produced from the nozzles. The instant measurement result, which was a stable case (the steady droplet sizes after the droplets had formed and settled and taken before ignition), is shown in Figure 7a as an example. The software derived the value from the laser device, calculated periodically, and developed an instant histogram showing the droplet size distribution at the exact time. The sample table under the evaluation histogram is a detailed number value for the user's reference on actual percentages that droplets with various diameters occupied. Figure 7b shows the derived parameter of the $D_{[X]}$ values as well as SMD. From these diagrams it can be seen that aerosol droplets showed good mono-dispersity, and the internal distribution of droplets at one test can form a narrowly ranged normal distribution shape. The range was within 50-100 μm. If statistical analysis

is implemented either within equipment level or numerical studies, the data are capable of the random distribution estimation.

a.

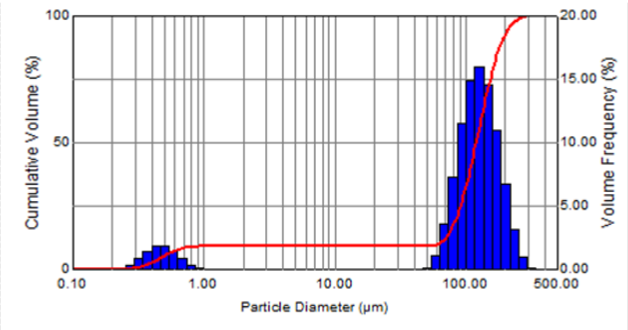

b.

Title	Value	Average	σ	Min	Max
Trans (%)	99.8	99.8	0.01316	99.8	99.8
Dv(10) (µm)	61.2	83.6	2.18	61.2	87.89
Dv(50) (µm)	119.4	127.4	2.639	119.4	145.5
Dv(90) (µm)	188.5	193.6	12.92	183.4	536.5
%V < 10µ (%)	9.085	0.0543	0.6184	0	9.438
D[4][3] (µm)	119.7	134.1	3.903	119.1	210.3
D[3][2] (µm)	4.717	108.3	10.78	4.717	126.5
Cv (PPM)	0.004532	0.1097	0.04088	0.004105	0.1452
Span	1.066	0.8635	0.08733	0.7825	3.199

Averaging period = 60.0 (s)

Figure 7. The Malvern Spraytec Testing Results Example. (a) The instant droplet distribution histogram. (b) The derived value table for measurements. Value: the directed measured value according to laser signal into the captured droplets in the testing region; Average: the mean value of the -60 seconds counting from this time point; σ: the standard deviation; Min & Max: the minimum and maximum values occuring within the measurement until this captured point. (Huang, Li, and Mannan, 2013)

As the analysis continued, the relations of droplet size distribution and volumetric concentration values were derived. The manipulating factors are (1) applied voltage and (2) liquid flow rate. By changing the applied voltage, the droplet size as a whole group behavior will deviate. The flow rate, though not directly, affected the volumetric concentration of the testing space. However, with the similar fuel feeding rate but different applied voltage, the droplet density would change in a manner with no specific tendency. For example, when the flow rate increases from 1 mL/s to 2 mL/s and 8.5 kV is applied to the droplets, the resulting concentration is increased from 0.23 ppm to 0.52 ppm; however, increasing the flow rate to 3 mL/s resulted in a concentration of 0.36 ppm. This may be due to the electric field distribution while different amounts of fuel are being charged, so that there were various cases of concentration readings in the laser testing region. This phenomenon of concentration instability, however, appeared to be occurring in every re-testing process. For the fine reproduction of the tests, when the experimental conditions were controlled to make the experiment processing in the specific, limited conditions, the errors produced within each test should be negligible. The results of applied voltage and flow rate changes are shown in Figure 8.

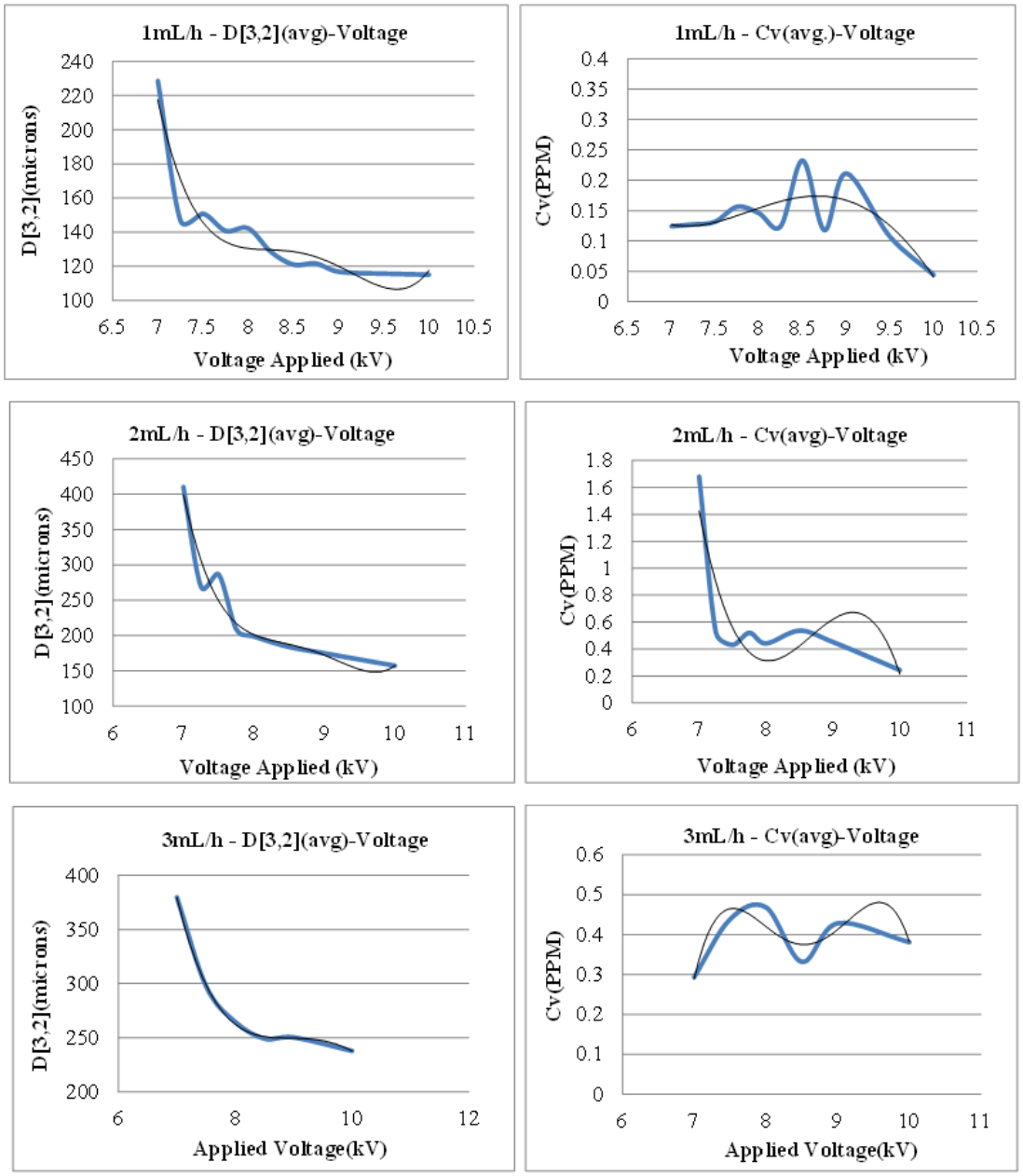

Figure 8. Droplet size/volumetric concentration changes according to applied voltage.

(Huang, Li, and Mannan, 2013)

From the data results, it can be seen that droplet size has a tendency to decrease as applied voltage increases; however, the volumetric concentration was not similarly stable for this tendency. The reason should be the unstable condition; the charged stream flowing in a twisted manner rather than straight lines, as well as the droplet size change within the same liquid feeding rate could result in the concentration reduction or deviation.

After the initial formation of aerosol droplets became stable, an ignition source was applied to the system. With the ignition taking place, the signal of the laser detection was highly affected by the flame; also, the droplets in the stream were rapidly evaporating as the flame burned through the droplets. The process begins with aerosol production, and the huge peaks were the combustion region; each peak is a flame produced by entering or exiting the laser detection area. After the ignition source was removed, the flow quickly returned to the original state; however, the droplet sizes were slightly smaller than before ignition.

Except for SMD values, the group behavior could also be reflected from other $D_{[X]}$ values. In the testing device, settings used were X = 10, 50 and 90 to evaluate the group distribution. As mentioned above, the distribution was close to random, and more narrowly focused on specific high peaks which could be considered as the representative value of droplet size. Figure 9 shows the timely change process of those statistical droplet sizes. The SMD values changing with applied voltages are shown in Figure 10 to

display the influence on the significant diameter used to describe the liquid droplet size in general.

a.

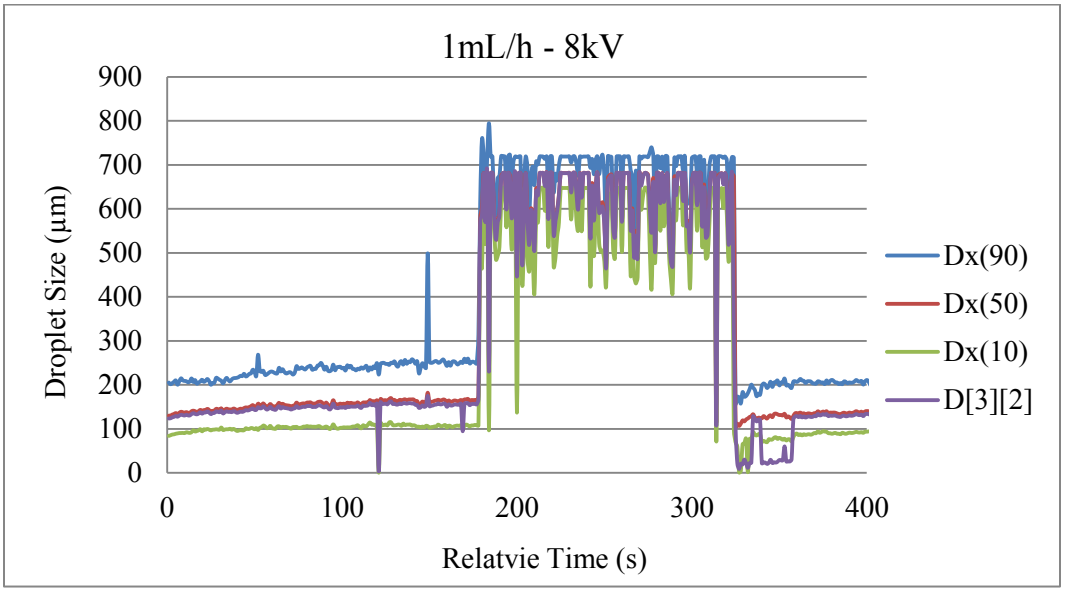

b.

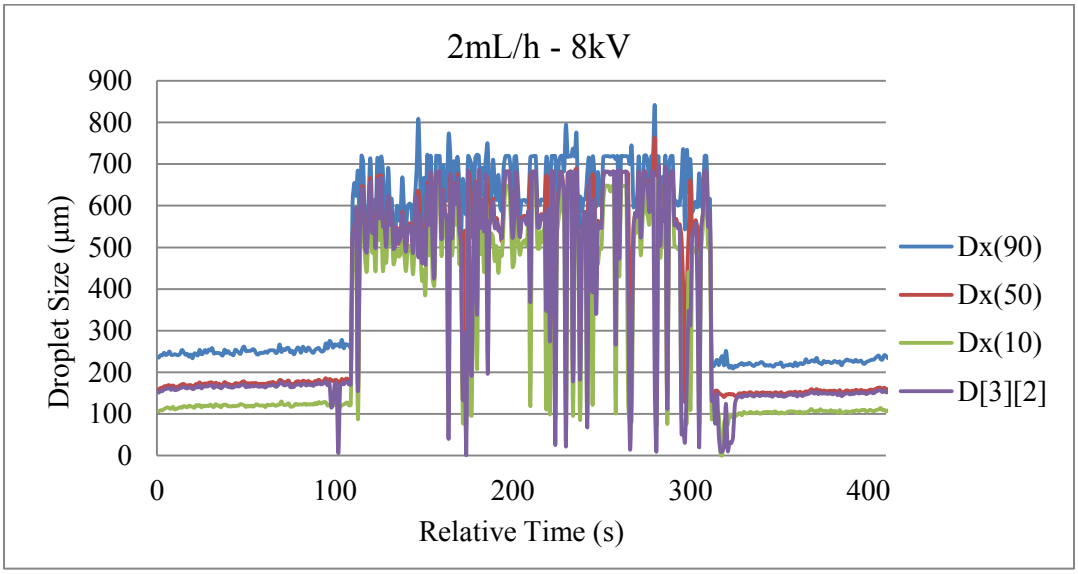

Figure 9(a-b). Droplet size timely changes. (part of P-NF results as example; 1mL/h, 2mL/h, 3mL/h liquid flow rate during syringe propelling with 8 kV applied). (Huang, Li, and Mannan, 2013)

c.

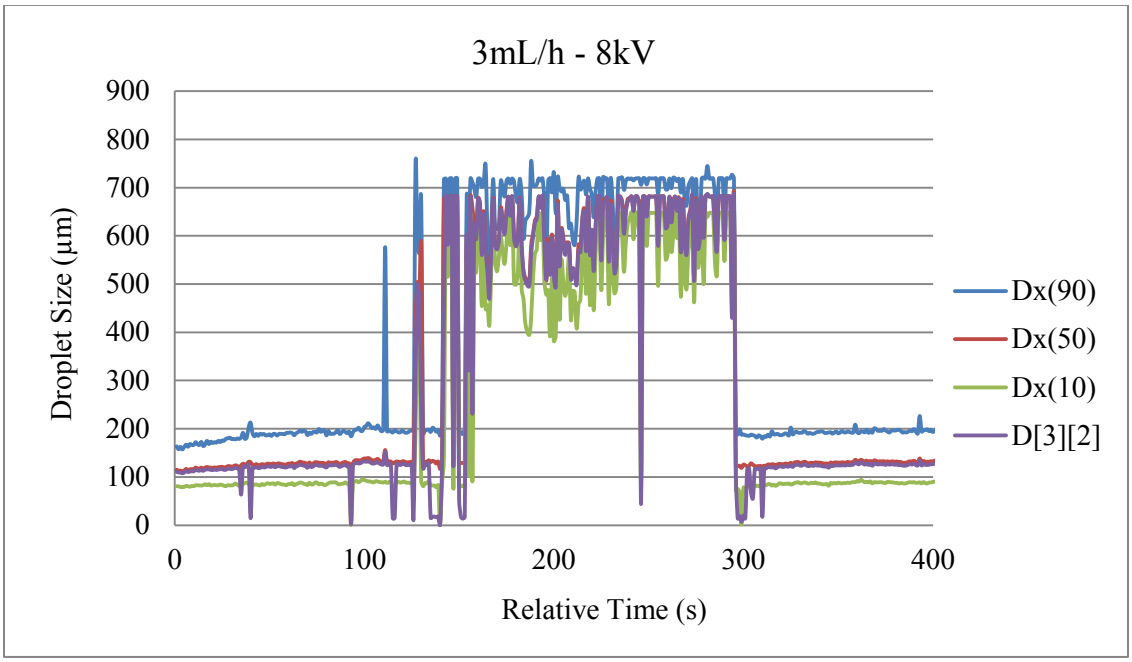

Figure 9(c). Droplet size timely changes. (part of P-NF results as example; 1mL/h, 2mL/h, 3mL/h liquid flow rate during syringe propelling with 8 kV applied). (Huang, Li, and Mannan, 2013)

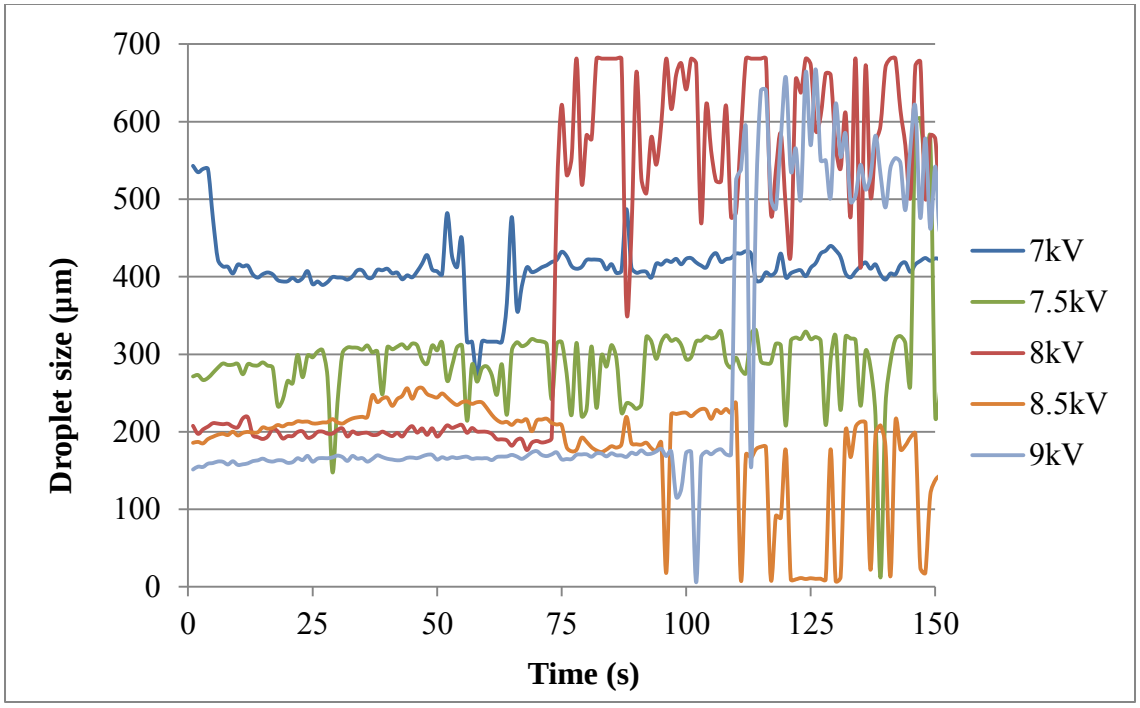

Figure 10. Droplet size timely changes. (Sauter Mean Diameter among different applied voltages; flow rate 3mL/h)

Comparing these four statistical droplet size values, the $D_{[50]}$ value showed that the droplets are in good mono-dispersity. At the beginning, with a droplet diameter range of ~150 µm, SMD and $D_{[50]}$ are close in numerical values, which also showed the narrow deviation among the produced droplets. When it came to the combustion, the signals of all values were approaching a similar region; however, after the aerosols were taken out of flame influence, $D_{[50]}$ and SMD were also the least changed values. The two diameters decreased about 2.3 – 4.1% (average value of each test with the same applied voltage and flow rate), while the decreasing of $D_{[90]}$ and $D_{[10]}$ deviated by closer to 5.0 – 6.6%. The reason is possibly due to the larger droplets within each test having unstable

droplet size distribution right after the combustion (compared to the beginning of the test), since the heat produced by ignition and flame propagation was still influential to the new aerosols in the testing space within 30 seconds after the former combustion was over. The burned droplets and new feedings tended to collide and coalesce, so that the droplet sizes were in a relatively chaotic state while measuring. Thus, the range of droplet size would be abnormally large or small for a short time, which was the source of possible deviation for the aerosol system to show specific trends in $D_{[90]}$ and $D_{[10]}$; these were the extreme sides of statistic values leaning close to smaller and larger fractions of group phenomenon. The similar numerical results were observed for D-600 and PHE as well.

The comparison of different liquid feeding rates is shown in Figure 11, with the variation of average concentration and SMDs. The higher feeding rates resulted in relatively high concentrations, while the 3 mL/h case shows the stability of concentration values when droplet size was changed. It can be seen that in this flow rate the concentration change with respect to droplet size is much smaller than the case of 1 mL/h and 2 mL/h. That is, a feeding rate as high as 3 mL/h can result in better control over a relatively constant concentration in each test and may change SMD simply by applied voltages to test the flammable region. The concentration and droplet size with influence on the electric field issue mentioned in Figure 8 shall be reduced more, as the fuel feeding rate is as high as 3 mL/h or higher.

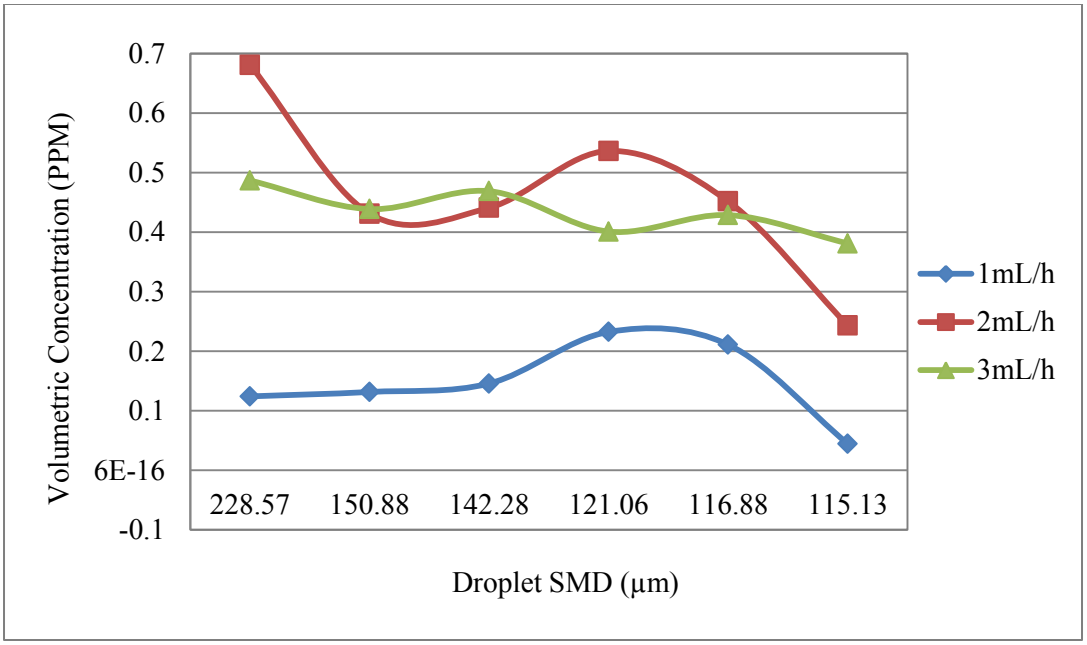

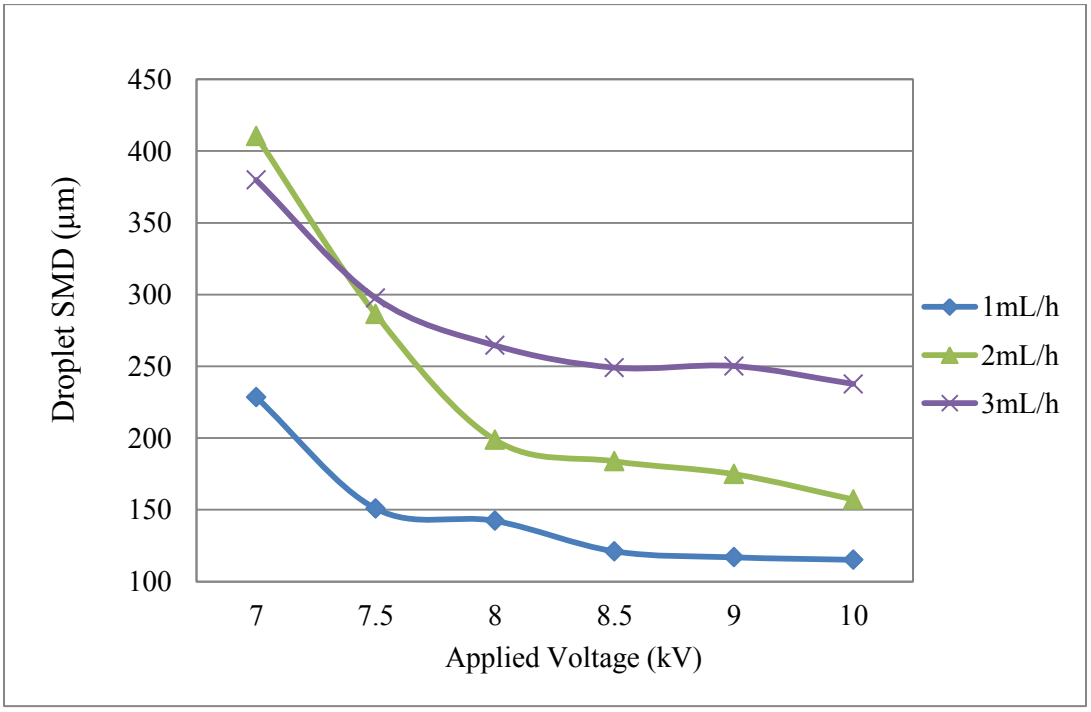

Figure 11. SMD and Cv values among different liquid feeding rates. (Huang, Li, and Mannan, 2013)

Ignitability and Flame Development

After the ignition begins in the aerosol system and the aerosol is available in the combustion conditions, the flame will form and propagate all the way to the top of the spraying point. Figure 12a shows the flame images on some general combustion processes; the large flame (at the bottom of each figure) is the ignition source, or the pilot flame. It can be seen that in lowering the amount of feeding in unit time, the flames tend to only form a series of small flame pieces and go up for a short distance (around 2-3 inches); however, while the fuel feeding was abundant enough with the increasing flow rate, the flame of P-NF aerosols tended to compose a "flame lumen" with evaporated droplets, vapors, and small flame pieces to make a luminous global flame. This is how flame appearance is a determinant of successful aerosol combustion. A successful combustion, as defined in this study, should have the clear, complete flame development of a global flame, and the flame should propagate from bottom to top of the metal meshes.

The flame formed during the process of combustion was analyzed by Peng Lian (2010, Mary Kay O'Connor Process Safety Center interior experiment safety analysis) in the terms of three stages: initial flame pieces, global flame, and quench state. The flame and relevant images are shown in Figure 12b.

a.

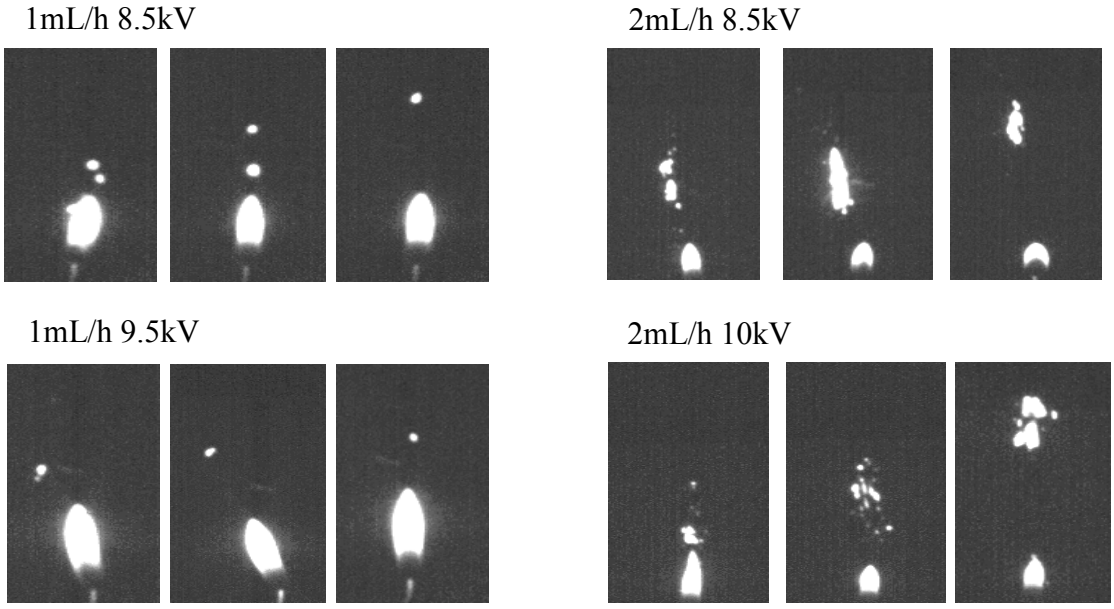

Figure 12(a). Typical, Complete Flame formed within an aerosol system. Flame captured from part of tests in different flow rates [liquid flow rate 3mL/h, Applied Voltage 8.5kV] (Huang, Li, and Mannan, 2013)

b.

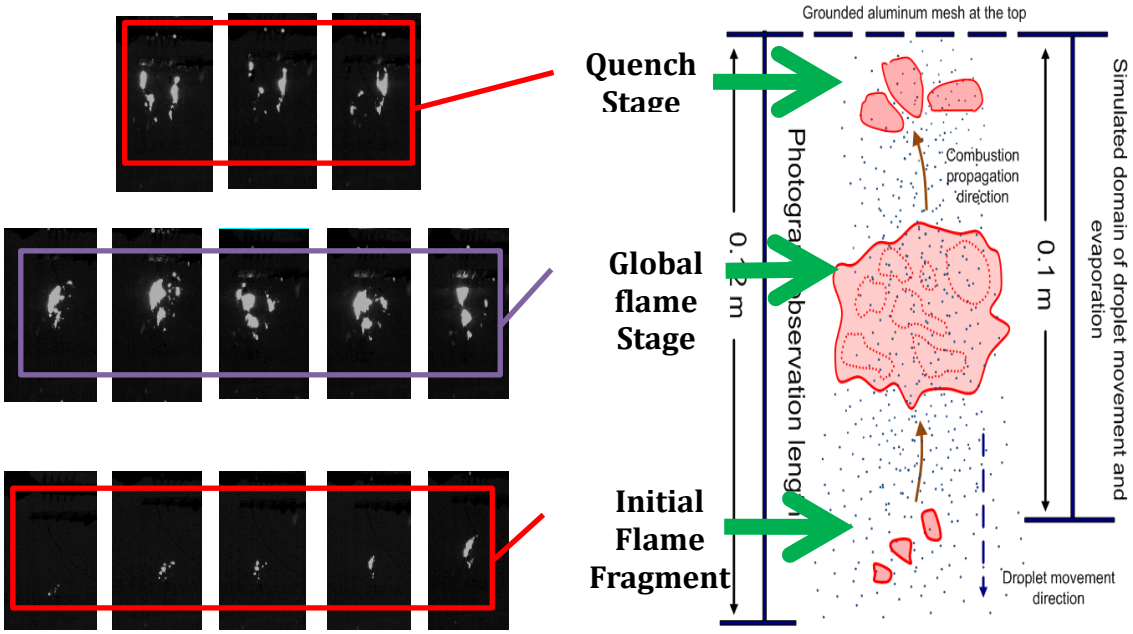

Figure 12(b). Typical, Complete Flame formed within an aerosol system. Flame development stage. (Huang, Li, and Mannan, 2013)

The definition of the flame development is considered to be the fact that five or more flames, following the three-stage process, were formed and captured from the experiment devices during the existence of the ignition source. The "successful" ignition attempt was considered to be under "ignitable" conditions. Table 2 to 4 show the ignitability evaluation with the experimental result analysis.

Table 2. The ignitibility test results of P-NF. (Huang, Li, and Mannan, 2013)

	7kV	7.25kV	7.5kV	7.75kV	8kV	8.5kV	9kV	9.5kV	10kV
1mL/h	No	No	No	No	No	**Yes**	**Yes**	**Yes**	**Yes**
2mL/h	No	No	No	**Yes**	**Yes**	**Yes**	**Yes**	**Yes**	**Yes**
3mL/h	No	No	**Yes**	**Yes**	**Yes**	**Yes**	**Yes**	**Yes**	**Yes**

Table 3. The ignitibility test results of D-600.

	7kV	7.25kV	7.5kV	7.75kV	8kV	8.5kV	9kV	9.5kV	10kV
1mL/h	No	No	**Yes**	**Yes**	**Yes**	**Yes**	**Yes**	No	No
2mL/h	No	No	No	**Yes**	**Yes**	**Yes**	**Yes**	**Yes**	No
3mL/h	No	**Yes**	**Yes**	**Yes**	**Yes**	**Yes**	**Yes**	**Yes**	**Yes**

Table 4. The ignitibility test results of PHE.

	7kV	7.25kV	7.5kV	7.75kV	8kV	8.5kV	9kV	9.5kV	10kV
1mL/h	No	No	No	**Yes**	**Yes**	**Yes**	No	No	No
2mL/h	No	No	**Yes**	**Yes**	**Yes**	**Yes**	**Yes**	**Yes**	No
3mL/h	No	No	No	**Yes**	**Yes**	**Yes**	**Yes**	**Yes**	**Yes**

The ignitibility test results provided the criteria of the flammability reference. This is the region of applied voltages and flow rates that result in a clear idea of "flammable conditions" for further analysis. For lower flow rates of liquid feeding, the ignitibility tended to show successful attempts near higher voltages, which can produce smaller droplets and can be ignited at lower concentrations; on the other hand, when fuel was fed at higher rates, the aerosol formed tended to be ignited over a wider range than that of lower feeding rates. Olumee, Callahan, and Vertes (1998) mentioned that substantial amounts of charges associated with the droplets, their collision, and coalescence are considered unlikely even at large particle densities.

Here in the higher concentration levels (from 2 mL/h – up to 3 mL/h), even larger droplet size particles could be ignited due to the balancing between droplet diameters, tendency of motion during spraying or coalescence, and concentration of the mixture during the combustion process. The reading value of larger droplet sizes with smaller applied voltages was likely to be the coalescence phenomenon; however, in highly-charged cases with the higher applied voltage conditions, this effect was more unlikely to happen due to the expansion of the spraying column (Ganan-Calvo *et al.*, 2006). Thus, with lower voltage, not only were droplet sizes larger, but also due to coalescence, there were less chances for the aerosol under those conditions to ignite and sustain flame formation. Comparing the three different fuel properties, the range of successful ignition within our setting criteria increase as the carbon number increases. The heavier hydrocarbon has the essential tendency to have a wider range of ignition condition. With

a higher voltage applied in higher feeding rate of fuel, the small and abundant droplets offer a stronger support for the flame appearance.

Flammability Table of Aerosol Flammable Region

After 25 sets of tests performed with better control (achieved from the concepts gathered in previous sections) of equipment either in droplet sizes or concentration, organized tables of the heat transfer fluid aerosol flammable regions were produced and are shown in Table 5 to Table 7. The tables were obtained from the results measured and calculated from the computational equipment connected to the measuring systems. The statistic accuracy is based on the droplet sizing deviation achieved from experiment results. The purpose of the study is needed for analysis on liquid handling. After the data from the detection of hazardous leaks are obtained, the droplet size usually has a wider range of distribution compared to electro-spray results. The updates on the system shall be considered when a new kind of fluid and process are being used.

Table 5. P-NF Flammable Region Table. (Huang, Li, and Mannan, 2013)

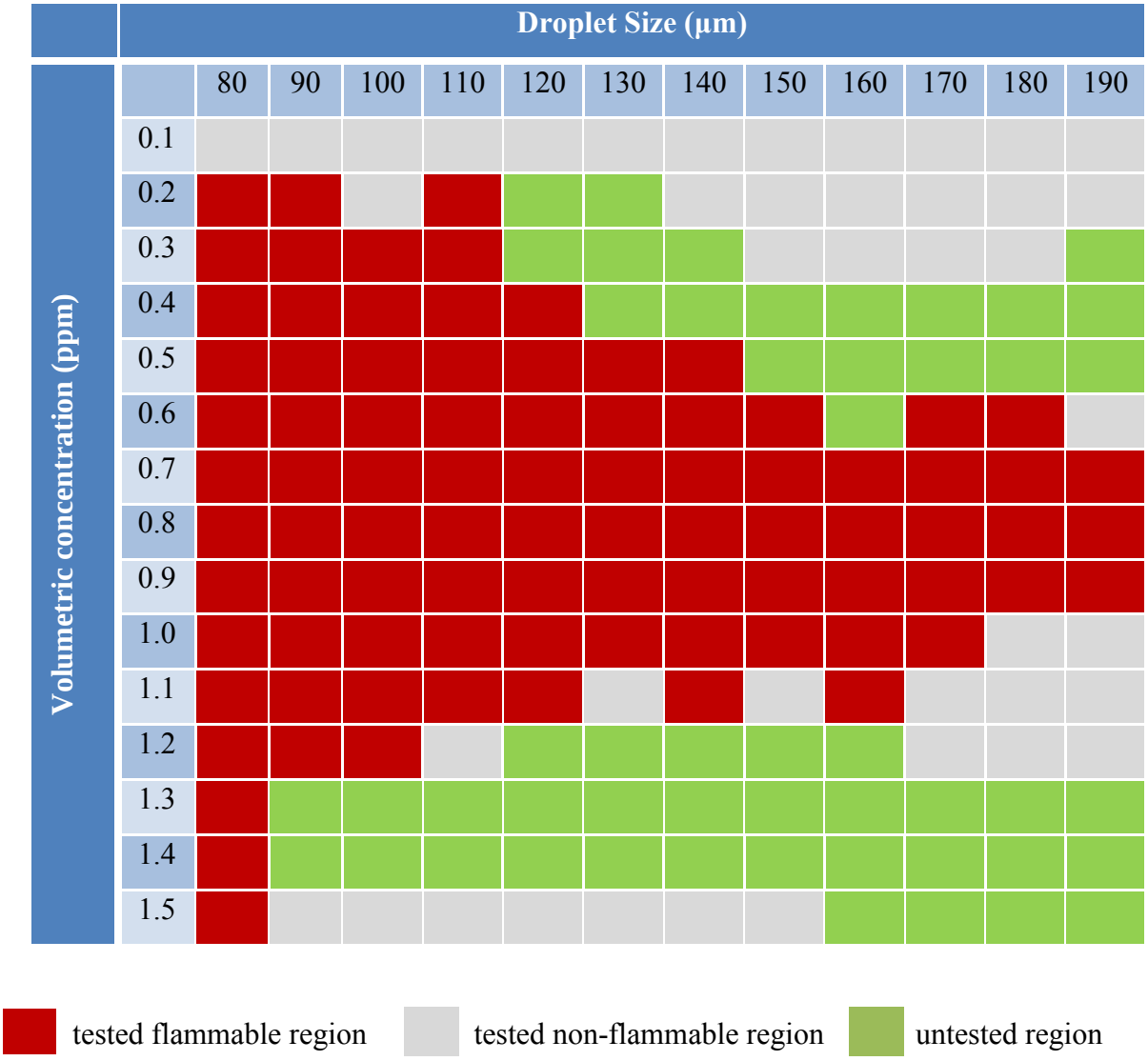

Table 6. D-600 Flammable Region Table.

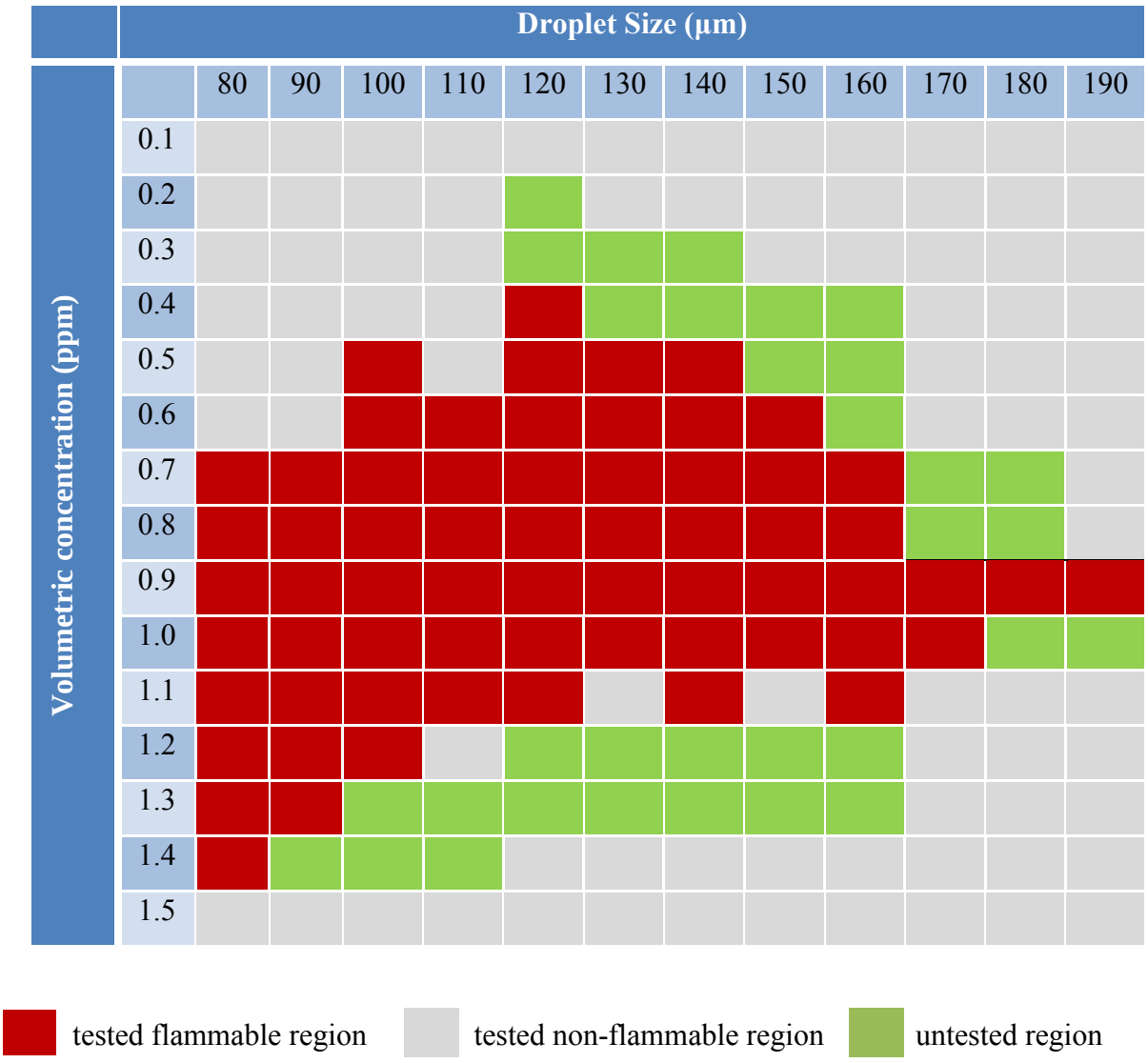

Table 7. PHE Flammable Region Table.

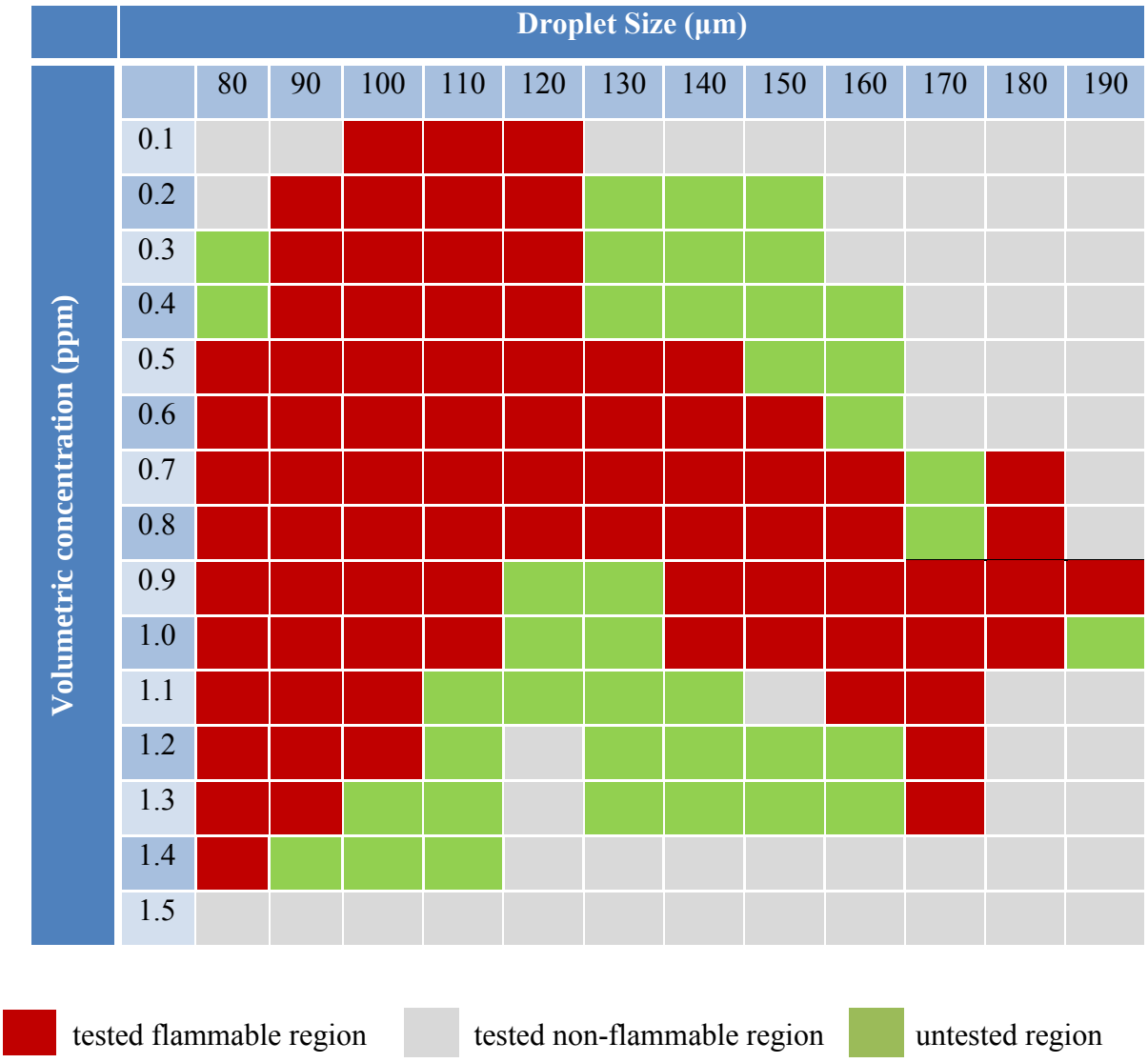

The flammability of aerosols is described in Tables 5-7 by both concentration and droplet size, assuming an ideal mixing case in the experimental setup. The experimental conditions were averaged as a flow rate of 3 mL/s, and an applied voltage of 8.5–9.5 kV. This offered a lab scale reference for further study in aerosol flammability. The fuel types still affect the potential flammability results, but for hydrocarbons with similar

thermal properties to heat transfer fluid (mineral oil and these operating conditions applied well. It is possible to see from this table that smaller droplets still gave a wider range of flammable concentrations.

The droplet sizes we were able to produce in our setup thus far were 80-110 μm droplets that could be ignited within a 0.9 – 1.3 ppm concentration range. For larger droplets, such as those larger than 170 μm, we achieved a range of only 0.2 ppm, which was highly non-flammable considering the real cases. The range of the flammable region can be observed in another direction as well. For an aerosol fuel cloud with a concentration of 0.7-0.9 ppm, it is likely to be flammable within a wide range of average droplet sizes. For higher or lower concentration cases, the droplets will be smaller to achieve similar flammability. More tests should be done to fill out the table and expand it horizontally and vertically. This is an initial tool for material hazards screening while handling liquids with potential to form aerosols during operation, filling, and storage.

To make better use of the flammability chart, a statistical formulation should be added into the region derivation while using the comparison value in real cases. The droplets are kept under the same pressure (atmospheric for this case) and same temperature (room temperature was controlled at 75 °F constantly), so that density and other physical properties are kept consistent among tests. Thus, the distribution of real-case droplets can be analyzed as an arithmetic mean in terms of diameters. The future study will also compare the aerosol flammability region with pure vaporized fuels to achieve a more

universal model of aerosol flammability; in addition, the influence on aerosol droplets to hydrocarbon combustion can be obtained through this approach as well.

The Impact of Aerosol State on Materials

A main concern of the research of a mixed physical state is to analyze the effect of aerosolization. Comparison between an aerosol and vapor state of the same fluid material is significant to verify the hazards and quantify the ignitability. For high flash point fluids with low volatility, it is difficult to directly analyze the pure vapor phase portion among the whole aerosol system. Abramzon and Sirignano (1989) published a coupled model which calculates the evaporization rate and amount of heavy hydrocarbon spray (more saturated carbon number than n-decane) under high pressure release, which is the origin of aerosol formation. This is known as the Abramzon-Sirignano model and is useful in predicting flammable vapor phase during instant spot heating, which is a precise tool for the initial sustainable flame appearance (*i.e.* ignition delay time in aerosols), which will be fully discussed in Chapter III.

For constant heating on droplets absorbing energy to evaporate, with flowing fluid turbulence, a more fundamental model is used, the "Spalding spray droplets" model (Amsden, O'Rourke, and Butler, 1989):

$$\rho_d \frac{2}{3} \gamma^2 c_l T^*{}_d = K_{air}(T - T_d) Nu_d - L(T_d)(\rho D)_{air} B_d(T_d) Sh_d$$

$$B_d(T_d) = \frac{Y_1^*(T_d) - Y_1}{1 - Y_1^*(T_d)}$$

The d indicates the droplet properties; T_d is the implicit temperature in the system; Nu is the nusselt number of the fluid flow; Sh is the Sherwood number regarding the turbulent Reynolds system; C_l is the liquid specific heat; $L(T_d)$ is the latent heat of evaporization; B_d is the droplet breakup transition probability function which is estimated by binomial distribution of spherical droplets within 1 cubic meter space of aerosol cloud; K_{air} is the heat conductivity of air; and $(\rho D)_{air}$ is the fuel-vapor diffusivity in ambient conditions.

From the equations, we can convert the experimental results of fuel-vapor system concentrations into the real flammable vapor contents:

$$\text{Molar concentration of fuel} = \frac{\left[n\times\left(\frac{\pi d^3}{6}\right)\times\frac{\rho_F}{\mu_F}\right]}{\left[n\times\left(\frac{\pi d^3}{6}\right)\times\frac{\rho_F}{\mu_F}\right]+\left[\frac{\rho_A\times 1}{\mu_A}\right]}$$

Where ρ_F = Density of liquid fuel (kg/m^3); ρ_A = Density of Air (kg/m^3).

Using the molar flammability of the pure vapor phase, assuming under a specific amount of heat, a portion of fuel vaporized can be obtained using Le Chatelier's Rule of Mixing to calculate the flammability limits. Using different vaporization energy rates, droplet characteristics, and other parameters, the model can be used for other kind of fuels as well. The results of the experimental result conversion are shown in Figures 13 to 15:

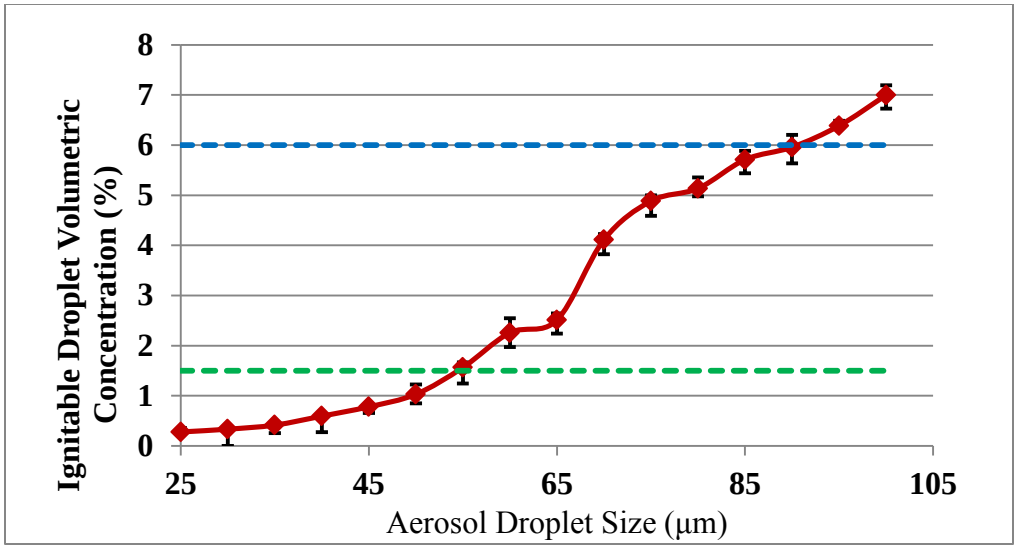

Figure 13. P-NF aerosols and vapor flammability limits comparison with fuel vaporization conversion

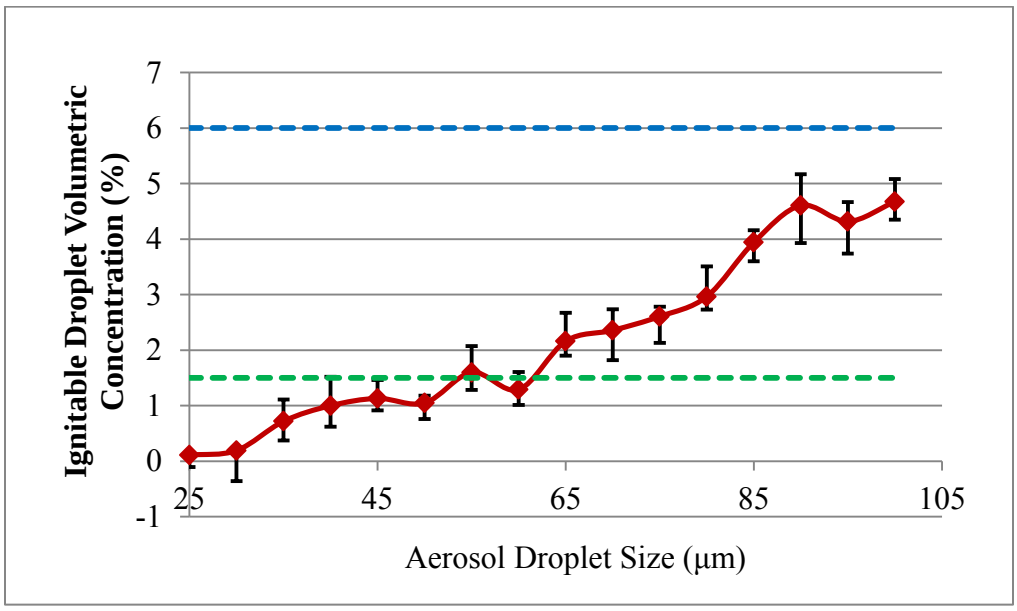

Figure 14. D-600 aerosols and vapor flammability limits comparison with fuel vaporization conversion

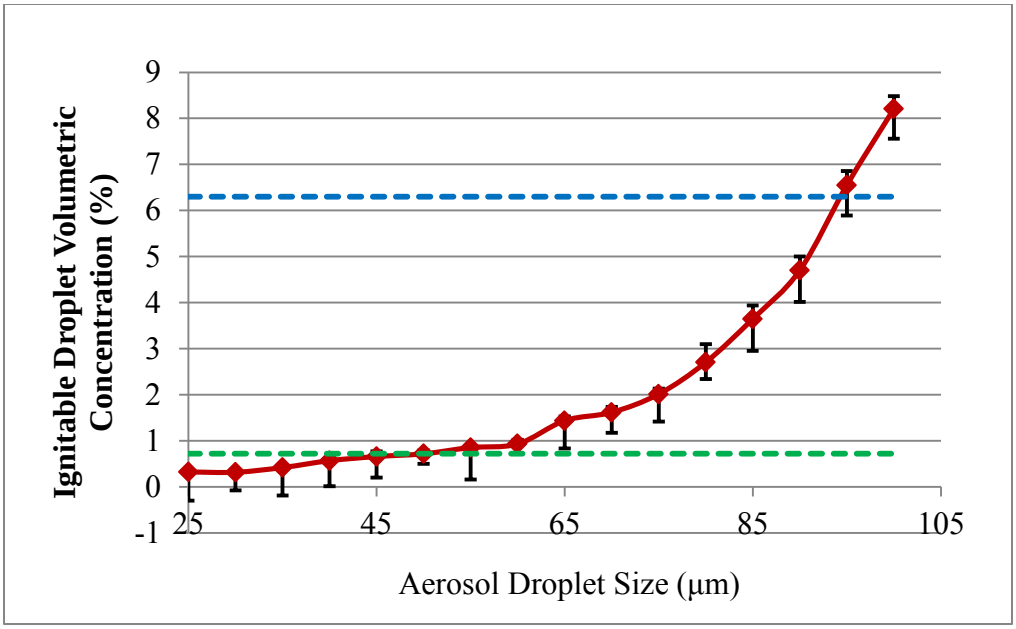

Figure 15. PHE aerosols and vapor flammability limits comparison with fuel vaporization conversion

A qualitatively clear trend, can be observed that aerosolization is able to change the flammability range within specific droplet sizes and concentrations. The fraction of ignition droplet volumetric concentration is for calculated vapor content in the heat and time applied. These vapor phase fuels, not including small droplets that can consider to be burned directly with negligible time of evaporation, expand the volume of combustion. The vapor evaporated from liquid contains significantly more matter (~10^4 more in hydrocarbons with C15-C20; ~10^6 more in regular inorganic materials) and energy content (~38.7kJ/mol due to molecule decomposition or combustion of liquid contents, and ~860kJ/mol phase change heat release).

CHAPTER III

STUDY ON IGNITION DELAY TIME AND SUSTAINABLE FLAME TRIGGERING OF FLOW SYSTEM AEROSOLS

Background and Problem Statement

Aerosol droplets are formed from pressurized materials, such as accidental rupture, pipeline breakage, and storage unit corrosion. A common scenario of incidents would be the accumulation of an aerosol cloud to flammability limits of mist combustion, with a surrounding ignition source to make the initial flame appear. Some understanding of flammability has been studied in relatively highly flammable materials, such as iso-octane, diesel oil, n-decane, n-heptane, and methanol (Atzler *et al.*, 2007; Atzler and Lawes, 1998; Danis, 1987; Hayashi and Kumagai, 1974; Hayashi *et al.,* 1981; Lawes *et al.,* 2002; Myers and Lefebvre, 1986; Singh, 1986). Compared with gaseous flammable mixtures, data on aerosol flammability are rare. One reason for this is the huge complexity of the aerosol ignition process, and the difficulty of carrying out experiments with setups sophisticated enough to account for various factors in the process (Ballal and Lefebvre, 1981). Commercial heat transfer fluids usually have specific characteristic of high flash point to make them difficult to be ignited in pure liquid states. They are also hard to exist in a pure gaseous state in process conditions, so the ignition and combustion data in the vapor phase are still lacking. However, there are more than 200 reported incidents from the previous 20 years, which were considered to

be related to heat transfer fluids in accidental leaking conditions. Aerosols formed by high flash point materials need to be studied to find a better explanation of the ignition, flame appearance, flame sustainability, and the mechanism of droplet combustion.

Aggarwal (1985) analyzed the fuel spray ignition models, having found that the influential factors of the one-dimensional, mono-dispersed system ignition are the droplet size, ignition source temperature, cold gas temperature, initial fuel vapor concentration, distance between the hot wall and the nearest droplets, equivalence ratio, and fuel type. Those factors, as well as the affect of the initial heat transfer to bring the energy for flame formation up to the fuel-vapor mixture further away, have potential influence on the combustion and flame propagation (Suard *et al*., 2004). Also, from the study of Lian *et al*. (2010), we realized a phenomenon that the flame tends to start from a series of small fragments, propagating upwards into the fuel-rich region where the streams of spraying are not deviated in directions due to an electric field. However, after these flame pieces formed, there was a delay of time and distance before the huge global flame formed. This "flame disappearance" region, about 4-6cm in length, was thought to have relations to the further delayed ignition. The mechanism within this area has not been discussed in any kinds of aerosol or spray studies and remained unknown even though the delay of ignition was analyzed in other research.

In this study, we tried to analyze from experiment and adapt models used in energy materials coupled with the flame speed development process, which is based on the flame front propagation theory in aerosols, to the flame kernel growth model applied in

spark ignition modeling for flammable mixtures (Lian *et al.*, 2010). Other than the ignition energy input, we added the sub-model on droplet evaporation during the process of a "traveling heated kernel" (discussed in detail in next sections), and observed the flame appearance-to-quench procedure comparing to experiment results on the temperature distribution among this tested space, hoping to conclude a better model to predict the ignition delay and the timing for mitigation application in practical cases.

Methodology: Experimental Approach

The ignition delay testing took place at the same time as the ignition testing. The goal is to capture the sustainable flame appearance between stage 1 and stage 2 of aerosol flame development (see Figure 12). A high speed camera was set to have the sensitivity of frame speed of 1000/second, with a resolution 512*512 to trigger the best observation of ignition delay. The time required to show the first sustainable, propagating flame will be considered as the ignition delay time of the testing sample. Twenty attempts of each concentration-voltage-droplet size combination were conducted before the final average ignition delay time was obtained. The ignition source here was still the open flame, with adequate energy as a screening level ignition for the heat transfer fluid aerosol system. The part was conducted with the previous session of aerosol flammability and ignitability analysis, and the criteria remained the same while considering a successful ignition. Each experiment set was repeated for 10 rounds, as mentioned in general ASTM tests for minimum ignition energy on two-phase mixtures (dust cloud), British industrial testing standards for flammable liquid sprays, and DIN testing procedure in

ISO 2009-06. This can be extended to ensure the reproducibility of the test, and put a better framework on the way to put the aerosol ignition delay test method into standardized ones. The observation of sustainable flame appearance was reviewed using high speed camera with 512*512 resolution and a 1000 frames per second capturing rate. Laser signals were applied and collected for flame diffraction backup reference.

Methodology: Computational Approach

Model Description

The process of aerosol stream combustion is shown in Figure 16. This system is based on the cooperative aerosol project done at Mary Kay O'Connor Process Safety Center at Texas A&M University. Heat transfer fluids were contained in syringes for spraying use. The method used to produce aerosols from liquid is electrospray, which is mainly the application of high voltage (up to 10 kV) onto the droplet streams, making the droplets charged and form minute droplet streams. These are the aerosol states defined in this study. The method was from a study by Mejia, He, Luo, Marquez, and Cheng (2009), introducing the electric control of the fine distribution of aerosol droplets. The size and space distributions can be varied by applying different voltages and liquid flow rates. The liquid meniscus at the outlet of each capillary took a conical shape, *i.e.,* cone-jet mode under the influence of the electric field between the nozzles and the grounding electrode (Lian, Mejia, Cheng and Mannan, 2010). The distance between the grounding electrode (attached to a metal mesh) and the nozzle front is 2.5 inches and remains the same for every test. The ignition source for the testing system is liquid propane gas, or

LPG, flowing through a 1/8-inch ID stainless steel tube. The inside end of the tubing was bent 90° up as the flame tip, so LPG gas would flow upward before being ignited upon exiting the tubing. The aerosol droplets traveled downwards with the ignition occurring at the very bottom of the chamber.

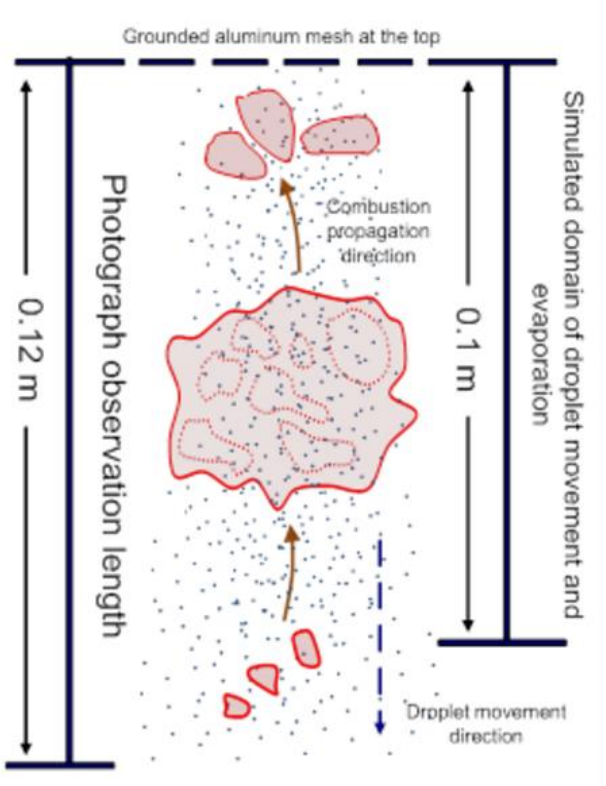

Figure 16. The flame development stages of generic, heat transfer fluid aerosol combustion (Lian *et al.*, 2010)

The whole procedure of the flame development in an aerosol system can be separated into three regions: (I) the flame pieces from the ignition source, (II) the global flame (which is the main flame we considered), and (III) the final quenching state when the

whole flame reaches the top with less heat supply. Since the behavior within region (I) is relatively complicated to describe, we focus on the (I) to (II) transition. The flame pieces travel up to the direction of the spraying point, and at certain distances of distance these flame pieces “disappear” with no illuminant flame shown. Then in a specific region above it, a large global flame would form and exist for a long period of time. This instability of flame appearance may be due to boiling point differences of the mixtures, droplet-droplet interactions, and the feeding-receiving rates of the fuel and local oxygen supplies. The potential factors will be reflected in our coupled model.

We are interested in the procedure of possible hot products heated by the flame from ignition sources, propagated in the form of a cool flame, and after the abundant fuel above the cool flame assists the formation of a hot flame, the huge flame can be observed. There is a delay time from the initial ignition to global flame existence, and this is our point of concern as the characterization indicator of aerosol flammability.

The model is designed to be like a space with dimensions as shown in the following figure.

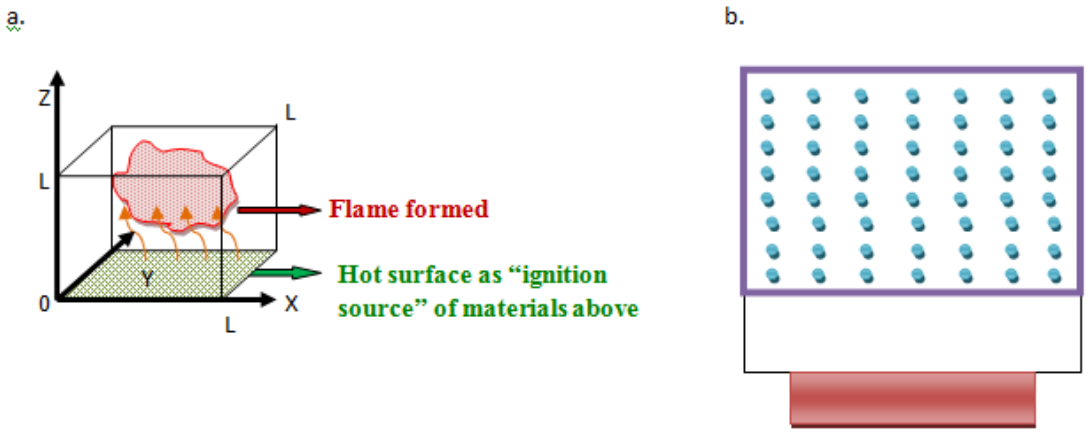

Figure 17. Schematic modeling domain in aerosol combustion. (a) The 3-axis simplified model setting of the system; (b) 1-D model domains

As we see in Figure 17a, the system is designed to be located in a box with L*L*L dimensions. The hot products (or cool flame) are treated as a surface with area L^2, heating up the materials above it. The surface is treated as static in the location, and only energy is transferred up to the aerosols.

Figure 17b will be our total 2-D modeling region. For more domain definition, we added two regions to describe the aerosols and the hot surface as an ignition source, which separates the whole region into three parts:

1) Unburned Aerosol Domain - Air (Purple Square): This domain is the target of the hot surface to produce energy transfer and flame front propagation.
2) Droplets Domain (Blue Dots): The droplets are described by the blue circles which do not have constant volume due to the evaporation of droplets. After we

consider the evaporation there will be another sub-domain set in this part defined as "fuel vapor" attached to them, changing the volume of the fuel drops.

3) Hot Kernel Domain (Red Square): The heated surface of the mixture at the bottom formed a volume we called "hot kernel." For simulation's sake we consider it as a cube, with the cut plane here as a constant-area region. The domain has heat flux into the Unburned Aerosol Domain, producing influence on droplets and the vapor-air system.

In summary, the overview of this model includes:

- Heat transfer (convection, conduction, radiation) between hot kernel and the aerosol system;
- Temperature change (time dependent) and distribution (spatial) to reflect the global flame appearance;
- Droplet evaporation model (the vapor and liquid mass/volume change); and
- Chemical kinetics factor (the reaction rate of fuel).

The equations included in this coupled model are listed as the following:

a. Heat transfer and temperature change

The heat transfer which occurs between mixtures of droplets with a heated mixture (hot kernel) can be written as the following: (Eisazadeh-Far *et al*, 2010)

$$\frac{dT}{dt} = \frac{Q_{comb} - Q_{cond} - Q_{vap} - Q_{cp}}{C_{pa} M_f}$$

$$Q_{comb} = \frac{dM_f}{dt} = \frac{\rho_f v_f H_c}{\rho_u M_w}$$

$$Q_{cond} = \frac{k_a A(T - T_{am})}{\delta}$$

$$Q_{vap} = \frac{dM_f}{dt} \frac{\rho_f E_{vap} v_f}{\rho_u M_w}$$

$$Q_{cp} = \frac{dM_f}{dt} \frac{\rho_f C_{pF} v_f}{\rho_u M_w} (T - T_{fb}) + \frac{dM_f}{dt} \frac{\rho_a C_{pa}}{\rho_u} (T - T_{am})$$

$$\rho_u = \rho_f \left(\frac{4}{3} \pi {R_d}^3 C_f \right) + \rho_a$$

Here, C_{pa} is the heat capacity of ambient air, v_f is the stoichiometric coefficient of fuel chemical, k_a is the thermal conductivity of air, and M_W is the molecular weight of the fuel chemical.

b. For the mass of fuel, we consider the following:

Concentration of fuel (C_f) $= \frac{Number\ of\ fuel\ droplets}{Total\ Volume} = \frac{N_f}{L^3} = \frac{\frac{dM_f}{dt} \times t}{\rho_f \times L^3}$

$M_f = L \times \sum_{k=1}^{k} \frac{\frac{3}{4} \pi \rho_{fk} N_{fk} {R_d}^3{}_k}{d_k}$

Where M is the mass, N is the number, subscript f denotes the fuel's cases, d is for droplet spacing in the axial direction, R_d is the droplet radius, and ρ is the liquid density of the fuel. Here the "k" is originally depicting the groups of droplets with different diameters in spraying, but in our simplified cases we introduce no statistical issue. The equation can then be simplified as:

$$\mathrm{M_f} = L\frac{\frac{3}{4}\pi\rho_f N_f {R_d}^3}{d}$$

with the value of each term representing the constant, initial values.

c. Droplet Evaporation (Abramzon-Sirignano Model):

$$\frac{dM_f}{dt} = 2\pi\rho_f D R_d Sh^* \ln(1+B_M)$$

$$Sh^* = 2 + \frac{(Sh_0 - 2)}{F_M};\ Sh_0 = 2 + 0.552 Re^{\frac{1}{2}} Sc^{\frac{1}{3}}$$

$$F_{B_M} = (1+B_M)^{0.7} \times \frac{\ln(1+B_M)}{B_M}$$

$$B_M = \frac{Y_{f_s} - Y_{f_\infty}}{1 - Y_{f_s}}$$

Where D is the mass diffusivity, Sh^* is the modified Sherwood number, B_M is the mass transfer number, F_M is the correction factors of mass diffusivity, Sh is the Sherwood number, Y_f is the mass fraction of vapor, and the subscript s means value at droplet surface, while ∞ means the infinity value. One thing to mention is that the case is good

for approximation in lower Reynolds number conditions, which is available in our experiment conditions.

The equations listed here are selected from the most probable cases close to our aerosol material and system. Eisazadeh-Far had mentioned (Eisazadeh-Far *et al*., 2010) in the ignition kernel study that the ignitor energy cannot exceed the level of 20mJ to 1kJ in the range of discussion. The kernel growth rate was limited to specific ambient conditions, which is usually around NTP, to have the exact estimation.

COMSOL-Multiphysics ver. 4.1 is the software we used for this modeling. The physical method was a mixture of differential equations and 2-D heat transfer, with the probes testing the temperature distribution within evaluation domains. The initial droplet distribution was set as the finite elements spreading equally in distance (of 0.002 m), and 100 droplets were initially set in the droplet domain mentioned before. The probe tested the temperature value from the margin to the center of the droplets, and the change in the droplet evaporation while heat applied. The changeable parameters are droplet size, initial temperature of heat kernel, droplet concentration (distance between each droplet; total droplet numbers), and heat transfer properties.

Results and Discussion

Ignition Delay Time of Aerosol Combustion from Experiment

The luminous flame fragments at the beginning stage disappeared for a time (from 2 s – more than 10 seconds), and then the global flame was shown at a position ~6-8 cm under

the spraying nozzle. The completely developed global flame of the aerosol system should contain a luminous shell with abundant fuel fed into the flame core as the vapor-droplet mixture forms. Each test calculated the flame number, selected the successfully ignited ones according to our criteria, and took the reciprocal to get the ignition delay time. The test results are listed in Tables 8 to 10.

Table 8. Ignition delay time of P-NF aerosol tests.

Applied Voltage	7	7.25	7.5	7.75	8	8.25	8.5	8.75	9	9.5	10
1mL/h Delay Time (s)	N/A	N/A	N/A	N/A	N/A	N/A	5.1	8.3	7.9	9.8	12.5
2mL/h Delay Time (s)	N/A	N/A	N/A	0.50	0.80	1.1	2.3	3.2	6.5	7.1	7.7
3mL/h Delay Time (s)	N/A	N/A	0.10	0.40	0.90	1.8	1.9	2.9	4.7	5.8	6.1

Table 9. Ignition delay time of D-600 aerosol tests.

Applied Voltage	7	7.25	7.5	7.75	8	8.25	8.5	8.75	9	9.5	10
1mL/h Delay Time (s)	N/A	N/A	N/A	1.2	2.8	1.9	2.22	3.1	3.9	N/A	N/A
2mL/h Delay Time (s)	N/A	N/A	N/A	2.2	2.1	1.9	3.1	2.9	3.8	3.4	N/A
3mL/h Delay Time (s)	N/A	0.86	0.98	0.12	0.9	2.3	2.1	1.7	2.6	4.1	5.0

Table 10. Ignition delay time of PHE aerosol tests.

Applied Voltage	7	7.25	7.5	7.75	8	8.25	8.5	8.75	9	9.5	10
1mL/h Delay Time (s)	N/A	N/A	N/A	N/A	N/A	1.8	3.4	3.7	N/A	N/A	N/A
2mL/h Delay Time (s)	N/A	N/A	0.40	0.50	0.30	1.7	2.1	2.0	3.3	3.1	N/A
3mL/h Delay Time (s)	N/A	N/A	N/A	0.20	0.10	0.70	1.0	1.6	2.2	2.1	3.0

From the ignition delay time table, the ignition of the aerosol system was delayed more with lower flow rates in general. For P-NF, when the concentration and droplet size approached more ignitable states, which were roughly described as higher concentrations and smaller sizes, the ignitions occurred at a higher frequency for flame formation. Due to the local value of droplet size reduction, the delay time increased with an applied voltage increase. The times range from 0.1 s to 12.5 s, which were all comparably shorter than the flame formation speed of other hydrocarbon vapors as reported. The ignition time length is influenced by properties of the aerosol, including aerosol droplet size, droplet number density, and droplet moving velocity. For D-600 and PHE, fuels that have a higher carbon value and molecular weight, the ignition delay time of each feeding rate do not deviate much comparing to lighter mineral oils. The larger particle interaction, tighter covalent bonds, and more gravitational related affinity between molecules made the heating process easier regarding heat transfer among particle layers. The chemical properties for droplet evaporation and oxidation are opposing each other.

The ignitability of P-NF has a wider range of successful attempts, while a longer delay time is needed for a sustainable flame to occur. We can draw an idea to the determining forces with changing of carbon numbers in the material molecules. Larger, bulk particles with tense molecule affinity has a higher energy request on the heating process; but while the affinity is large enough and the fuel supply is abundant in flammable range, the convective heat transfer will exceed the bulk density factor and turns out to have a shorter ignition delay time.

In these cases, applying different fuel feeding rates influenced droplet moving velocity. The ignition delay depends on how "rapidly" the heat and flow particles transfer to flame appearance location, which is usually the spot with the best flammable conditions; thus, the droplet velocity would increase with feeding rate, and this also increased the droplet flow rate. The heat transfer rate is higher in the liquid phase in the case of the two-phase system (gas and fuel), especially with the assistance of air flowing within the chamber. Liquid droplets brought more energy and transferred completely through the fuel fed above the heated region. This factor would make a huge force of flame formation, which results in a short ignition delay time. The change of applied voltage, or the attempts to change droplet size, will influence ignition delay time as well. A sustainable flame needs a stable system of aerosol to feed fuel into the "flame lumen" body. When smaller droplets form within a stronger electric field, the charge density on each droplet or droplet group will increase. These droplets tend to repulse each other, making the system more unstable. Thus, the moving droplets take a longer time to travel downwards and have more open spaces to coalesce and form more stable gatherings to

sustain a flame; also, smaller droplet cases, as we mentioned in a previous section, may result in lower local fuel concentration (in the same flow rate condition) at the flame formation region, which also affected the flame appearance.

Ignition delay time gave a clear reference of the flame appearance timing and when to expect the global flame. Possible mitigations or protections would be applied to processes and units in industrial cases, and the response time should be within the ignition delay time after the adequate ignition source resulted. More study about the combustion process and ignition delay mechanism will be carried out in later research.

Modeling Results: Horizontal Temperature Distribution

In the simulation part, the temperature changes in the direction of a plane which is parallel to the heat kernel/unburned domain boundary was typically shown as Figure 17. We need this information to know how the layers of aerosols are being burned. The probes numbering and locations are defined in Table 11. Six hundred probe values were averaged as the final value for analysis.

Table 11. Horizontal temperature analysis probe numbering

Probe 1	Center of droplets
Probe 2-3	Droplet side (left, right)
Probe 4	0.001m away from droplet margin

The heat transfer effects on aerosol droplets rely highly on the chemical properties of the fuel. Since we have done a series of experimental studies on heat transfer fluids, the droplet domain material would be set in its specific heat transfer parameters. We can see that in huge droplet cases, such as 500 micron droplets, the temperature change was mainly on the region outside droplets first due to the interior liquid heat transfer; when the droplets were heated properly and the temperature started to increase to ~1000K (the luminous flame temperature range), it took about 4-6 seconds, which was comparable to our experiment data, though slight higher due to the droplet size scale and the assumption of simplification.

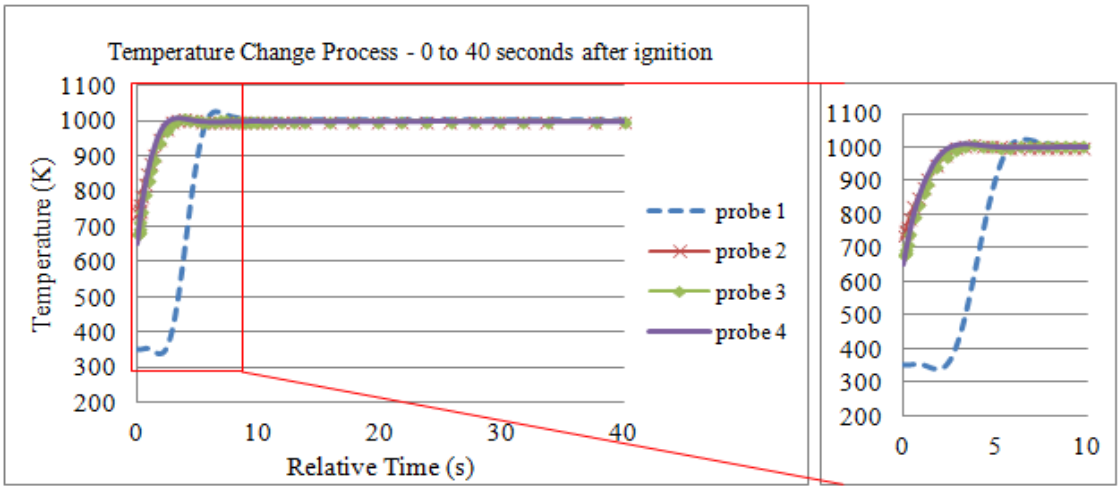

Figure 18. Temperature simulation results. [Fuel: P-NF; Droplet size: 500μm; Amount: 100 droplets/64cm^3 testing space; heat kernel moving velocity: 0.005m/s]

When the droplet sizes decreased into our experimental scale, the results of the temperature change of the probes were shown as the following Figures 19 to 21.

a.

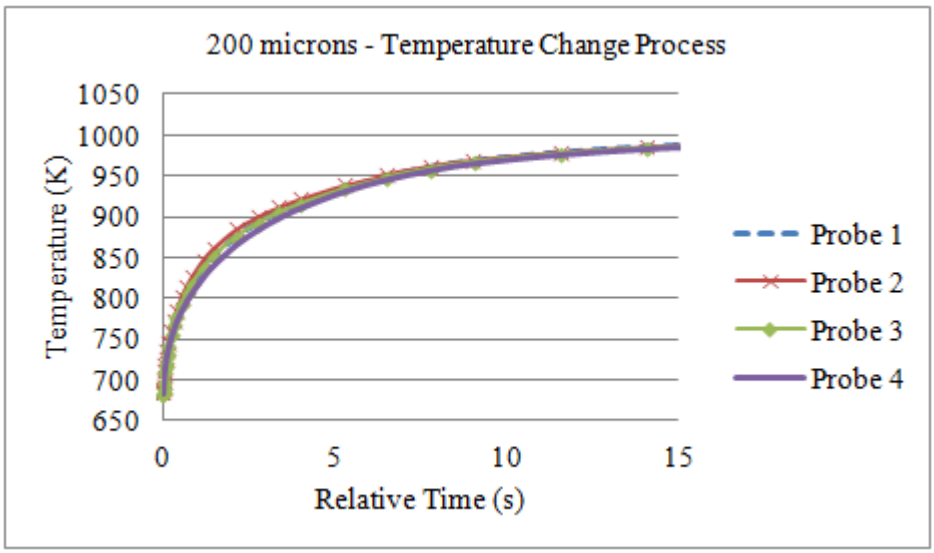

b.

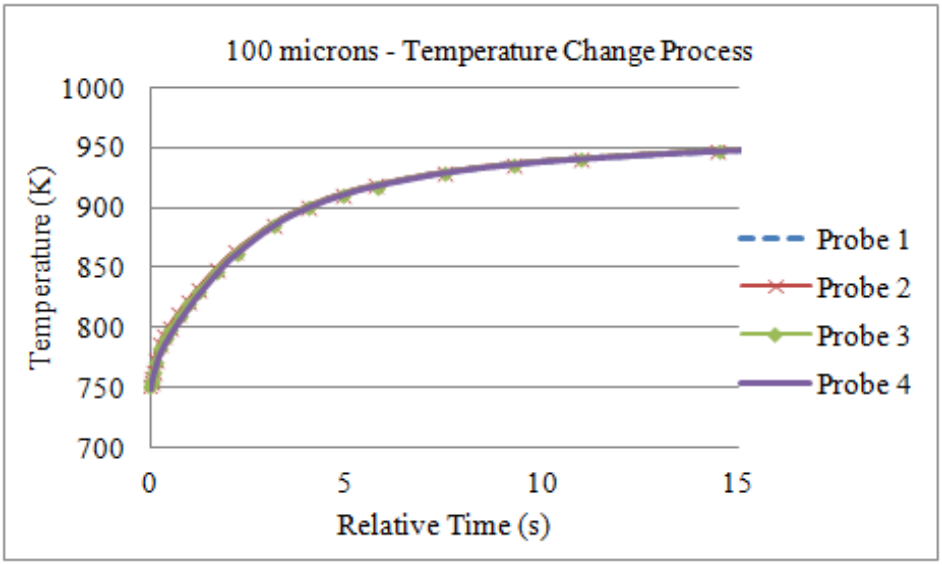

Figure 19(a-b). Droplets size and horizontal temperature change relations. [Fuel: P-NF; Droplet size: 200-80μm; Amount: 100 droplets/64cm^3 testing space; heat kernel moving velocity: 0.005m/s]

c.

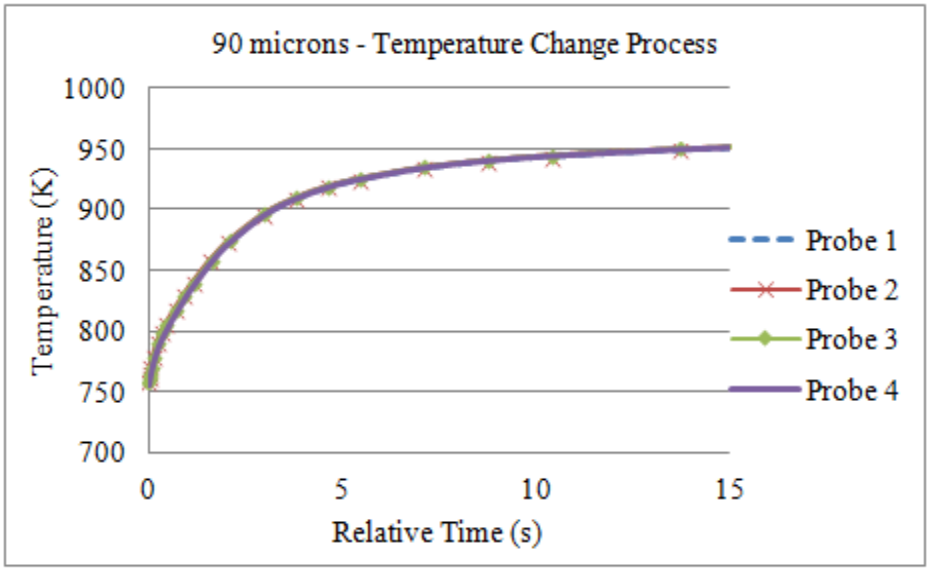

d.

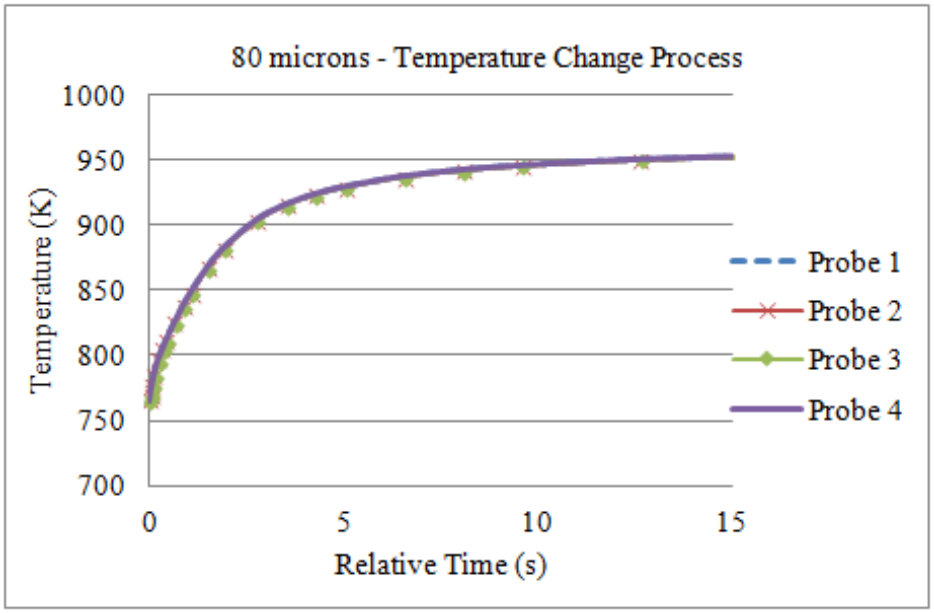

Figure 19(c-d). Droplets size and horizontal temperature change relations. [Fuel: P-NF; Droplet size: 200-80μm; Amount: 100 droplets/64cm^3 testing space; heat kernel moving velocity: 0.005m/s]

a.

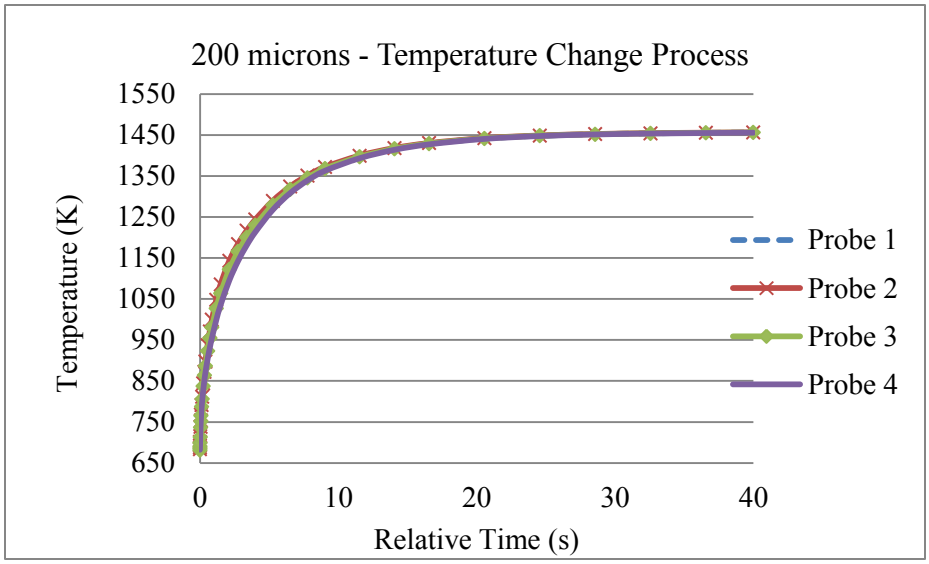

b.

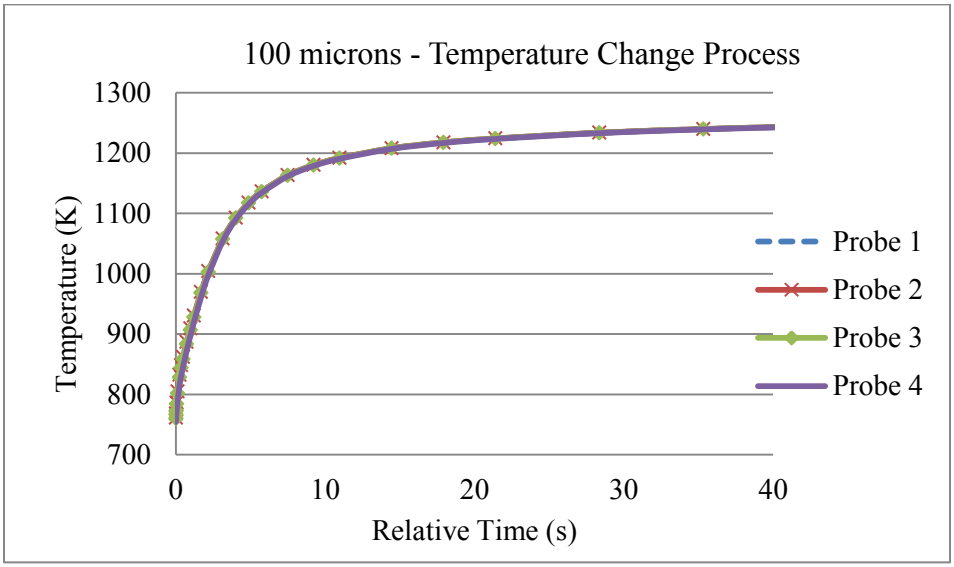

Figure 20(a-b). Droplets size and horizontal temperature change relations. [Fuel: D-600; Droplet size: 200-80μm; Amount: 100 droplets/64cm^3 testing space; heat kernel moving velocity: 0.005m/s]

c.

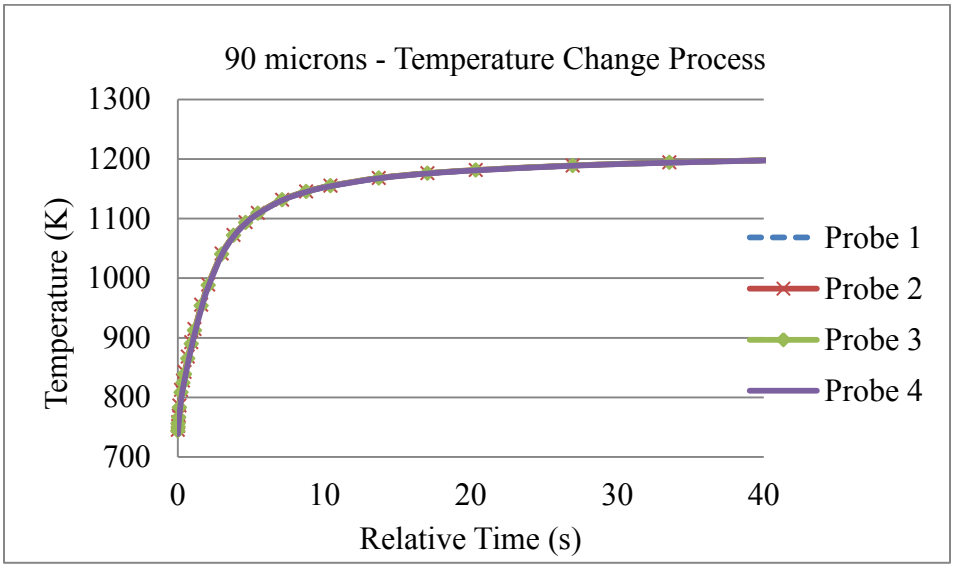

d.

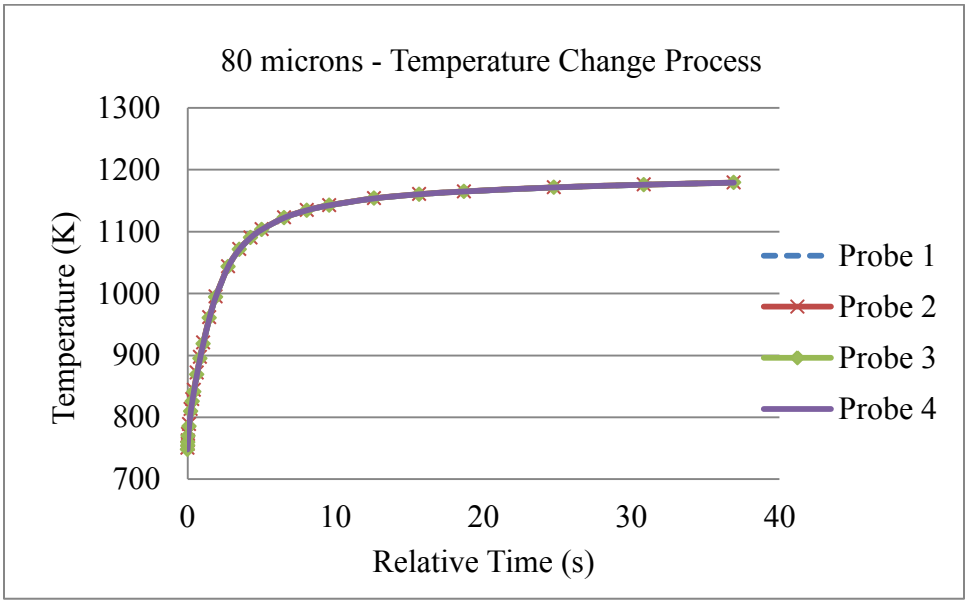

Figure 20(c-d). Droplets size and horizontal temperature change relations. [Fuel: D-600; Droplet size: 200-80μm; Amount: 100 droplets/64cm^3 testing space; heat kernel moving velocity: 0.005m/s]

a.

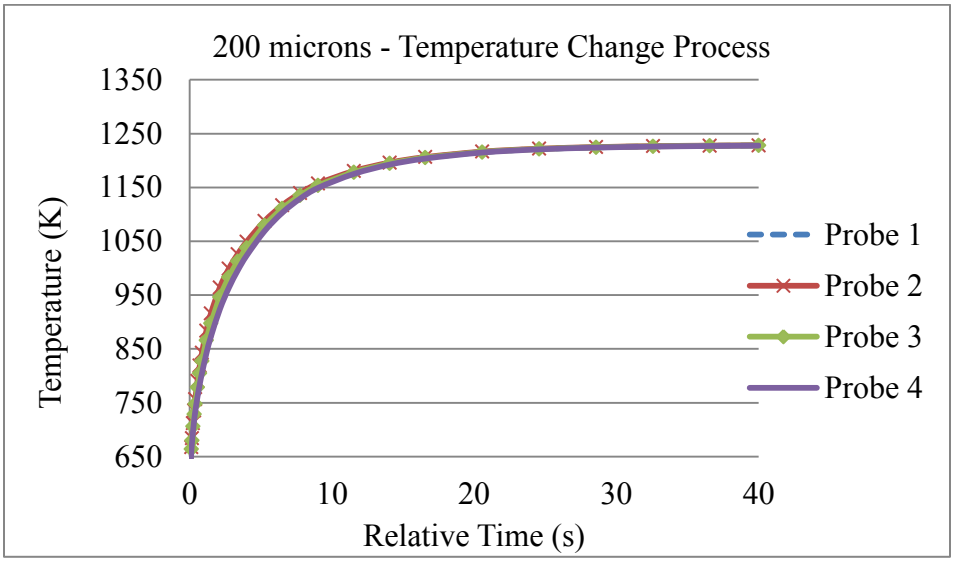

b.

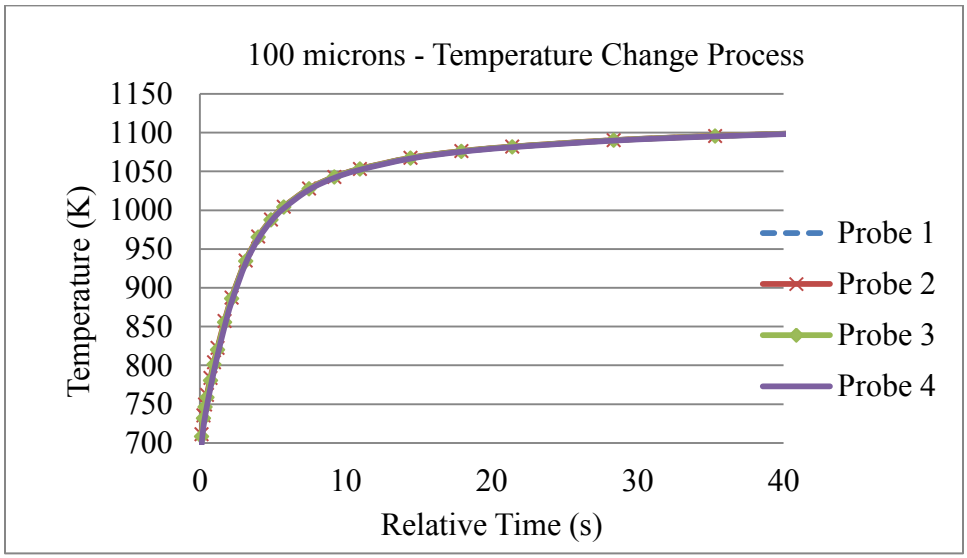

Figure 21(a-b). Droplets size and horizontal temperature change relations. [Fuel: PHE; Droplet size: 200-80μm; Amount: 100 droplets/64cm^3 testing space; heat kernel moving velocity: 0.005m/s]

c.

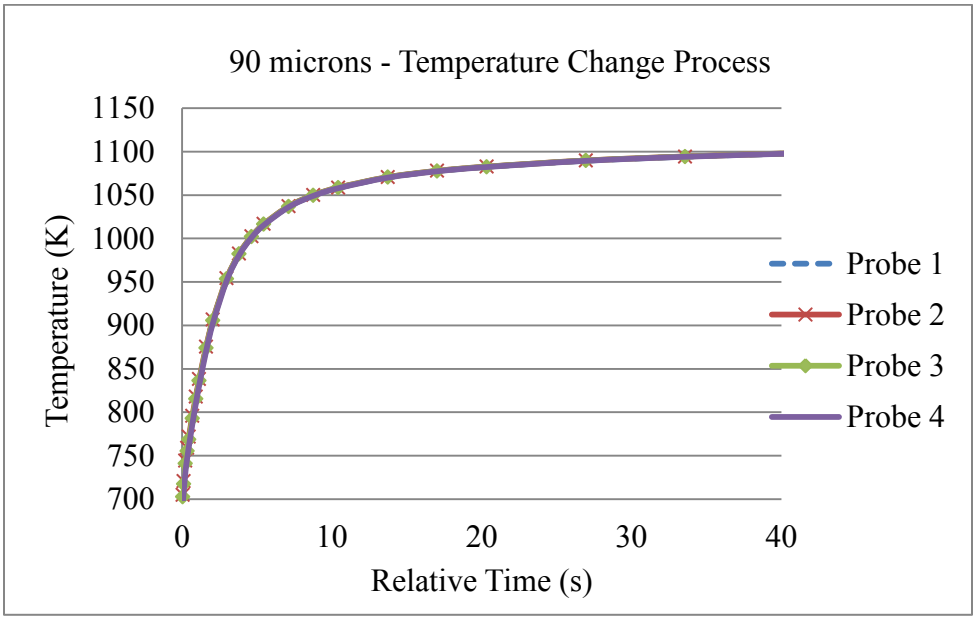

d.

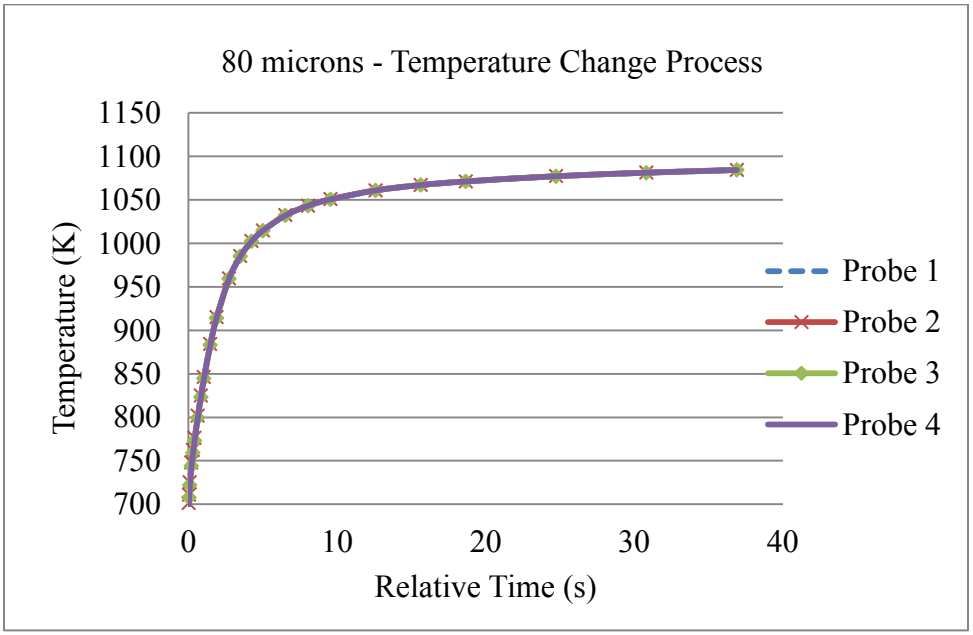

Figure 21(a-d). Droplets size and horizontal temperature change relations. [Fuel: PHE; Droplet size: 200-80μm; Amount: 100 droplets/64cm^3 testing space; heat kernel moving velocity: 0.005m/s]

We can see from the figures of three heat transfer fluids that the slope of temperature change increased with the decrease of droplet size. Larger droplets had better heat effects, and the luminous flame would appear in a shorter time range with horizontal direction homogeneity in terms of heating; smaller droplets reacted in the opposite way. This may due to the larger droplets having more combustible matter when the concentration was kept solid; the evaporation volume increases more in large droplet cases causing the probes to differ with each other in early stage of flame heating process and transfer the heat effectively to the surrounding "neighbor" area on the horizontal line as the kernel moved upwards. This allowed regions in parallel positions to be equally heated. For heavier hydrocarbons, the increase of temperature started in lower values due to the initial heating for a specific range of droplet group; however, the rate of heating and supply along the horizontal direction increased severely after the first 3-5 seconds, which is during the appearance of luminous flame. The result is close to the initiation of sustainable fire from experiments, while only a layer of the local droplet system was heated and burned during the measurement.

The horizontal heat transfer showed the direct explanation of the heat kernel layer and the unburned layer interaction, and we could describe the idealized phenomenon of an equally burning rate with the heat kernel covering the entire bottom mixture region after the ignition source offered enough heat. This made sure that our system could be predicted in the ignition delay with a steady state process.

Modeling Results: Vertical Temperature Distribution

The vertical temperature distribution required different probes. This part of study was mainly focused on the flame propagation mechanism and the vertical heat transfer phenomenon. This is important for the droplets in vertical positions taking sequence to sustain the flame by their combustible matters and to let us know where the global flame appeared by calculating the kernel travel distance and ignition delay time resulting from this part of the study. Table 12 shows the probes for vertical temperature testing.

Table 12. Vertical temperature analysis probe numbering

Probe 6	On the Boundary of kernel and unburned domain
Probe 7	One droplet distance above
Probe 8	Two droplets distance above

The temperature distribution results are shown in Figures 22-24. The vertical temperatures were distributed in a range of 350K – 1000K, with the changes showing special local slope differences in one droplet distance above the boundary of the kernel and unburned domain.

a.

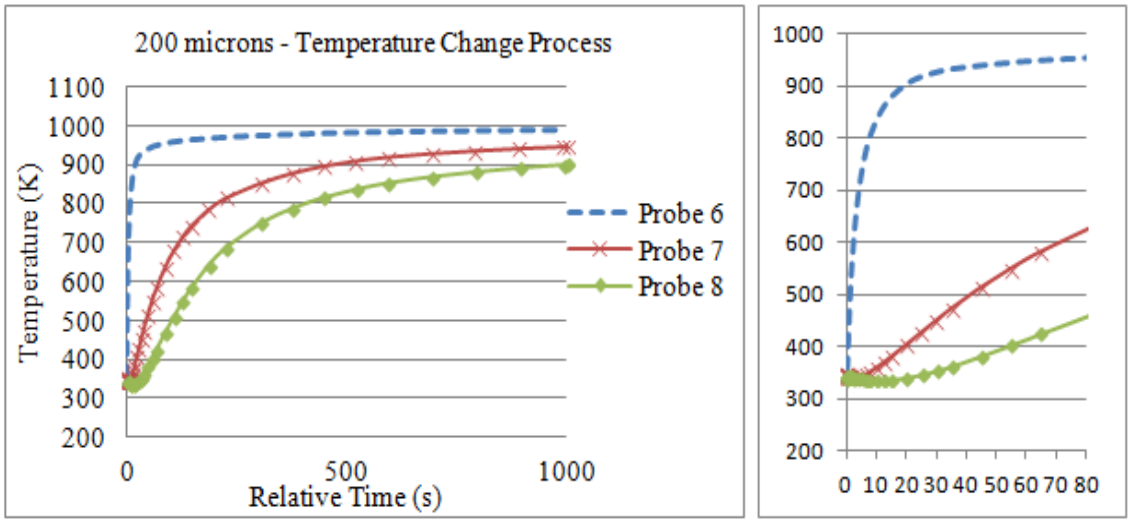

b.

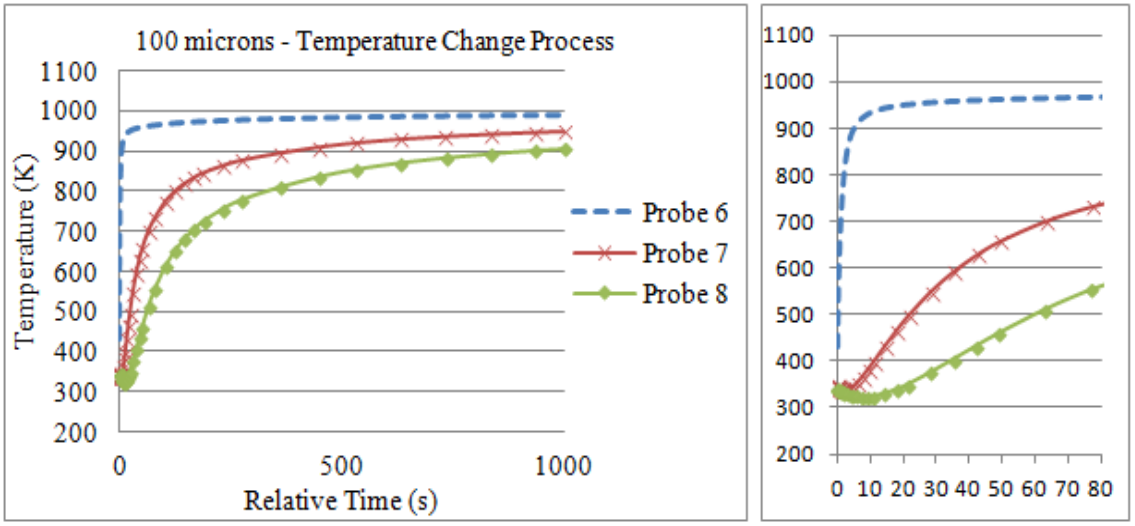

Figure 22(a-b). Droplets size and vertical temperature change relations. [Fuel: P-NF; Droplet size: 200-80μm; Amount: 100 droplets/64cm^3 testing space; heat kernel moving velocity: 0.005m/s]

c.

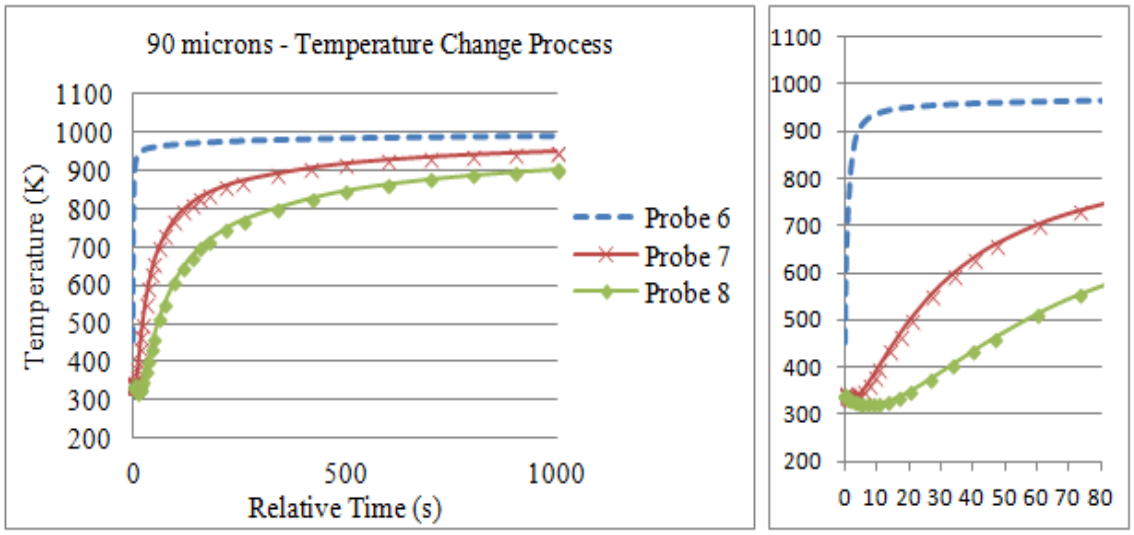

d.

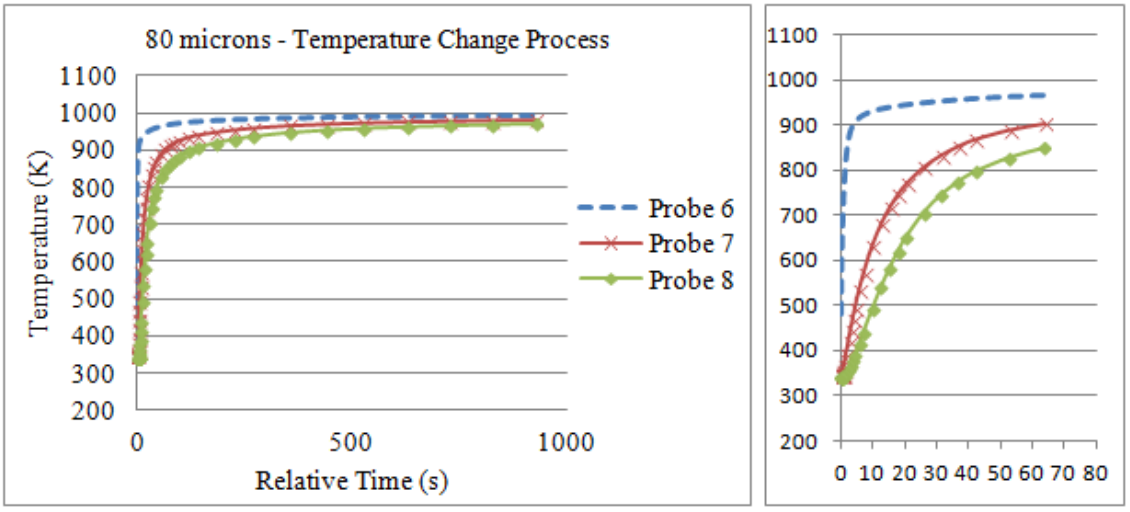

Figure 22(c-d). Droplets size and vertical temperature change relations. [Fuel: P-NF; Droplet size: 200-80μm; Amount: 100 droplets/64cm^3 testing space; heat kernel moving velocity: 0.005m/s]

a.

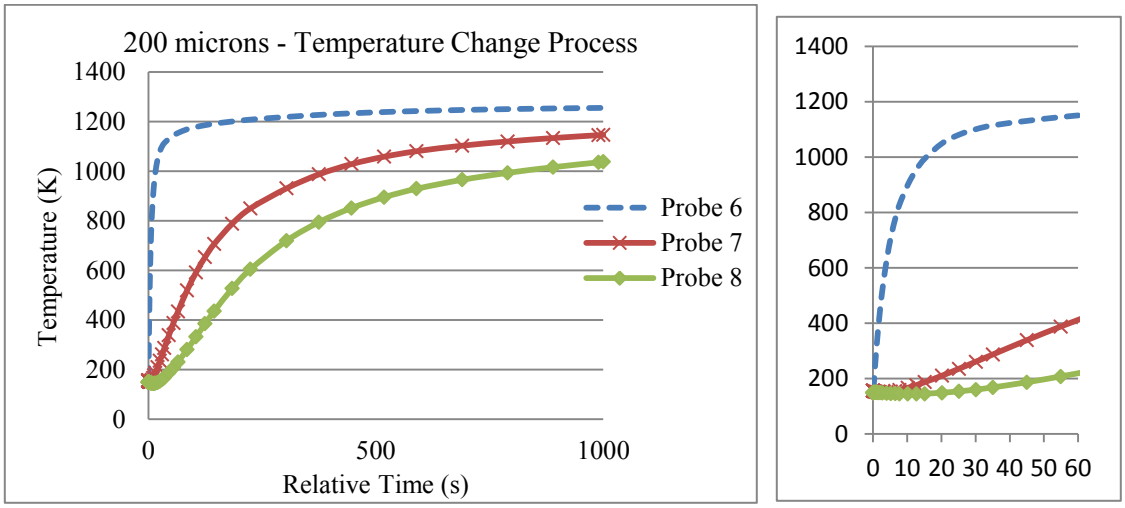

b.

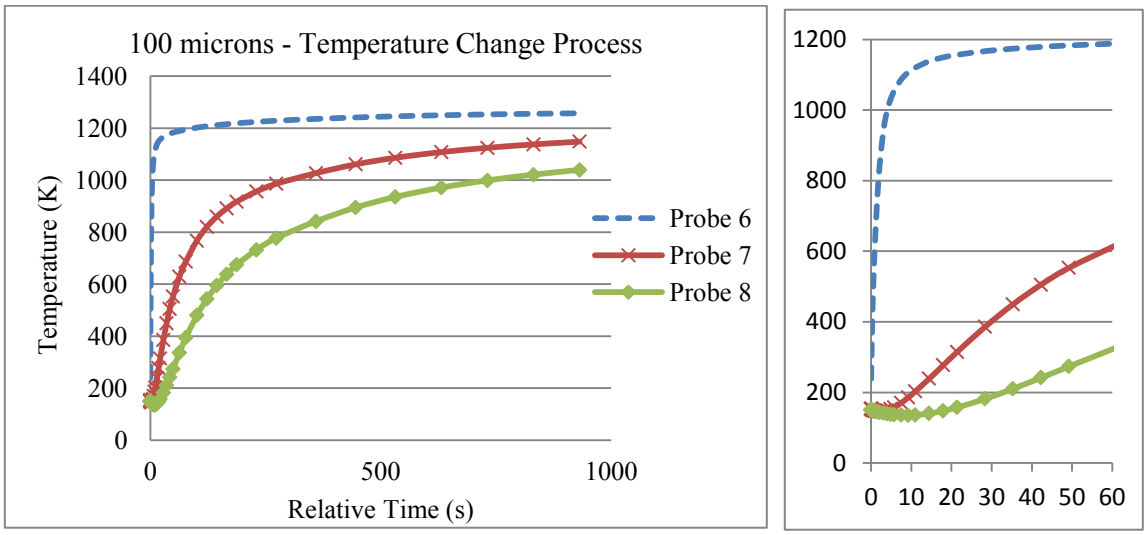

Figure 23(a-b). Droplets size and vertical temperature change relations. [Fuel: D-600; Droplet size: 200-80μm; Amount: 100 droplets/64cm^3 testing space; heat kernel moving velocity: 0.005m/s]

c.

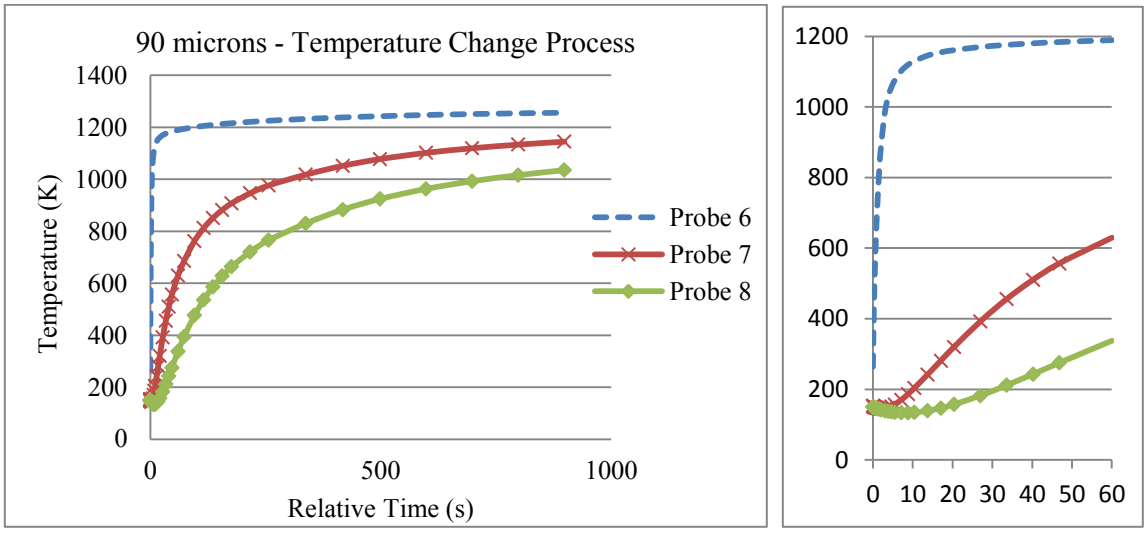

d.

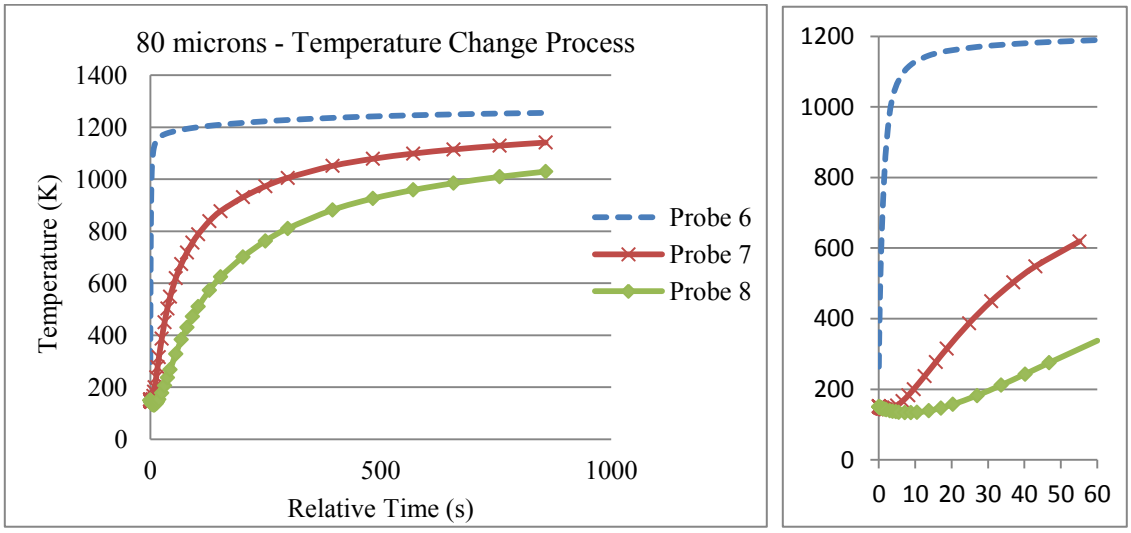

Figure 23(a-d). Droplets size and vertical temperature change relations. [Fuel: D-600; Droplet size: 200-80μm; Amount: 100 droplets/64cm^3 testing space; heat kernel moving velocity: 0.005m/s]

a.

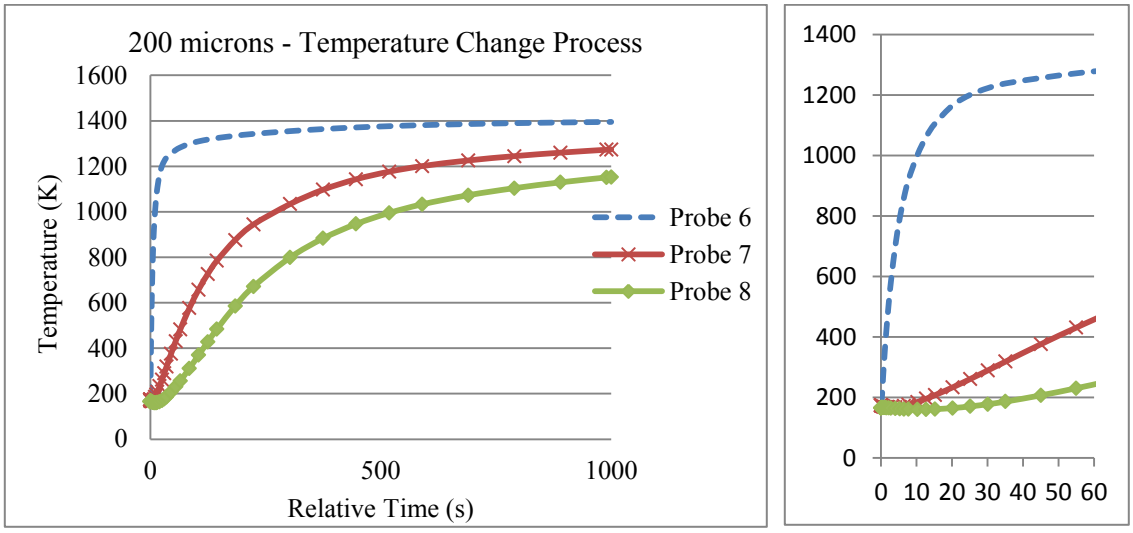

b.

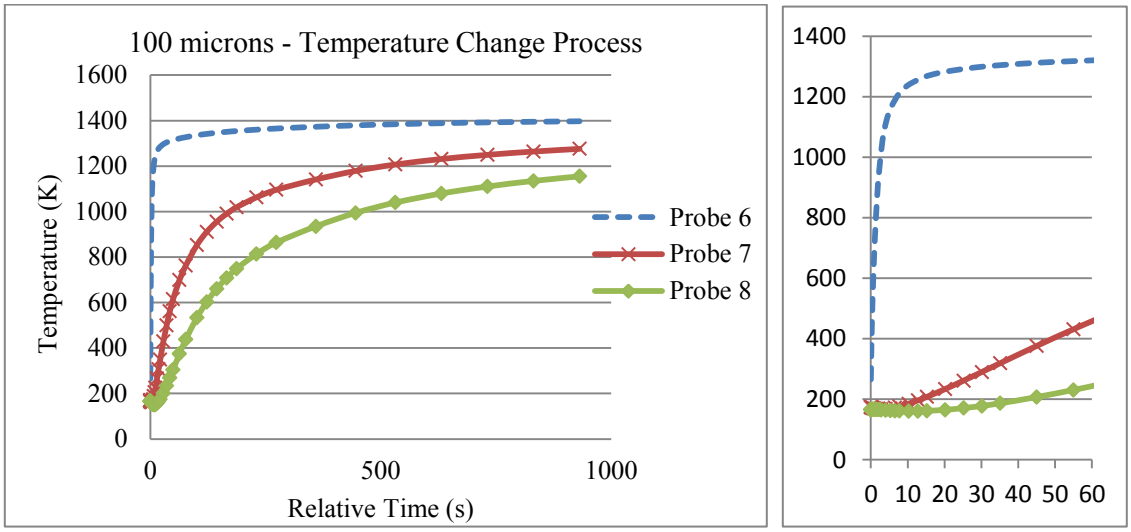

Figure 24(a-b). Droplets size and vertical temperature change relations. [Fuel: PHE; Droplet size: 200-80μm; Amount: 100 droplets/64cm^3 testing space; heat kernel moving velocity: 0.005m/s]

c.

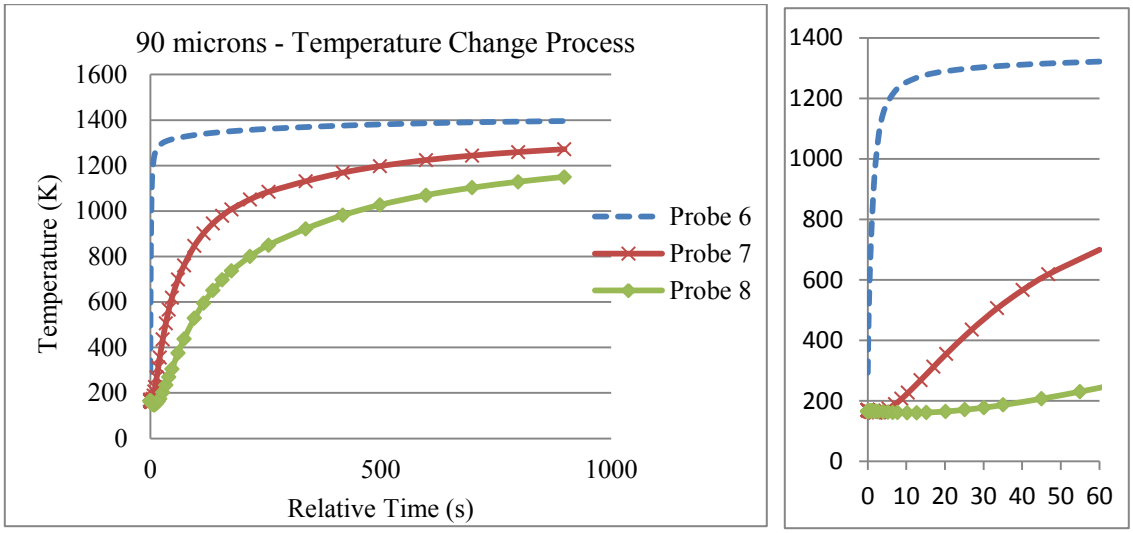

d.

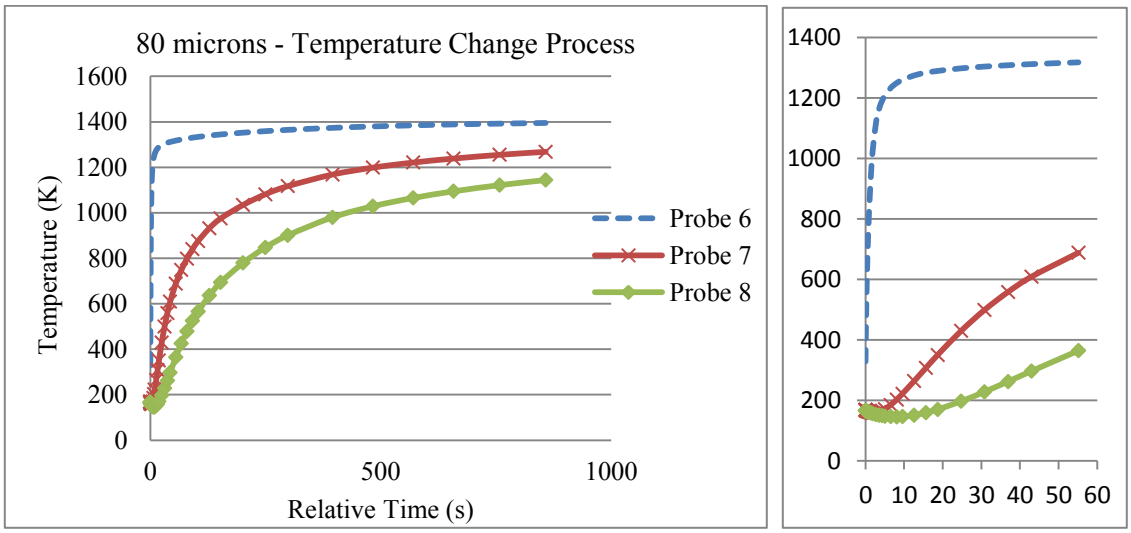

Figure 24(a-d). Droplets size and vertical temperature change relations. [Fuel: PHE; Droplet size: 200-80μm; Amount: 100 droplets/64cm^3 testing space; heat kernel moving velocity: 0.005m/s]

For larger droplet sizes, the temperature at the droplets center showed a tendency to take a smoother path to increase the temperature, possibly because of the more combustible matters included in individual droplets. For smaller ones, however, the heat transfer was faster through the droplet body and proceeded to the upper region, so that the ignition delay time was lower.

Regarding the temperature changes in probes located higher in the surrounding air, larger droplets cases would result in more time for heat transfer due to the thermal expansion rate in evaporation. The vapor fraction at the surface is higher since the surface area would be higher in same concentration conditions; then the associated Sherwood number would be higher by the correction factor effects, and finally the mass change rate of fuel would be relatively larger than the cases in smaller droplets. The more rapid change in combustible fuel mass would result in more time required to balance the influence of the gas/liquid heat transferring efficiency.

The vertical results are important indicators for upwards flame heating effects. Since there were steady flows (idealized assumption) feeding and the whole region was kept stable, the capability to form a sustainable, movable flame to proceed required enough time to develop.

The following figures showed the comparison of each position of probes and the local temperature change they indicated. We can see that smaller droplets (100 microns and under) required more heating time (up to 40+ seconds) to achieve the luminous flame temperature.

a.

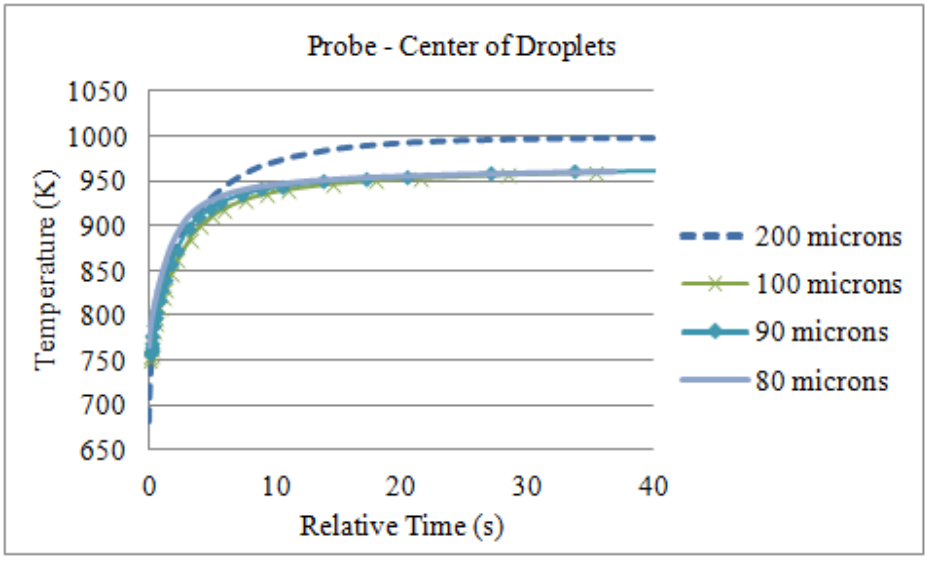

b.

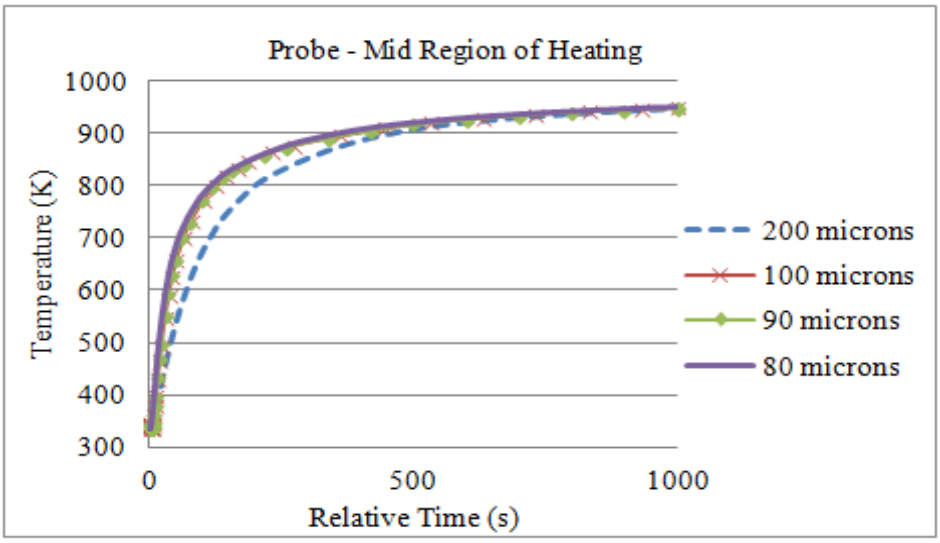

Figure 25(a-b). Droplets size / vertical temperature probe locations: a. center of droplets; b. mid-region between droplets. [Fuel: P-NF; Droplet size: 200-80μm; Amount: 100 droplets/64cm^3 testing space; heat kernel moving velocity: 0.005m/s]

c.

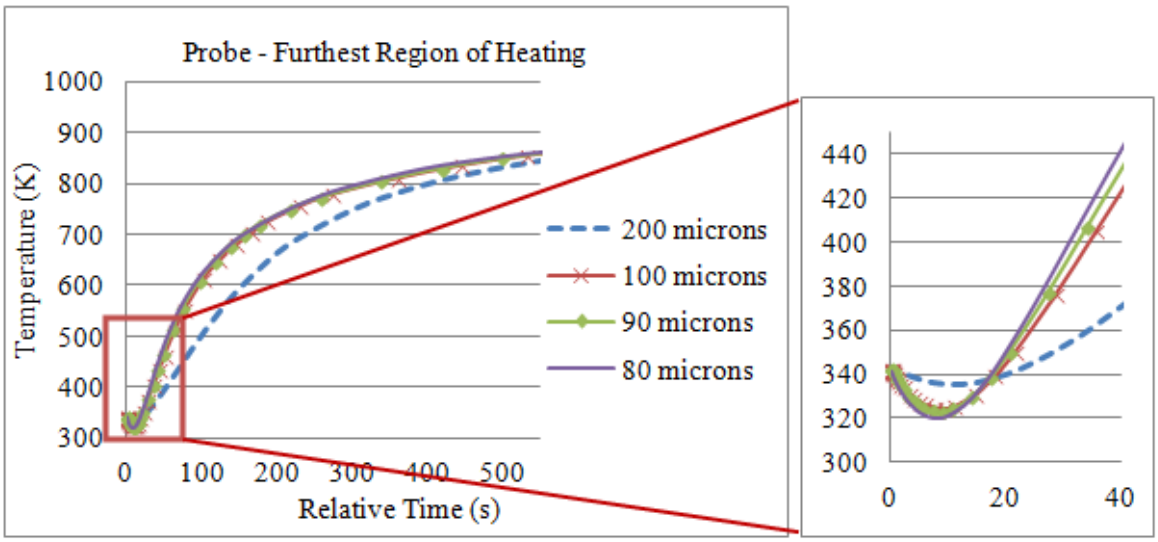

Figure 25(c). Droplets size / vertical temperature probe locations: further region of droplets. [Fuel: P-NF; Droplet size: 200-80μm; Amount: 100 droplets/64cm^3 testing space; heat kernel moving velocity: 0.005m/s]

a.

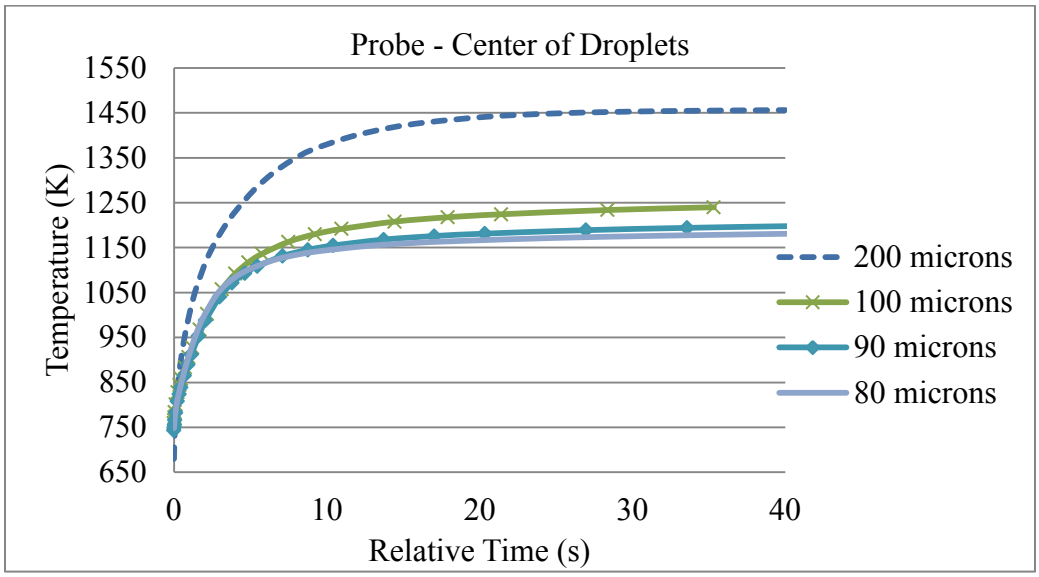

b.

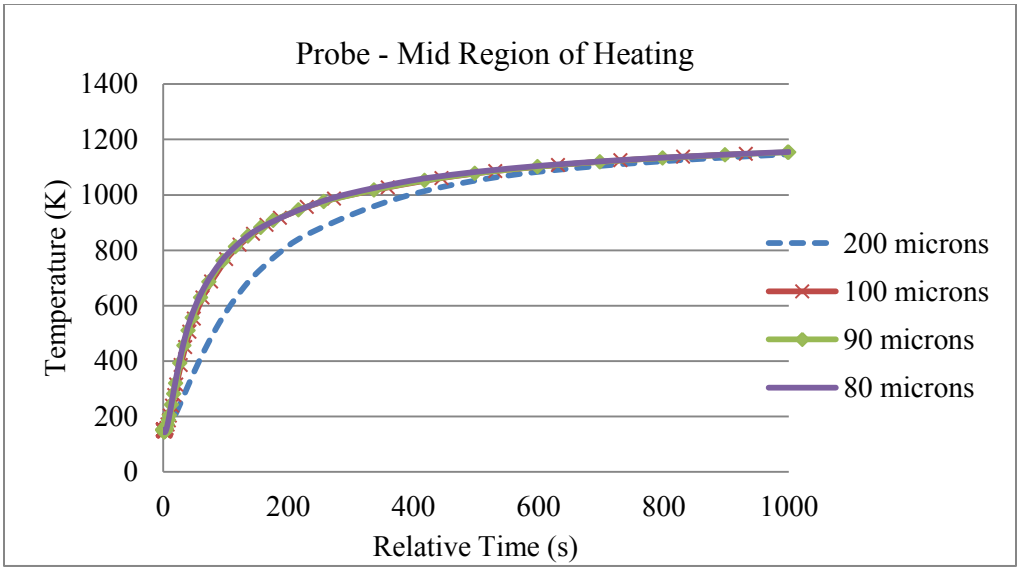

Figure 26(a-b). Droplets size / vertical temperature probe locations: a. center of droplets; b. mid-region between droplets [Fuel: D-600; Droplet size: 200-80μm; Amount: 100 droplets/64cm^3 testing space; heat kernel moving velocity: 0.005m/s]

c.

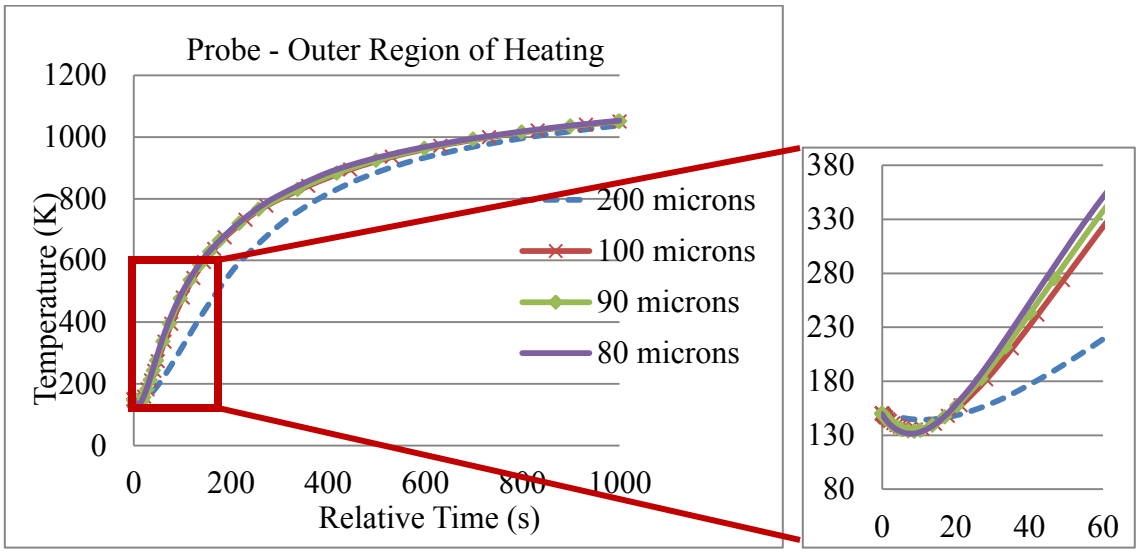

Figure 26(c). Droplets size / vertical temperature probe locations: further region of droplets. [Fuel: D-600; Droplet size: 200-80μm; Amount: 100 droplets/64cm^3 testing space; heat kernel moving velocity: 0.005m/s]

a.

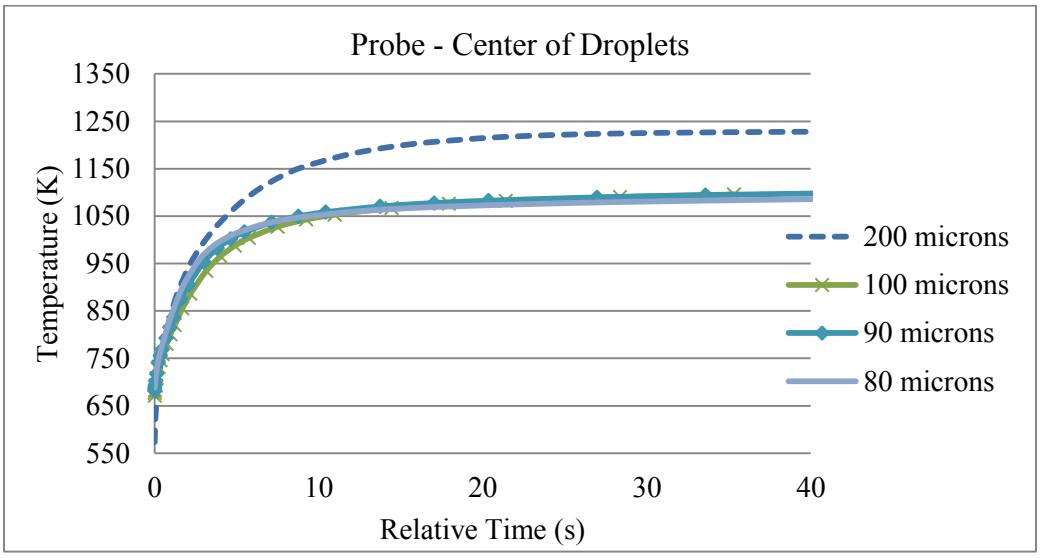

b.

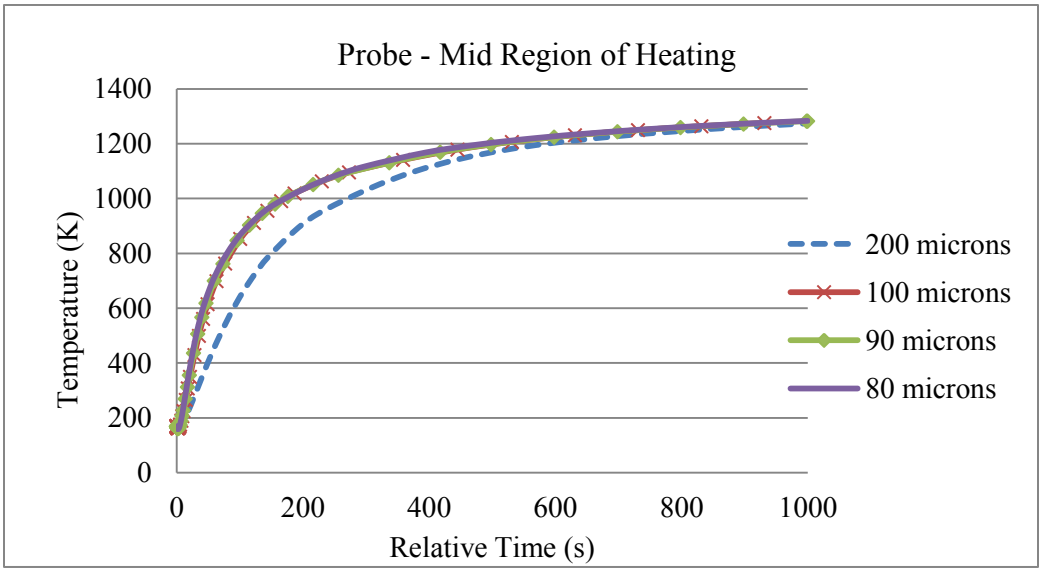

Figure 27(a-b). Droplets size / vertical temperature probe locations: a. center of droplets; b. mid-region between droplets [Fuel: PHE; Droplet size: 200-80μm; Amount: 100 droplets/64cm^3 testing space; heat kernel moving velocity: 0.005m/s]

c.

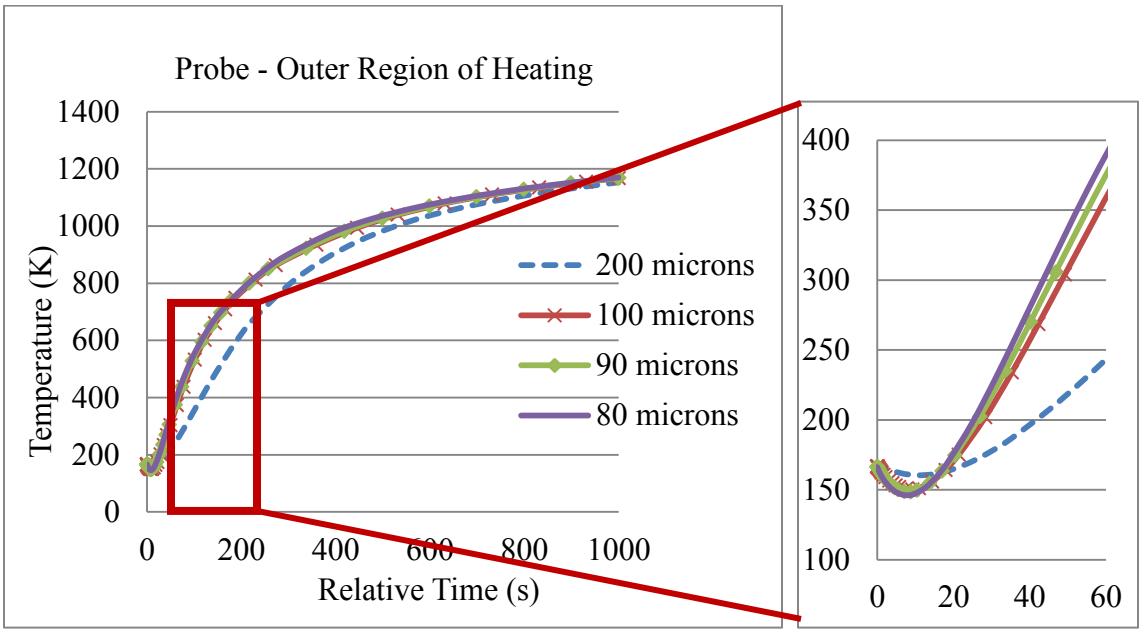

Figure 27(c). Droplets size / vertical temperature probe locations: further region of droplets. [Fuel: PHE; Droplet size: 200-80μm; Amount: 100 droplets/64cm^3 testing space; heat kernel moving velocity: 0.005m/s]

If reading with the horizontal flame temperature, we can see that there should be first ~10 seconds to sustain the flame to the parallel direction, due to the lower level heating supply; and the time after would be assisting the flame heat to propagate upwards and accept more droplet inputs to support flame from being quenched. From the probes located higher in the mixture region, at least 2 droplets above the boundary, there was a temperature drop in first 10 seconds, possibly resulted from the horizontal heat supply, and then the heating kernel travelled up with the flame it prepared and when there was enough fuel/vapor supply, the luminous flame would appear.

Among the different heat transfer fluids, though all have a similar tendency to change with droplet sizes, the variety of chemical components affecting temperature rise can still be observed. For instance, in the probe, droplet center, the heated system traveling upwards in D-600's case had a much higher slope (40K/s) than P-NF's (10K/s) in 200μm average droplet groups. In PHE, similarly, a 30K/s heating rate was recorded. It reflects that the large droplets have more heating effects within same amount of time, which indicates the energy applied, simultaneously, influences combustible matter evaporation (phase change) as well as flammable vapor temperature increase.

The starting point of a heavier fuel leads to a lower initial temperature state, but the following-up of rapid droplet-droplet / molecule-molecule interaction can bring the temperature of the whole system higher, with the microscopic and macroscopic positive effects. For the surrounding probes testing the secondary vapor phase induced from the original heated kernel, the fuel supplied played an important role in offering quenching effects to reach heat equilibrium; the thermal turbulence has similar results among P-NF, D-600, and PHE.

Summary

From the study of model coupling and the observation of simulation results, we have a better understanding on how the temperature distributes, the heat transfers from phase to phase, and how the primary, secondary, and final heat kernels carry the energy upwards. The ignition delay trend changing with droplet sizes under same number density fits the observed experiment results well according to the previous studies.

The main themes to interpret from the results are:

1) The “horizontal” heat transfer is the dominating effect at the beginning of the ignition source, allowing energy to flow into the aerosol system. Larger droplets had better heat effects, and the luminous flame would appear in a shorter time range with horizontal direction homogeneity in terms of heating. The more combustible matter exists in the initial heating system, allowing the whole secondary heat kernel to appear quicker.

2) The “vertical” heat transfer mainly dominates the secondary heat matter traveling upwards. Although most of the ignition delay time was for horizontally homogenizing the evaporated droplet sub-domain, the vertical heating was still the continuous energy transfer needed for the flame to propagate. The primary ignition source (pilot flame) does not have much impact on the continuous heating after the first 10-15 seconds due to the distance.

The smaller droplets, however, have a longer ignition delay. That is a phenomenon we hypothesized as the horizontal heating requires more time for energy transfer to induct the luminous flame. In this system of high flash point mixtures, the instability effect will be enhanced to lengthen the possible delay time. Once the homogeneous heated matters started to influence the upper region of the unburned aerosol system, the smaller droplets began to reduce the heating effect among the evaporated material domain so that more

time was required to have the vertical energy transferred into the flammable region. The conclusions also trace back to the results obtained from experimental approach.

This offered us a better understanding on when and where the sustainable, luminous flame would appear and propagate. In a practical case, once the flame front travels to the unburned region with adequate ignitability, mitigation shall be applied instantly on either reducing the concentration of droplets or lowering the temperature to avoid a luminous flame from occurring. This methodology can potentially be a starting point for future research on high flash point aerosol cloud fire hazards and loss prevention, and a design on the setting of flammable matter detectors.

Our stage of research is still on the fundamental aspect of the combustion phenomenon stage, with a more detailed focus on ignition delay time, which reflects the initial flame appearance in the induction of sustainable flame. The design of mitigation system will be a more complicated issue due to the targeting of multi-phase materials surrounding ruptured equipment, failed valves, and so on.

CHAPTER IV

THE INFLUENCE OF ELECTRIC FIELD AND CHARGE DENSITY ON AEROSOL IGNITABILITY TESTS INSTABILITY

Background and Problem Statement

Whenever research involves ignition regarding energy transfer and accumulation locally in an aerosol system, the electric field's influence on droplet size distribution and the energy transfer rate cannot be ignored. The electrospray method has long been used in NMR sample formation, surface spraying, and other detailed and delicate industry processes. It has the great benefit of droplet size and flow direction control, so that researchers can easily obtain a monodisperse spray. However, the charges surrounding droplets having an unknown influence on ignition, heating, and spray stability due to turbulence produced by electrostatic field with a high voltage attack. Not only does this charge the aerosols but also the scattering fuel vapor can be affected by the extra charges from the natural flow-performed electron density. Dunn *et al* (1994) analyzed electrically-charged droplet inter-spray mixing for both dynamic and kinetic process of the spray suspension of droplets. They found out that under specific circumstances, such as mean velocity component magnitude decreasing zero at the center of electrospray, the cone jet mode originally release by minute nozzles from spray head (Mejia, He, and Cheng, 2009) would move laterally away from the center; the velocity component would then fluctuates before returning to a scale around zero. This transition of electro charges

might have an impact on droplet trajectory during evaporation, change of density, and temperature rise. Mullins *et al* (2010) also indicates from their research on surface tension with an electrostatic charged aerosol collector, that the Reynolds' number of aerosol flow in ambient air shall be highly dependent on the airflow rate, making it is the source of turbulent friction charge accumulation on the traveling droplets (Figure 28).

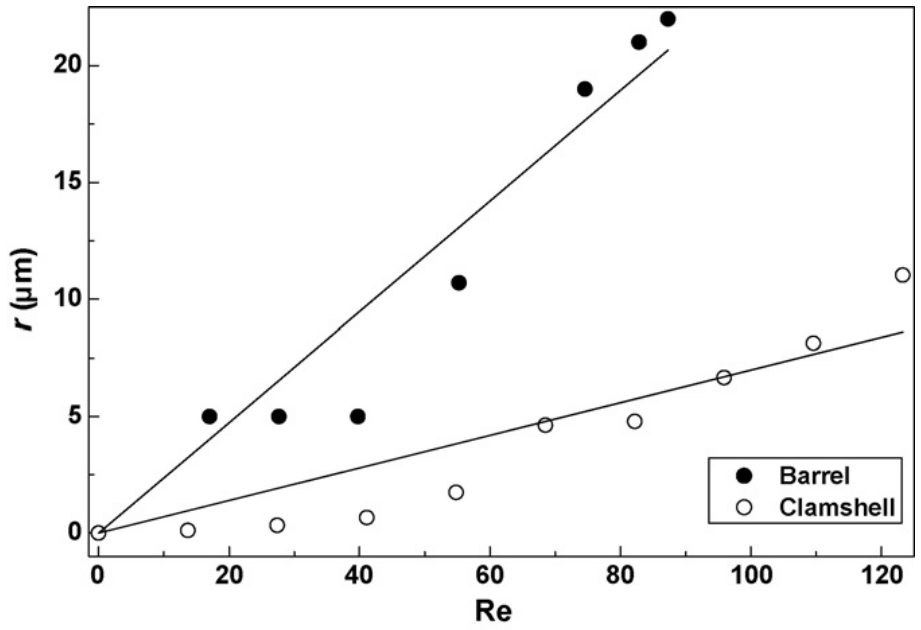

Figure 28. Extension of droplets with increasing airflow (Re); Barrel and Clamshell are the two target aerosol liquid droplet collectors in the study. (Mullins *et al.*, 2010)

A fundamental way of explaining the microscopic droplet-charge interaction by Wilm (2011) had proposed a methodology of mass spectra ionization of a material spray, saying that the charged droplets would have been evaporated and sustained by the electrons added to their surface; this procedure included the droplet evaporation and electron residue. Once the droplets are formed, their solvent starts to evaporate while

they are in flight. Solvent molecules leave the droplet as neutral particles, leading to an increase in the field density at the surface of the droplets. In less than a few microseconds, the threshold field density is reached, and a new Taylor Cone mode forms on the droplet, which ejects highly charged small droplets. If the droplet is not perfectly spherical, this process will occur at an apex point of the droplet, which is the point with the smallest curvature radius. The plot of the mechanism is shown in Figure 29.

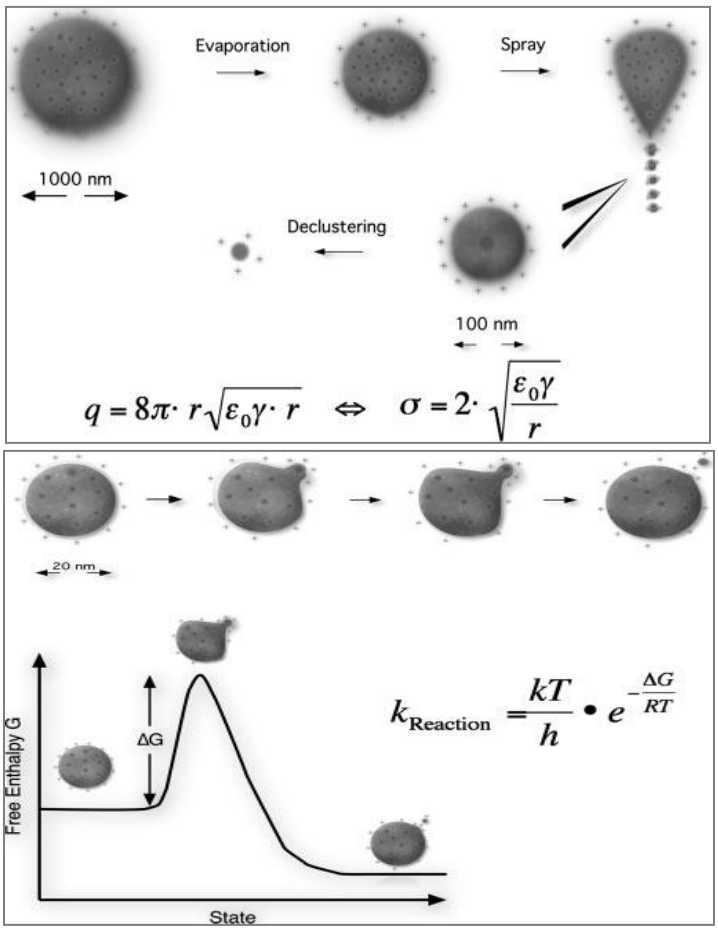

Figure 29. The Fuel droplet Evaporation and Charge Residue Mechanism of Electrospray Process (Matthias Wilm, 2011)

According to the figure, the droplet can be said to have a clear relation of charges with electrospray formation method. The two main parts are (1) the ion evaporation process, and (2) the charge residue process. The ion evaporation process is when an individual ion leaves the charged droplet in a solvated state. The electric field strength at the surface of a droplet is so high that the energy required to increase the droplet surface is rapidly compensated by the gain due to the Coulombic repulsion. (Variables: $k_{Reaction}$, reaction rate constant; k, Boltzmann constant; T, temperature; h, Planck's constant; R, ideal gas constant). The charge residue process is when a highly charged droplet shrinks by solvent evaporation until the field strength at the location with the highest surface curvature is so large that a Taylor Cone forms. From the tip of the Taylor Cone, other highly charged smaller droplets are emitted. This process can repeat itself until droplets are formed that contain only one analyzed molecule. This molecule is released as an ion by solvent evaporation and de-clustering. The equation describes the maximum charge a droplet can carry before the Coulomb repulsion overcomes the surface tension. Locally, it is the condition for the formation of a Taylor Cone. (Variables: q, droplet charge at the Rayleigh instability limit; r, droplet radius; ε_0, electric permittivity of the surrounding medium; γ, surface tension; σ, surface charge density.) Similarly, Mullins *et al* (2010) also mentioned the breakage of droplets after a series of charge application and droplet motion (individually and interactively) that the diameter changes from the very early stage of spraying, and since droplet size is a significant flame propagation index the ignitability of the aerosol system may change (shown in Figure 30).

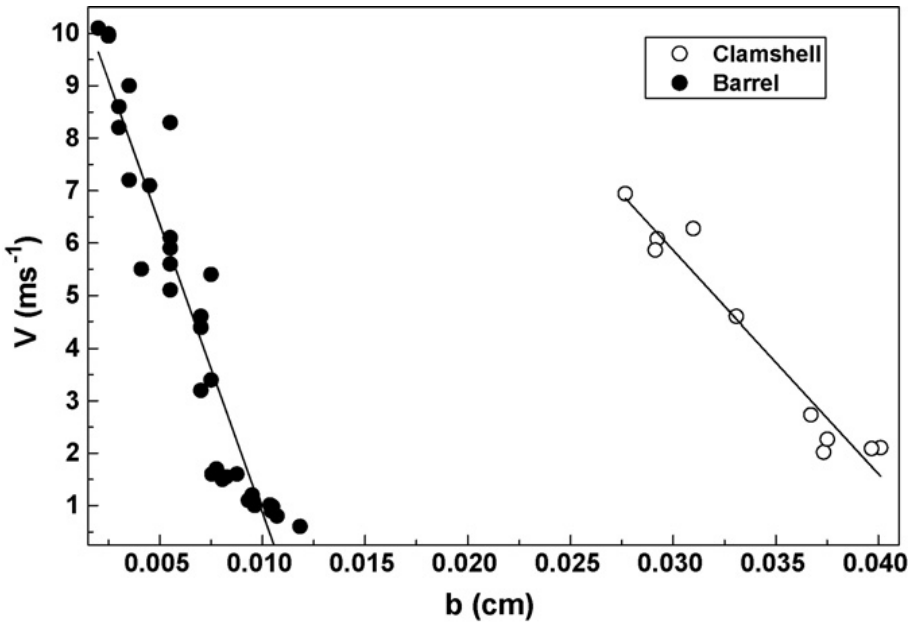

Figure 30. Air velocity at which droplets flowed down the surface in relation to droplet diameter. The flow velocity changes charge density in this case. (Mullins *et al.*, 2010)

In our proposed study, as long as we consider the energy transfer to droplets for the sustainable flame, experimental system stability, and the ignition source heat transition procedure, the electric field shall be eliminated in the effects by introducing models while analyzing experimental data, and comparing the error percentage which would not purely come from an ignition source. Also, for electro-sparks as an ignition source, we still need to consider the extra charges applied with the electrode discharge, and the reflection on ignition energy, droplet size distribution, and the traveling of the flow aerosol system while considering dispersion in a controlled space if we reach further to the aerosol explosion field. Studies conducted in this chapter will explain the actual impact that charges have on droplets, and which part of properties is majorly deviated.

Methodology

To take a more accurate control of ignition with a charge density, the source of ignition was changed to a controlled igniter. The pair of electrodes protrudes into the ignition chamber through the opening at the same height of the viewports on the chamber wall, in the direction that is perpendicular to the axis through the viewports' centers. Ignition sparks are delivered to the sprays by the electrodes. A custom-made circuit which receives power from a power supply (Topward 6603D) supplies the electric voltage to the electrodes while sending the voltage and current information upon the appearance of sparks to the computer PCI board for data recording.

The spark energy is mainly controlled by the voltage setting of the power supply, and the current during the spark is limited by the current limit setting of the power supply. The optimum spark energy range is 10 to 200 mJ. The gap width between the two electrodes can be adjusted with the optimum range from 1 to 4mm to create the optimum spark energy range. Spark frequency is controlled by the spark generation circuit, which receives a signal from a function generator (Stanford Research System, DS345). Spark frequency can be adjusted by the function generator's frequency setting. The spark frequency ranges from 0.01 to 5 Hz. A LabView program is designed to calculate the spark energy from the voltage and current data received in the PCI board.

The experimental process of spark ignition on aerosol is:

(i) Connect the spark electrode to the chamber. When the aerosols droplet properties become stable, electric sparks are generated from the spark generation system.

(ii) Electric sparks are generated, under the same ignition energy and spark gap width (for example 50mJ and 2mm), for 50 times. Ignition and subsequent combustion of aerosols in the chamber are detected by the Spraytec and visual observation through the viewports. Times of the successful aerosol ignitions are recorded, and the ignition frequencies are calculated. If no ignition occurs during the spark generations, spark energy is raised until ignition is observed.

(iii) Test of influence of different spark electrode configurations: under the same ignition energy level, spark gap width or spark current limit value is adjusted separately, following similar steps in (v) to get the ignition frequency values.

(iv) Test of influence of different spark energy values: for different spark ignition energy values, follow similar steps in (v) to get the ignition frequency values.

(v) Test of ignition behavior of aerosols with different droplet size and concentration values: change the aerosol droplet size by adjusting the electrospray syringe pump flow rate and electric voltage on the spray nozzle. When the aerosols droplet properties become stable, steps in (i),

(ii), and (iii) are followed to get the ignition frequency values for aerosols with different droplet size and concentration values.

The electrosparks lighting the aerosol system are segregated into two major categories: high end (which is close to the literature ignition energy for heat transfer fluid vapor cloud); and low end (which is 10-30mJ less than the lower limit of high end electrospark energies). This is to ensure that all the standard testing methods from ASTM are supplied as reference for potential aerosol testing standardization. The higher end ignition energies are the successful ignition case in the aerosol system. Furthermore, aerosol ignition energy shall cover the range from the highest reported ignition energy, which is supposed to be the vapor case, and the energy adequate to ignite liquid release in a normal temperature and pressure condition. After obtaining the ignitability with regard to the igniter energy, a series of coupled models can be discussed and launched from the experimental results to describe the changing of charge density regarding the aerosol flammability parameters studied in previous chapters. Since there is no accurate way to measure it directly, the igniters' energy input is assumed to have an average of 76.2% absorbed into the aerosol system from a droplet motion study of diesel engine electro-ignition testing (Chrigui *et al*., 2010). The excess energy applied into the aerosol system of P-NF, D-600, and PHE are fully used to sustain flame. A comparison list on applied voltages from electrospray and the flammability change with specific igniter energy, the change on droplet sizes / concentration, and the ignition temperature rise locally among aerosol systems was obtained. This can be considered as a combination of previous two parts of study under a defined ignition source.

Results and Discussion

The experimental results were calculated with the Coulomb electric energy law for obtaining surface density regarding the absorbed energy. The energy density is defined as the total electric energy applied onto each droplet, which was estimated from $D_{[3][2]}$ of each test with various voltages in the aerosol formation process. Figures 31 to 33 shows the three heat transfer fluid results.

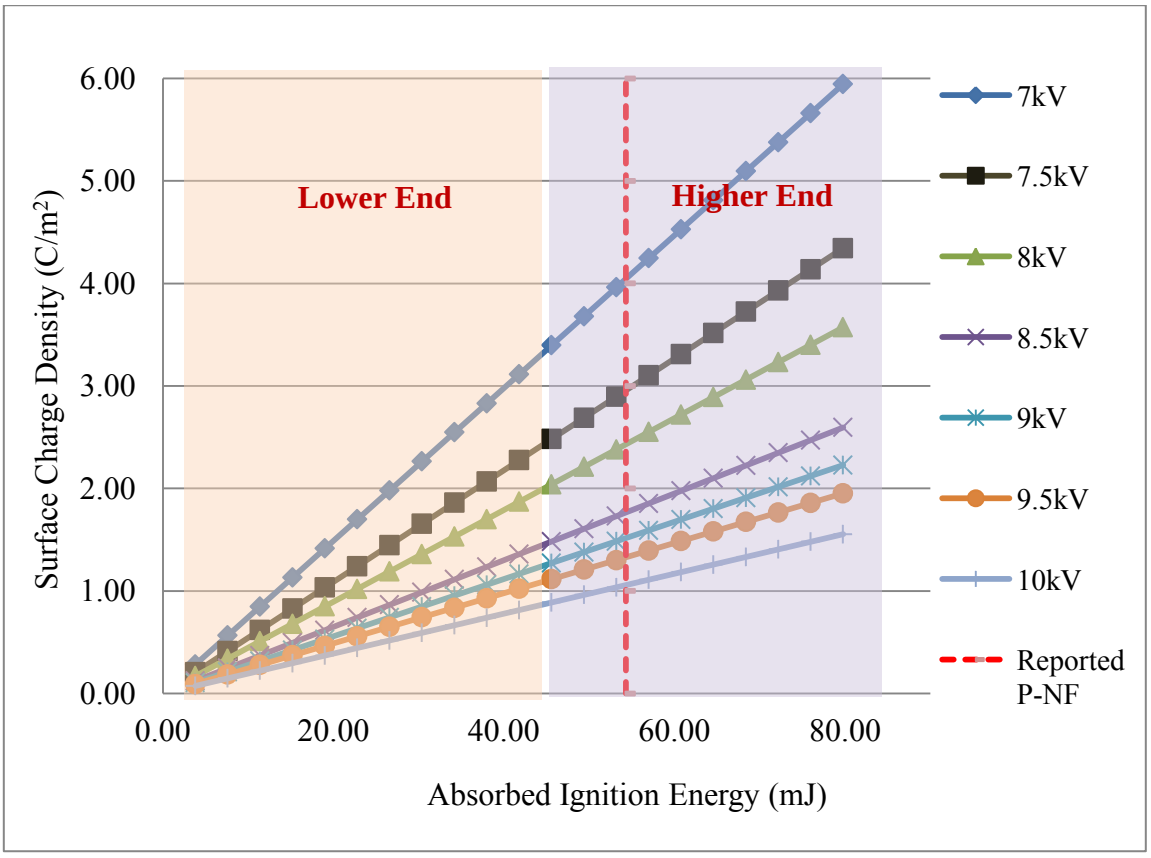

Figure 31. Electric Field Application on P-NF aerosol system with Ignition Energy

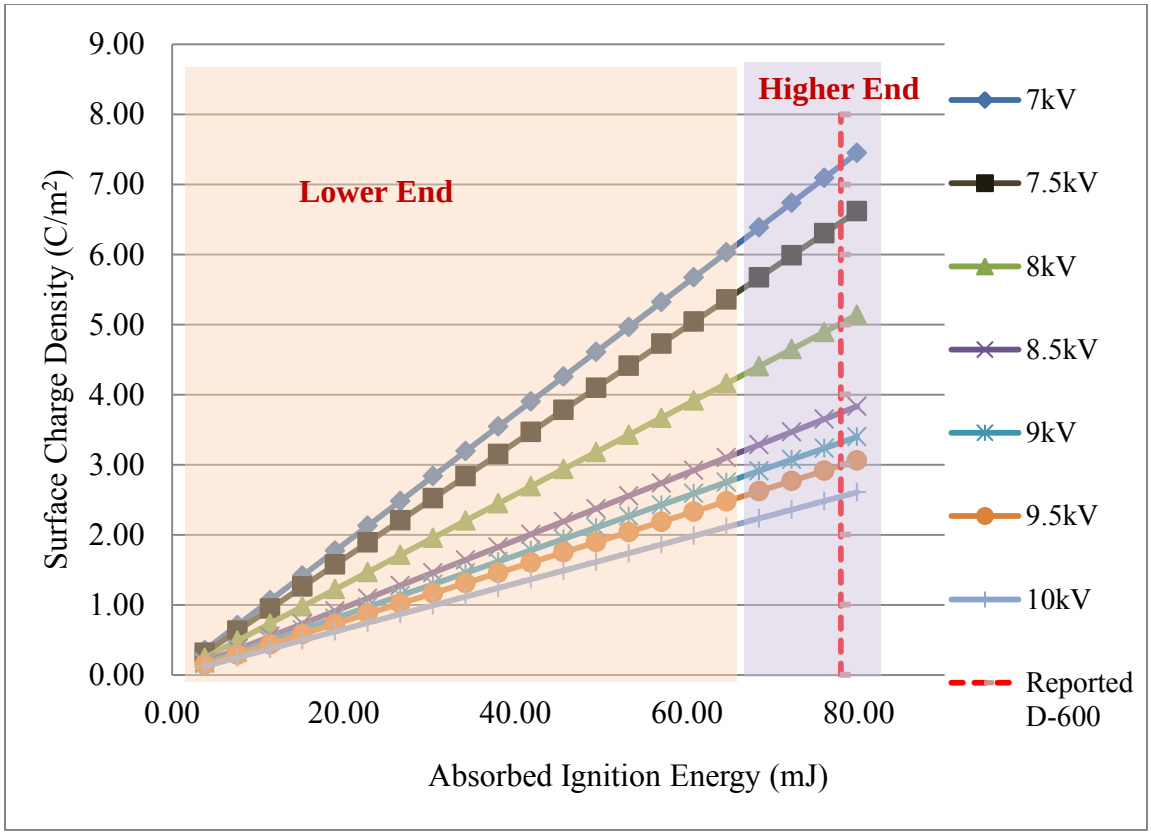

Figure 32. Electric Field Application on D-600 aerosol system with Ignition Energy

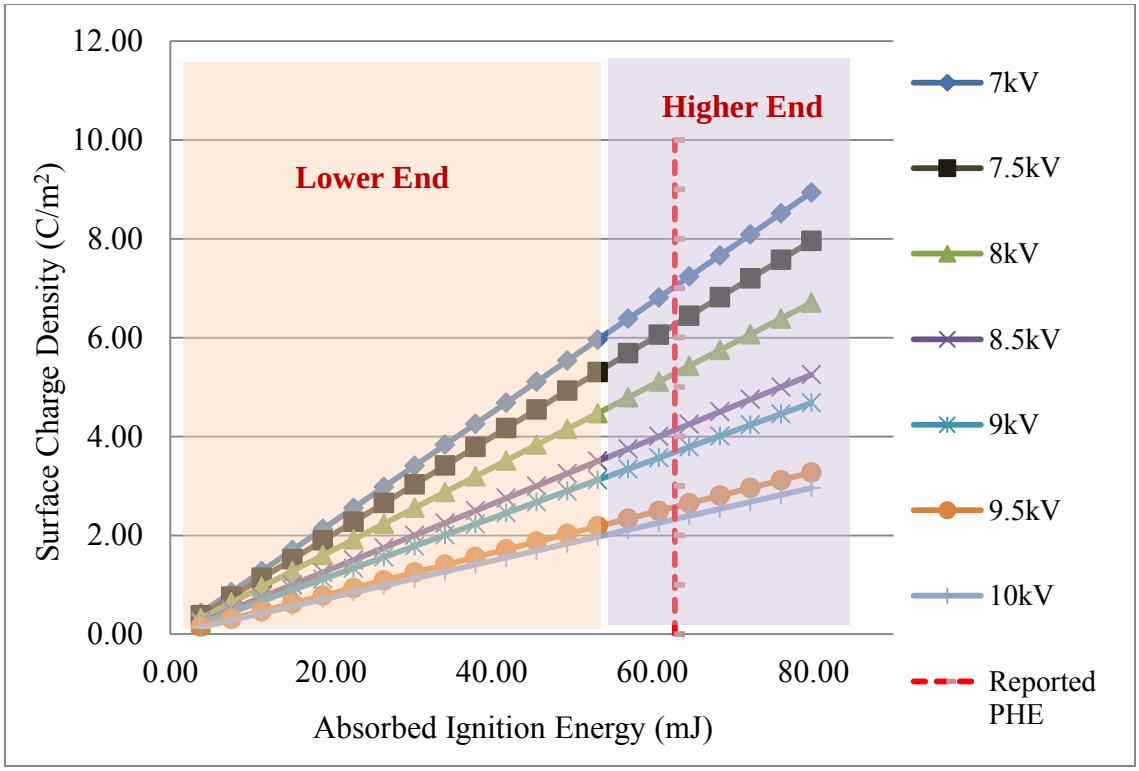

Figure 33. Electric Field Application on PHE aerosol system with Ignition Energy

From the ignition energy trend, the charge density change, and the reported ignition energy on flammable vapor state, we see that in lower electrospray voltages given the slope of charge density change dropped more. With a more rapid change in the Sauter Mean Diameter, a weaker electrostatic field applied a wider range of ignitable surface charge density increments. This explains the tendency of an aerosol with a higher voltage applied shall have more time to increase the whole system into an adequate state to ignite. In the energy aspect of aerosol ignition, initial charges applied by electrospray may cause a positive effect on the heating rate; however, when the voltage goes higher, the increased surface charge density tends to result in droplet breakout and instability in

the traveling trajectory, which may be the root cause of turbulent conditions making the system less likely to be ignited.

On the other hand, the sufficient droplet surface area for ignition is considered to be the area in the reaction zone at the time of flame occurred. Those parts can most efficiently absorb energy from an ignition source, cover the surrounding liquid phase of fuel, and then burst into flame once the condition permits. Electric fields of the high voltage applied is significant in the beginning of heating, as mentioned, while the droplet interaction due to charge accumulation and opposing effects among the system individual particles played important role for the heat transfer in the later process. Even though the charge offers energy which may be up to 5-10% of the ignition energy; however, for each droplet or droplet group with similar Sauter Mean Diameter, the anti-affinity reduces the chance for droplets to evaporate with constant air flow locally.

Except for the issues listed above, for most cases, the electric field still offer a positive effect on expanding aerosol ignition energy range by 12-15% away to towards the reported value from heat transfer fluid under normal condition. The extent of this impact is far lower than the aerosolization itself on ignitability of fuel comparing to pure vapor. Electron motion is difficult to keep track comparing to the macroscopic influence of vapor domain behavior with a sufficient pilot flame as the ignition source. Thus, there is a need to evaluate the results from experiment by modeling.

We modified the model derived from the previous chapter, and checked the ignition delay time under various applied voltages; the results of sustainable flame appearance delay time are shown in Figures 34 to 36.

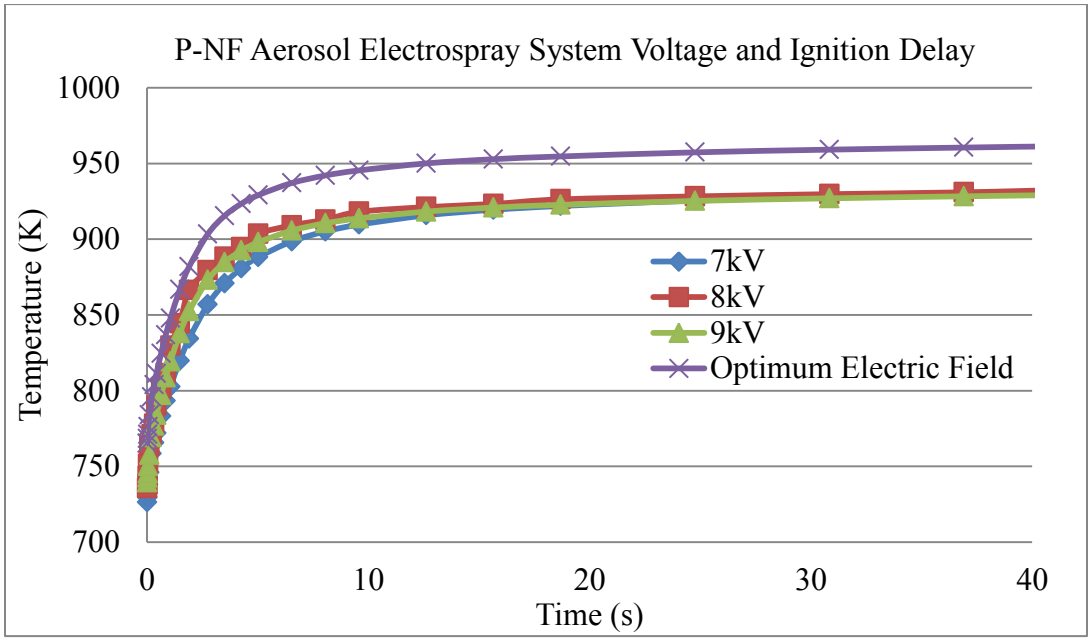

Figure 34. Ignition delay time of temperature reflected by droplet center, P-NF

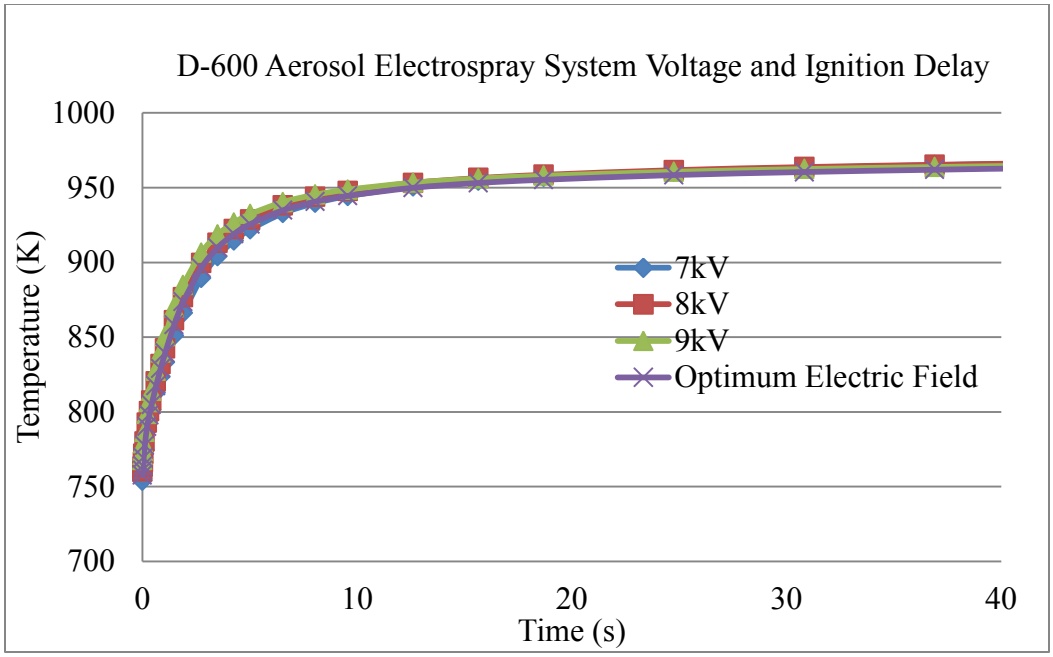

Figure 35. Ignition delay time of temperature reflected by droplet center, D-600

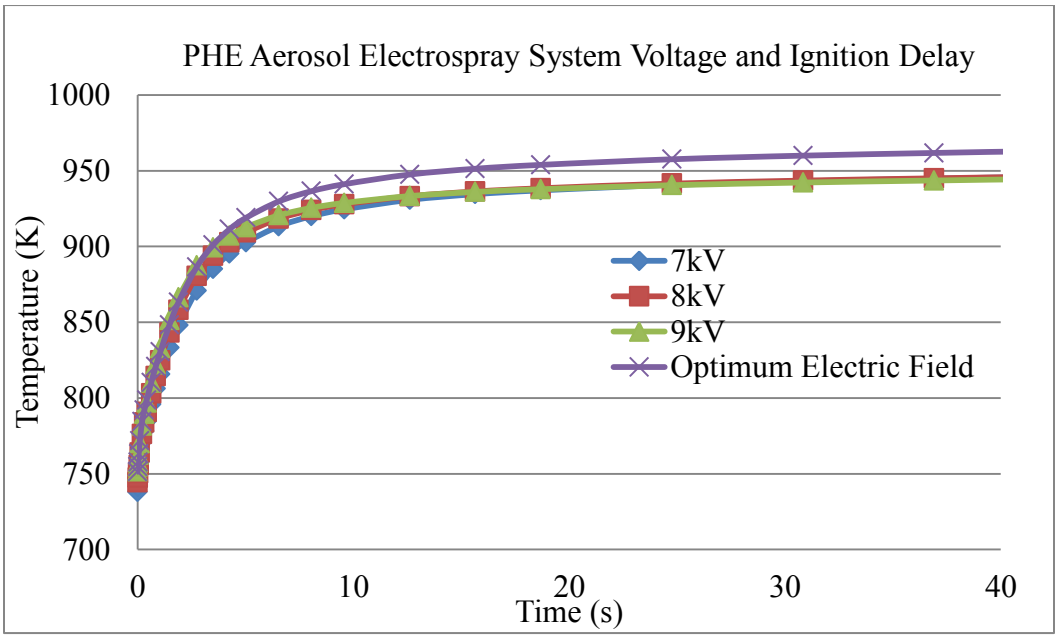

Figure 36. Ignition delay time of temperature reflected by droplet center, PHE

The droplet center domain temperature monitoring is the reflection of heating effects directly on the fuel system. The optimum electric field is derived from dynamic averaging of the voltage applied and from the electrosparks given upon the initial droplet (the heated kernel, as in the previous chapter). For P-NF and PHE, the optimum voltages tend to bring a stiff slope to temperature increase, which means the luminous flame would appear earlier under the same ignition source energy; on the other hand, D-600's optimum voltage among the setting condition is close to the segregated applied voltage estimation, which means the electric field was more homogeneous in its case.

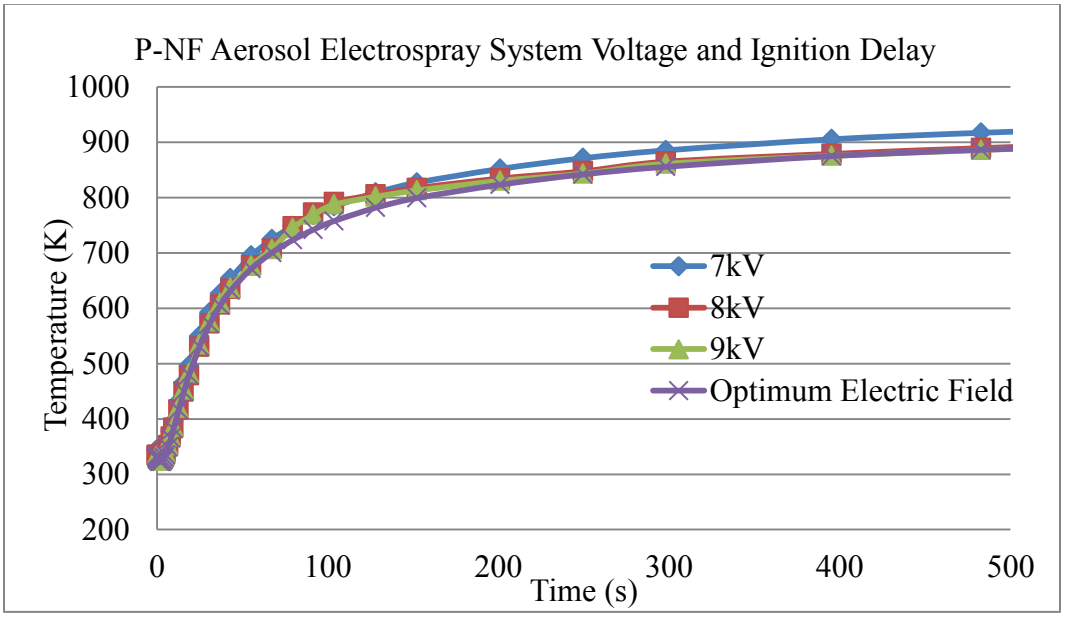

Figure 37. Ignition delay time of temperature reflected by vapor domain, P-NF

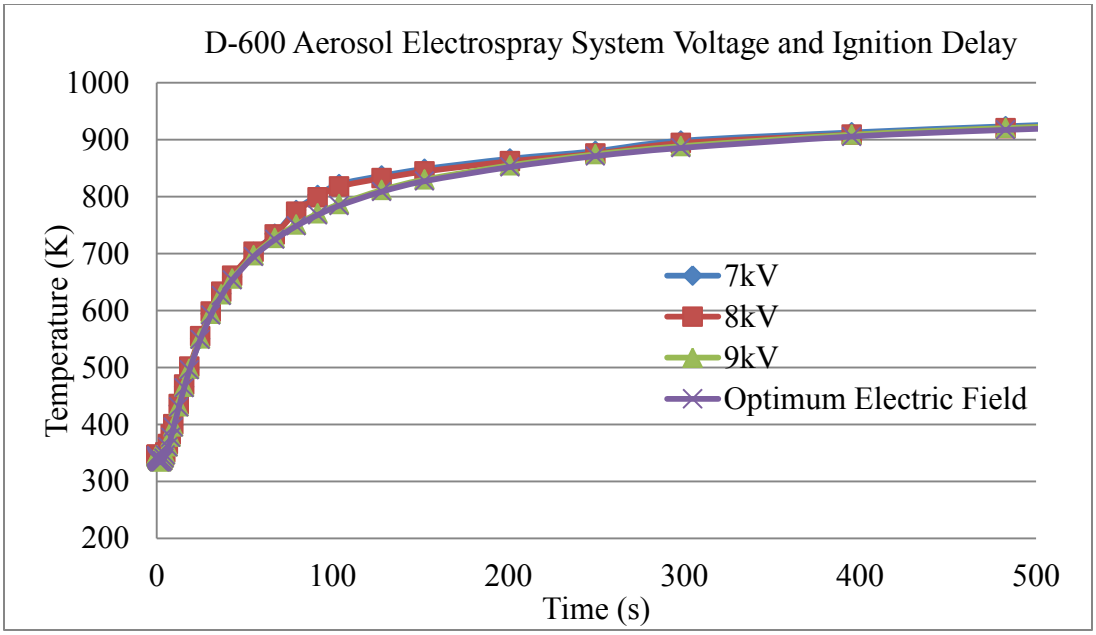

Figure 38. Ignition delay time of temperature reflected by vapor domain, D-600

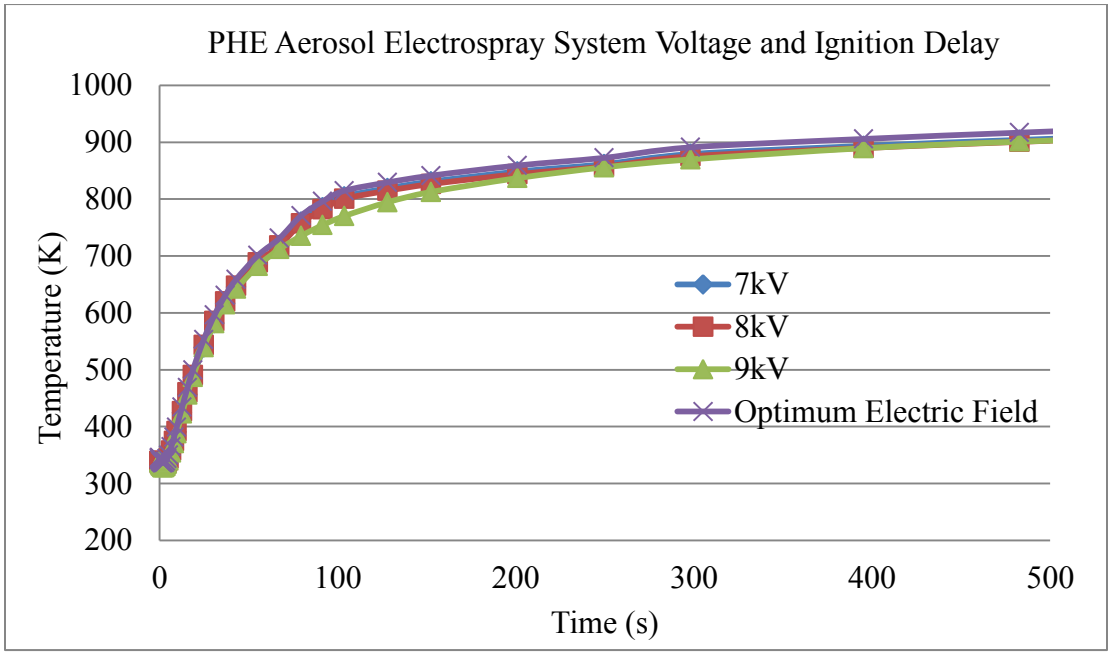

Figure 39. Ignition delay time of temperature reflected by vapor domain, PHE

In the case of vapor domain surrounding the droplet system, the optimum electric field has shown a very close relation with possible experimental conditions. Those vapor domains are the parts being heated before the droplet center, with a lower convective coefficient comparing to the pure liquid phase with droplets. The charges accumulated upon droplet surface slowly generate the heating for evaporation to occur. Once the droplet evaporated with the external heat source and the charges on it, the size would shrink and produce a higher charge density locally on the droplet surface; thus, the charges resulted in a higher repelling effect on the droplet interaction, reducing the heat transfer efficiency and lessening the temperature increase rate.

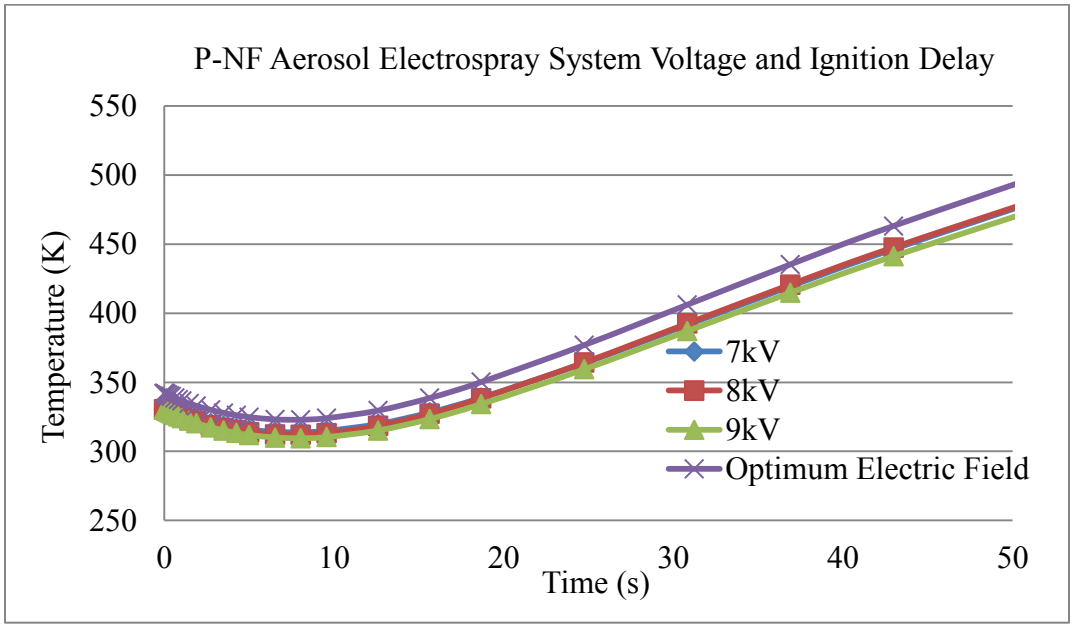

Figure 40. Ignition delay time of temperature reflected by kernel heating surroundings, P-NF

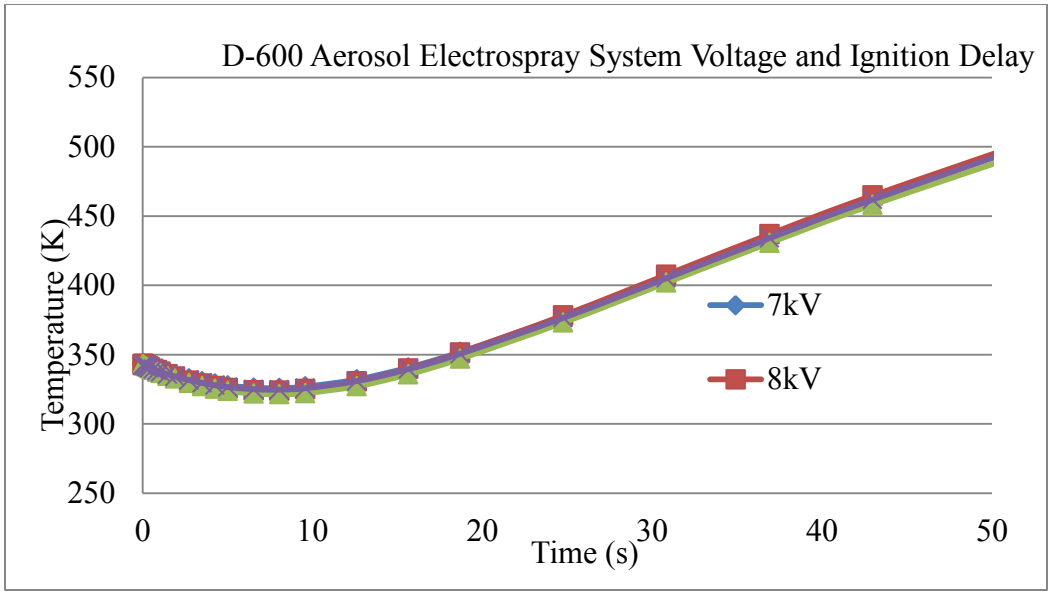

Figure 41. Ignition delay time of temperature reflected by kernel heating surroundings, D-600

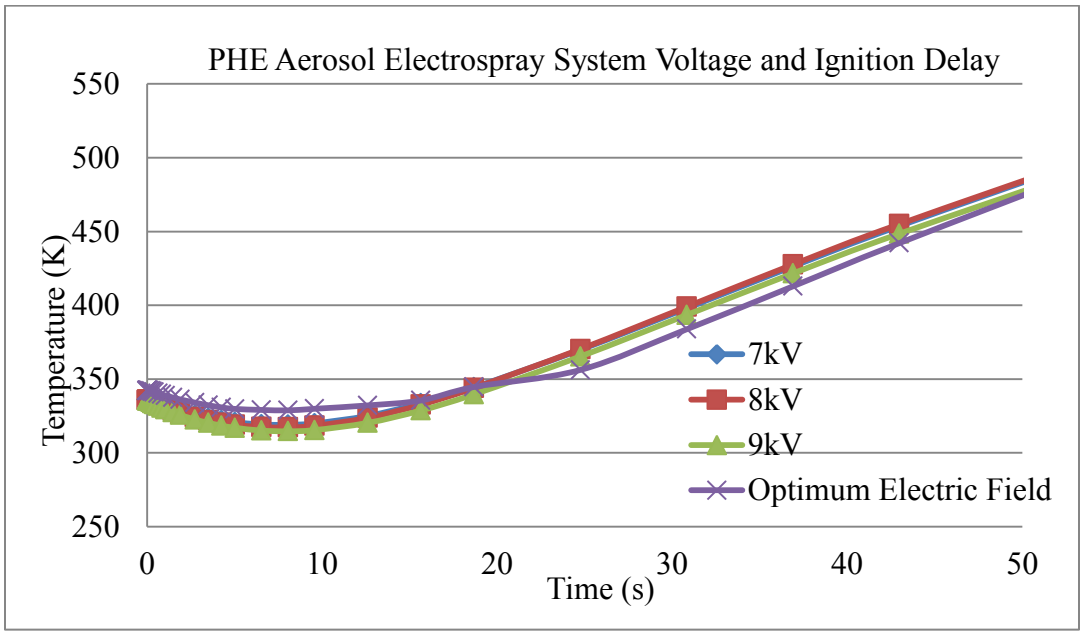

Figure 42. Ignition delay time of temperature reflected by kernel heating surroundings, PHE

The kernel heating surroundings is the domain covering 50% to 100% of the distance between the initial heating kernel (produced by electrosparks) and surrounding vapor domain of droplets. In this potentially ignitable region of the aerosol system, the vapor property regarding electric charge density are less likely to be considered in specific trend of change. For P-NF, since the lighter vapor content evaporated a higher portion of fuel in the fuel-air mixture under same time of initial heating, the optimum electric field suspended among droplets are more homogenous statistically; thus, the voltage dynamic average is higher in unit time.

For D-600 the optimum electric field is lower in general compared to original voltages applied each time, which means that within ignition delay time for droplet and vapor domains the heating effects for surrounding air is negligible. This is supposed to be the property of mineral oil with higher surface tension in liquid phase, and the transition of charges might occur while droplet size becomes larger (yet not too large to eliminate the flammability limits). The air-fuel mixing effect of PHE, however, resulted in a temporarily higher optimum electric field due to the turbulence at the first stage of evaporation with fresh input; then when more flammable vapor had been produced and the heated kernel with most vapor contents began to heat up its surroundings, the charge density, again, reduced the effects which are more likely to be determining forces in higher liquid contents. The optimum electric field reduced and increased temperature locally with a slower pace. The electric field had an impact on droplets, especially the liquid phase transitioning to vapor.

Most of the influences were observed and verified by modeling under initial heating of ignition source and in the beginning stage of evaporation. Charges applied energy and shrinking effects on droplets to assist in heat transfer. Nevertheless, while more flammable vapor started to take place increasing fuel-air fraction, charges started to suspend in gas molecules and further segregated the remaining droplets, causing an opposite effects on heating and ignition delay time. The average time for P-NF is around first 10-15 seconds, while D-600 and PHE have less regular trends due to fuel component complexity and heavier weight per unit volume. Dense vapor with higher molecular weight contents transfers energy easier. Paraffins and heavier mixtures, according to petroleum studies, do have a better chance to form colloids during heating/cooling and external electric field attendance (Mansoori, 1997). The internal electrons and external charges of droplet-air groups are the driving force for turbulence of flow system aerosols traveling from the spray nozzles to ignition source area, and this time is also significant while discussing the ignition delay.

CHAPTER V

CONCLUSIONS

The study of aerosol ignitability testing method, flame development procedure, and the re-visit of electric charges influence to refine the research tool, are the main concerns of this dissertation. This is not a new field for analyzing aerosols and flammability, but it is certain that our approaches, points of focus, and framework opened from results are innovative enough to close the potential hollows in the aerosol studies. Two-phase flow has been discussed over years on flammable liquid-formed aerosols, and the chemical properties regarding molecule level reactions with heating process. Based on previous studies, a series of testing and modeling were conducted in our research process, obtaining important findings which may result in different ways to think over the "ignition" and "sustainable flame appearance" phenomena.

From Chapter II, the useful tool for aerosolized materials with high flash point in the liquid state was generated in terms of droplet size and reactive fuel concentration under a controlled, open-flow system. This simulates perfectly the practical case on pipeline or vessel leaking in storage or operating conditions, with the surrounding under ambient pressure/temperature and the fuel under high pressure and specific flow rate. The ranges of ignitable droplet-air mixture systems are from 0.5 ppm to 1.5 ppm in lower droplet sizes, and generally narrow down when droplet sizes grow larger by controlling the feeding rate and applied voltages. The control of electrospray was tested and analyzed to

the extent of its impact on fuel aerosol properties, which is comparable to previous studies. As chemical properties on flash point, viscosity, and average molecule weight (*i.e*. carbon numbers) increases, the ignition became more difficult under the same stable pilot flame as an ignition source. Besides, the influence of aerosolization on fuel comparing to its pure vapor case was also assessed. From the results, a clear trend can be observed that aerosolization of a fuel is able to change the flammability range within specific droplet sizes and concentration. With higher carbon numbers, the fuel tends to draw close to lower the LFL relatively more to its on UFL. For lighter heat transfer fluid such as P-NF, aerosol state can expand clearly both on the LFL and UFL, which means it is harder to reach fuel-rich conditions.

From Chapter III, the experimental observation and computation modeling on aerosol system ignition delay were discussed. Since heat transfer fluids are mostly mixtures from various ranges of hydrocarbons, such as mineral oil, the system stability is sure to be much lower than pure materials. By coupling the models of fuel input, droplet evaporation, and heat transfer among vapor and liquid domains, we obtained a more complete model which can track down the temperature changes from various probes set in different regions of the aerosol system. As heating effects took place and traveled upwards to form a new ignition source upon the primary pilot flame, the droplet groups' interaction revealed an ignition delay time change depending on the mixed effects from horizontal heating homogeneity and vertical convection for new fuel feeds. The temperature change can be observed to determine when the luminous flame would appear. As the results showed, we concluded that heavier fuel has better heating effect

sustainability with a shorter ignition delay time. The initial temperature increase was lower due to more combustible matter; however, the slope of the temperature increase grew steeper once the initial horizontal heating was over, which contributes to the first ~10 seconds of ignition delay. The vertical temperature rise, on the other hand, determines the secondary heating effects which forms 10-40+ seconds of ignition. For mitigation and droplet detection design in process plants, this "response time" from ignition source existence to hazardous flame occurrence can be adapted to adjust the setting.

Finally, from Chapter IV, a more fundamental analysis on the testing method itself was discussed for future research as a reference. All tools for flammability testing have their deficiencies. Electrospray is a good way to generate droplets in minute, specific sizes under control; however, the charges existing on the droplet surface may have great impact on the energy level required to cause fire hazards. From what has been developed in other electrospray applications, such as NMR, a higher charge density is proven to increase the change and shorten the time for droplet breakage to happen, making smaller droplets and inducing turbulence within the aerosol system. From the simulation results we designed from experimental conditions, it is descriptive that for achieving the optimum voltage applied in heat transfer fluid aerosols, the ignition delay time can be reduced due to higher energy addition to each droplets. On the other hand, under the same amount of electrostatic field, lighter chemicals more easily form smaller droplets which have more positive effects from the electric charge heating. However, this difference from no electric charge addition with high voltage supply reduces the

significance in heavier molecules with tighter affinity between droplets, especially in the further time of heating, which the original heat source energy has been suspended and the evaporated vapor phase increases in fraction. The final combination of impacts concludes the performance on D-600 and PHE with a lower, unstable optimum average voltage. Thus, we shall be able to claim that the charges are more effective in chemicals with higher volatility, since the energy supplied from electric field can rapidly increase the rate of evaporation and during the droplet breakage stage more combustible matter can be heated efficiently.

This research covers a more refined study based on previous analysis on electrospray-generated aerosols from heat transfer fluid. The ignitability is re-defined from the criteria used by pure vapor material states; the ignition delay and flame appearance are analyzed in a completely coupled model; the potential deviation from heat transfer fluid testing is pointed out through charges among droplet surface and assessed. The whole logic can be used to cover high flash point fuel aerosols and their complicated flammable conditions.

CHAPTER VI

FUTURE WORK AND SUGGESTIONS

A General, Broader View on Lab Scale Aerosol Formation and Ignition

First, much more data are needed to provide ignitibility evaluation from the control attempts to apply on the experimental equipment. Now the smallest electrospray droplets we produced with this setup is around 80 microns (stable; there were other sizes appearing in a short range of time), with more stable cases occurring in the range of 100-150 microns. We want to achieve a more specific range of droplet sizes, have confined space to analyze the concentration and fuel-air ratio for discussion on closed system leaking hazards, and expand the flammability table both horizontally and vertically.

Second, the ignition delay time and combustion process will be introduced into the flammability characterization criteria. To better understanding the ignition process, we plan to study the reaction system and the combustion tail gas by using the methodology introduced by E. Gutheil (1993) that the ignition delay time might be highly related to the chemical kinetics of the combustion of radical concentration profiles. The droplet size distribution, fuel spraying temperature, equivalence ratio (fuel-vapor), and spray lifetime will be considered as the 4 parameters of dominating influential forces to understand the ignitability or aerosols.

Third, more heat transfer fluids that had been evaluated in terms of combustion process and flame propagation by former researchers shall be tested in terms of a supply in database, as well as the other potentially hazardous chemical species. There is a strong need to find out more hazardous scenarios which have been reported as incident causes or near-miss event reasons, such as spraying surface operations, droplet streams impingement, and other potential scenarios. This will help us solve the real-case problems in the industry and lab-scale liquid handlings.

Fourth, for the simulation part, we have not applied more detailed statistical droplet size distribution into our model, using the direct read and Gaussian estimation from the equipment and software settings; in our theorectical studies, instead, we add only the lab scale Bayesian modification onto it with COMSOL Multiphysics. The flow state was assumed to be steady, but in real cases we should consider the droplet spraying deviations in route, and the local coalescence of droplets due to electric field instability. We need to find out how those factors influence our experiments and apply the estimated errors into our simulation as well. Other than this part, we will keep on developing more models and their own specific error fittings to better describe different chemicals and their ignition delay. Furthermore, the Reynolds' number in various processes in pilot plant scale shall require more statistical distribution error interval while making plans on process safety analysis.

Finally, we want to combine the minimum ignition energy models developed by previous studies and complete the combustion behavior of aerosols in general. The

minimum ignition energy of heat transfer fluids are affected by chemical species, thermodynamic properties, and aerosol profiles. We want to understand the combustion behavior about how to sustain the flame by our continued research, and introduce different models into the system of study, trying to understand the relation of minimum ignition energy and the ignition frequency.

Further Studies on Ignition Delay

The detailed modeling procedures to improve this ignition delay and combustion mechanism requires many chemically analyzed sub-models on kinetics (surface reaction and tail gas analysis), gas-phase and liquid phase interaction (regular droplets), and extreme cases of mass transfer dominating/vapor-like approach (large drops/small drops). Here is a list of modeling works I propose to add to the aerosol system simulation approach:

Macroscopic Model

Since in most cases, the liquid fuel is a mixture, we have to consider the boiling point difference of the materials. This is one of the reasons the sustainable flame needs more time to form than the initial ignition source that was placed into our aerosol system. We plan to think of a scenario of the real case, applying the parameters of temperature, pressure, and heat addition in each step of the PFD. For the model itself, we will introduce the boiling point range of the material, and add chemical kinetics of the fuel oxidization into the explanation. An early study pointed out potential reactive parameters

including in this model (Jokiniemi et al, 1993): gas phase reaction, chemical affinity, binary nucleation of fuel species, and particle surface reaction rates. This will give an explanation to ignition delay and the "successful flame" appearance mechanism due to surface chemical reactions. When the surface reaction is done, the droplet evaporation will be the dominating force instead of kinetics, which is, the mass transfer of combustible matters. This leads to the next model system: single droplet model.

Single Droplet Model

To achieve the combustion profile of sustainable flame appearance and compare with ignition energy and ignitable conditions, a single droplet model is considered to be the first step of individual droplet behaviors before their distance grows close enough for them to interact with each other. The schematic figure of the domains is shown as Figure 43.

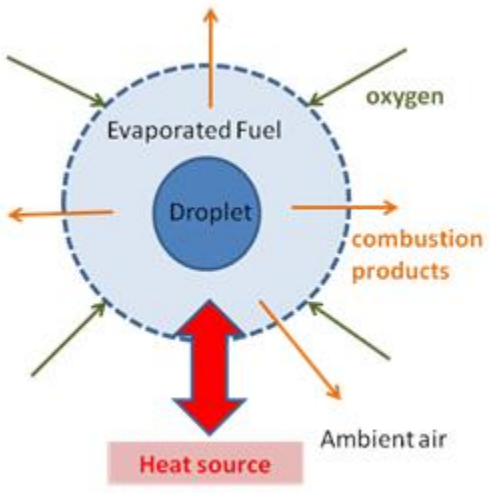

Figure 43. Single Droplet Model Domains

The droplet is surrounded by vapors, with oxygen input and combustion products outputs. The heat source is considered to be in the gravity direction to simplify the flow system model. This shall be a steady-state mass flow process influenced by the following sub-systems:

- Droplet Size
- Oxygen diffusion
- Combustion products
- Heat transferred from heat source
- Liquid evaporation extent
- Vapor diffusion and mixing

These would be highly relied on experimental results of the combustion extents by GC studying of tail gas. However, the experiment results are based on group behaviors. To achieve a better estimation of combustion extent of this oxidation reaction, we need the assistance of multiple droplets model.

Multiple Droplets

This part of the model, as in Figure 44, shall be similar to the single droplet model. The differences are: (1) extreme droplet sizes, (2) droplet-droplet interaction: heat transfer in evaporated domains, and (3) heat transfer in radial direction. Very large droplets (but still light enough for suspending in air) are mainly mass-transferring with much time spent on evaporation of matters, with the less consideration of vapor diffusion and

mixing; very small droplets (<40 microns), however, are likely to go directly to vapor mixing since their liquid fuel amounts are relatively few. The droplet-droplet interaction, the heat transfer portion (just like our simulation in preliminary results, the “heat kernel” hypothesis), is another important point of view. The coordination selection shall be carefully evaluated as long as this is a radial model in energy transport.

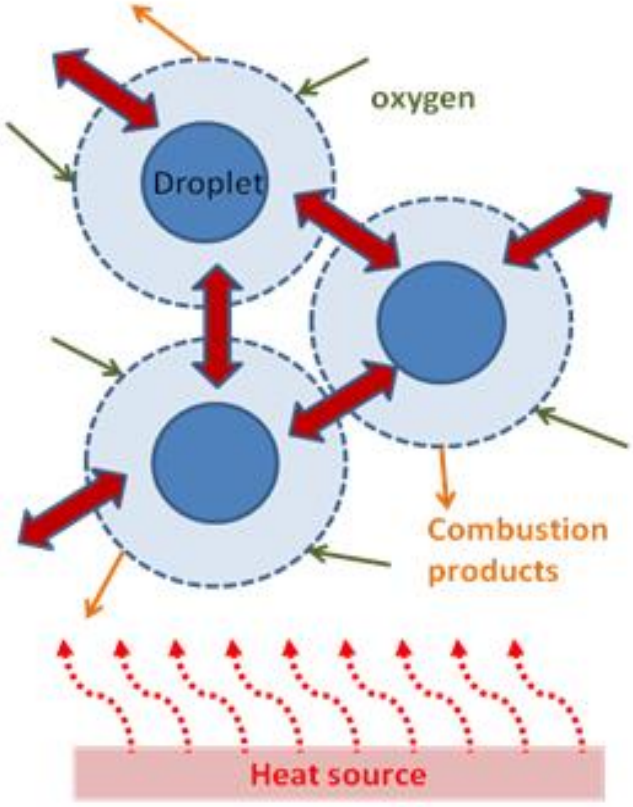

Figure 44. Multiple Droplets Model Domains

REFERENCES

Abramzon, B., Sirignano, W. A. (1989). Droplet Vaporization Model for Spray Combustion Calculations. *Int. J. Heat Mass Transfer*, 32, 1605-1618.

Aggarwal, S. K., and Cha, S. (1987). Further Results on Spray Ignition and Comparison with Experiments. *IN AIAA 25TH AEROSPACE SCIENCES MEETING*.

Aggarwal, S. K., and Sirignano, W. A. (1984). Ignition of Fuel Sprays: Deterministic Calculations for Idealized Droplet Arrays. *TWENTIETH SYMPOSIUM (INTERNATIONAL) ON COMBUSTION*, 1773-1780.

Aggarwal, S.K. (1997). A Review of Spray Ignition Phenomenon. *33RD AIAA/ ASME/ SAE/ ASEE JOINT PROPULSION CONFERENCE & EXHIBIT*, Seattle, WA

Amsden, A. A., O'Rourke, P. J., and Butler, T.D., (1989). KIVA II: A Computer Program for Chemically Reactive Flows with Sprays, Los Alamos National Laboratory, LA-11560-MS.

Atzler, F., Lawes, M. (1998). Burning Velocities in Droplet Suspensions. *ILASS-EUROPE'98*, Manchester

Bowen, P. J., Shirvill, L. C. (1994). Combustion Hazards Posed by the Pressurized Atomization of High-flash Point Liquids, *J. Loss Prev. Process Ind.*, 7(3), 233-241.

Buchanan, J.S., (1994). Analysis of Heating and Vaporization of Feed Droplets in Fluidized Catalytic Cracking Risers, *Ind. Eng. Chem.,* 33, 3104-3111

Chrigui, M., Zghal, A., Sadiki, A., and Janicka, J., (2010). Spray Evaporation and Dispersion of N-heptane Droplets within Premixed Flame, *Heat Mass Transfer,* 46, 869–880

Cui, C., Fritsching, U., Schultz, A., and Li., Q. (2005). Mathematical Modeling of Spray Forming Process of Tubular Performs: Part 1. Shape Evolution, *Acta Materialia*, 53(9), 2765-2774

Dunn, P.F., Grace, J. M., and Snarski, S.R. (1994). The Mixing of Electrically-Charged Droplets between and within Electro-hydrodynamic Fine Sprays, *J. Aerosol Sci*., 25(6), 1213-1227

Durkee, I. J. B. (2003). Solvent Safety II: Aerosols and Mists. *Metal Finishing*.

Eichhorn, J. (1955). Careful! Mist Can Explode, *Petroleum Refiner* 34 (11), 194–196.

Eisazadeh-Far, K., Parsinejad, F., Metghalchi, H., Keck, J.C. (2010). On Flame Kernel Formation and Propagation in Premixed Gases. *J. of Combust. Flame,* 157, 2211-2221.

Febo, H.L., Valiulis J.V. (1995). Heat Transfer Fluid Mist Explosion Potential: An Important Consideration for Users, *Proc. of the AIChE Loss Prev.*, Norwood, Maine, Factory Mutual Research Corporation.

Ganan-Calvo, A., Lopez-Herrera, J., and Riesco-Chueca, P. (2006). The combination of electro-spray and flow focusing, *J. Fluid Mech.*, 566, 421-445.

Gutheil, E. (1993). "Numerical Investigation of the Ignition of Dilute Fuel Sprays Including Detailed Chemistry," *J. of Combust. Flame*, 93, 239-254

Huang, S., Li, X., and Mannan, S. (2013) The Characterization of Heat Transfer Fluid P-NF Aerosol Combustion: Ignitable Region and Flame Development, *J. Loss Prev. Process Ind*., accepted manuscript, in press.

Huang, S., Li, X., and Mannan, S. (2013) Paratherm-NF Aerosol Combustion Behavior Simulation: Ignition Delay Time, Temperature Distribution of Flame Propagation, and Heat Kernel Hypothesis of Combustion Process Analysis, *J. Loss Prev. Process Ind*., accepted manuscript, in press.

Jorma, K., Jokinemi *et al* (1994). Numerical Simulation of Vapour-Aerosol Dynamics in Combustion Processes, *J. Aerosol Sci*., 25(3), 429-446

Krishna, K., Rogers, W. J., Mannan, M. S. (2003). The Use of Aerosol Formation, Flammability, and Explosion Information for Heat-transfer Fluid Selection, *J. of Haz. Mat.*, 104(1-3), 215-226.

Lian, P., Mejia, A., Cheng, Z., and Mannan, M.S. (2010). Flammability of Heat Transfer Fluid Aerosols Produced by Electro-spray Measured by Laser Diffraction Analysis, *J. Loss Prev. Process Ind*., 23(2), 337-345.

Lian, P., Ng, D., Mejia, A.F., Cheng, Z., and Mannan, M.S. (2011). Study on Flame Characteristics in Aerosols by Industrial Heat Transfer Fluids, *I&EC*, 50(12), 7644-7652

Lian, P., Gao, X., Mannan, M.S. (2012). Prediction of Minimum Ignition Energy of Aerosols Using Flame Kernel Modeling Combined with Flame Front Propagation Theory, *J. Loss Prev. Process Ind*., 25(1), 103-113

Lawes, M., Saat, A. (2011). Burning Rates of Turbulent Iso-octane Aerosol Mixtures in Spherical Flame Explosions, *Proc. of Combust. Inst.*, 33(2), 2047-2054

Mansoori, G.A. (1997) Modeling of Asphaltene and Other Heavy Organic Depositions, *J. of Petro. Sci. and Eng.*, 17(1)–2, 101-111

Maragkos A., Bowen P.J. (2002). Combustion Hazards Due to Impingement of Pressurized Releases of High-flashpoint Liquid Fuels, *Proc. of Combust. Inst.,* 29, 305-311.

Mejia, A. F., He, P., Luo, D., Marquez, M., Cheng, Z. (2009) Uniform Discotic Wax Particles via Electrospray Emulsification, *J. Colloid Interface Sci*, 334(1), 22-28

Mullins, B.J., Braddock, R.D., Agravski, I.E., (2010). Modelling Droplet Motion and Interfacial Tension in Filters Collecting Liquid Aerosols, *MATCOM*, 81(7), 1257-1271

Nomura, H., Kawasumi, I., Ujiie, Y., Sato, J. (2007). Effects of Pressure on Flame Propagation in a Premixture Containing Fine Fuel Droplets, *Proc. of Combust. Inst.*, 31(2), 2133-2140

Olumee, Z., Callahan, J. H., and Vertes, A. (1998) Droplet Dynamics Changes in Electrostatic Sprays of Methanol-Water Mixtures, *J. Phys. Chem*., 102, 9154-9160.

Suard, S., Haldenwang, P., Nicoli, C. (2004). Different Spreading Regimes of Spray-flames. *C.R. Mecanique*, 332, 387-396

Wilm, M. (2011) Principles of Electrospray Ionization, Tutorials, by the American Society for Biochemistry and Molecular Biology, Inc.